SHORT TERM CONTRACT FOR THE BIOLOGICAL STUDIES (ICCAT GBYP 06/2019) OF THE ATLANTIC-WIDE RESEARCH PROGRAMME FOR BLUEFIN TUNA (GBYP Phase 9)

Final Report

for:

ICCAT

Scientific coordinator:

Dr. Haritz Arrizabalaga (AZTI-Tecnalia)

Pasaia, April 10th, 2020

This project is co-funded by

the European Union

PARTNERS:

Fundación AZTI-AZTI Fundazioa

IFREMER

Universitá di Genova

National Research Institute of Far Seas Fisheries

Texas A&M University

GMIT

Universidad de Cádiz

Instituto Español de Oceanografía

University of Cagliari

SUBCONTRACTORS and COLLABORATORS:

Institute of Marine Research

IPMA

INRH

INDEX:

EXECUTIVE SUMMARY:....7
1. CONTEXT....10
2. SAMPLING....11
2.1. Sampling accomplished....11
3. GENETICS....18
3.1. Introduction....18
3.2. Material and methods....19
3.2.1. DNA extraction and SNP genotyping....19
3.2.2. Generation of genetic informed baselines....20
3.2.1. Assignment of samples of unknown origin....20
3.2.2. RAD-loci assembly and SNP calling....21
3.2.3. Estimation of recent migration rates....21
3.2.4. Loci under selection....22
3.2.5. Tests for nuclear introgression....22
3.2.6. Generation of new subset of SNPs for traceability....23
3.3. Results and discussion....23
3.3.1. DNA extraction and SNP genotyping....23
3.3.2. Improved baseline for origin assignment....24
3.3.3. Comparing assignment of feeding aggregate samples using a location informed or a genetic-informed baseline....25
3.3.4. New subsets of SNP for traceability....28
3.3.5. Origin and role of the Slope Sea in the ABFT populations connectivity...29
3.3.6. Mechanisms for the maintenance of stock structure despite observed mixing at spawning site and season....31
3.3.6.1. Genomic signatures of natural selection....31
3.3.6.2. Introgression from albacore....34
3.3.6.3. Origin of the linkage groups....36
3.4. Conclusions....38

3.5. Future work and management implications 40
4. OTOLITH MICROCHEMISTRY 43
4.1. Determining nursery origin of bluefin tuna captured in the potential mixing zones 43
4.1.1. Introduction 43
4.1.2. Material and Methods 43
4.1.3. Results and Discussion 45
4.2. Individual origin assignment 48
4.2.1. Introduction 48
4.2.2. Material and Methods 48
4.2.3. Results and Discussion 48
4.3. Discrimination of nursery areas within the Mediterranean Sea by trace element and stable isotope composition in young-of-the-year bluefin tuna 50
4.3.1. Introduction 50
4.3.2. Material and Methods 51
4.3.3. Results and Discussion 55
4.4. Otolith oxygen isotopes measured by high-precision secondary ion mass spectrometry (SIMS) reflect movements between the Mediterranean Sea and the Atlantic Ocean 61
4.4.1. Introduction 61
4.4.2. Methods 63
4.4.3. Results and Discussion 65
4.4.4. Conclusions 77
5. CALIBRATION OF FISH AGEING SERVICES OTOLITH AGE ESTIMATES AND CREATION OF AN OTOLITH REFERENCE COLLECTION. 79
5.1. Introduction 79
5.2. Material and methods 80
5.3. Results and discussion 82
5.4. Conclusions 91
6. ATLANTIC BLUEFIN TUNA (*THUNNUS THYNNUS*) LARVAE IDENTIFICATION IN THE BAY OF BISCAY 94
6.1. Introduction 94
6.2. Material and Methods 95
6.2.1. Field samples 95

6.2.2. Microscopic identification....97
6.2.3. Genetic identification....97
6.3. Results and discussion....98
7. SORTING AND IDENTIFICATION OF ATLANTIC BLUEFIN TUNA LARVAE FOR POTENTIAL CLOSE-KIN ANALYSES....103
7.1. Objective....103
7.2. Methods....103
7.3. Results....104
8. ACKNOWLWDGEMENTS....106
9. APPENDICES....107

EXECUTIVE SUMMARY:

The main objective of this project is to enhance knowledge about Atlantic bluefin tuna (ABFT) population structure and mixing, but also to focus on age dynamics.

During Phase 9, following sampling protocols agreed in earlier Phases, the consortium sampled a total of 747 bluefin tuna (1 YOY, 4 juvenile fish, 101 medium sized fish and 641 large fish) from different regions (107 from the Strait of Gibraltar, 50 from Morocco, 31 from Portugal, 56 from the Canary Islands, 184 from Norway, 314 from the Central North Atlantic and 5 from the Bay of Biscay). In total, 1079 biological samples (322 otolith samples, 154 fin spines and 603 genetic samples) were collected by the Consortium and incorporated into the tissue bank. The consortium also received samples from other ICCAT contracts with tagging teams and farm operators. In total, the consortium handled 4427 biological samples (1600 otolith samples, 598 fin spines and 2229 genetic samples from 2941 individuals.

On genetic analyses, we have generated an improved baseline for the existing 96 SNP traceability tool integrating genome-wide genetic background of the included samples, considering information on population dynamics complexity of Atlantic bluefin tuna. Improved assignment rates were obtained using the new genetic-informed baseline which, together with the original baseline, was used to assign genetic origin of >2400 samples from feeding aggregations including 470 newly genotyped samples, completing the mixing map of the Gulf of Mexico and Mediterranean genetic components along the Atlantic. Assignments using the new genetic-informed baseline produced lower unassignment rates than those calculated using the original location-informed baseline, both analyses confirming high mixing in Western locations. Regarding the population structure of Atlantic bluefin tuna, gene-flow from the Mediterranean Sea into the Gulf of Mexico, most likely through the Slope Sea, was confirmed analyzing RAD-seq data from 535 individuals.

Hypotheses that could explain maintenance of genetic structure despite gene-flow are formulated.

Regarding otolith microchemistry, new carbon and oxygen stable isotope analyses were carried out in 129 otoliths of Atlantic bluefin tuna captured in the Central North Atlantic, to determine their nursery area. $\delta^{13}C$ and $\delta^{18}O$ values measured in otolith cores indicated that these samples were dominated by eastern origin individuals. The comparative analysis with previous Phases suggests that mixing of the two populations occurs at variable rate, but Mediterranean bluefin tuna may be the principal contributors to the Japanese fishery operating in the central North Atlantic. Within the Mediterranean Sea, discrimination of Eastern Mediterranean nursery was possible in 2011 using otolith trace element concentration, but differences among the nursery areas in 2013 were not statistically significant.

High-precision secondary ion mass spectrometry (SIMS) was used to provide, for the first time, high resolution estimates of oxygen stable isotopes (δ18O) along otolith growth transects from Atlantic bluefin tuna. Measurements were markedly lower than the values previously obtained using IRMS, which is consistent with reports from other species and is likely due to methodological differences. δ18O signatures in individuals from the same environment (Mediterranean farms) showed considerable variability which will reduce the accuracy of life history reconstructions. Nonetheless, examination of relative patterns between individuals indicated substantial variability in environmental histories during the first few months of life. The results support the hypothesis that some individuals are retained within homogenous water masses during early life, while others are exposed to wide variation in water chemistry. Possible evidence of trans-Atlantic migration of adult fish was also recorded in some otolith chemistry profiles.

On the otolith age calibration exercise, the findings show that the band count is similar between Fish Aging Services (FAS) and the group of laboratories involved in direct ageing of Atlantic bluefin tuna otoliths. This is reflected by an acceptable precision between both readings. However, there is a one-year bias starting from 10-13 years of age in the count of bands in older specimens, with a lower count by FAS compared to the rest of the laboratories. This bias seems to be due to the fact that FAS counts the bands in a different area of the ventral arm of the otolith compared

to other laboratories. This counting discrepancy, although small, is significant and it would be necessary for FAS laboratory to reread the samples of specimens older than 10 years using the area close to the sulcus margin of the ventral arm.

Recently, ABFT larvae were found in the Bay of Biscay (Rodriguez et al.2019) suggesting that ABFT could have been spawning in this area. For that reason, the search for ABFT larvae in samples collected in past surveys in the Bay of Biscay was proposed for this study. The species identification was performed on historical samples preserved in ethanol, collected outside the continental platform, where the probability to find ABFT was considered to be higher. All larvae were extracted and identified through microscopic identification and genetic sequencing for confirmation. Among the 7,017 larvae checked for ABFT from 368 samples, preserved in ethanol, one larva collected in August 2009 was identified as bluefin. This sample was taken west of Santander (43º37'61N 4º10'92 W) in august 2009 in a mean sea surface temperature of 21.6ºC and a mean sea surface salinity of 34.88. Moreover, larvae from *Sarda sarda* (14 larvae), and *Auxis spp* (13 larvae) were identified after the genetic sequencing.

Finally, ABFT larvae from surveys conducted in the Balearic spawning ground were sorted and identified for potential close-kin analyses. A total of 339 bluefin tuna larvae were suitable for close-kin analyses after sorting and identifying fish larvae in more than 60 stations. Collaboration with CSIRO confirms only ethanol-preserved larvae, and not cytoscan, allows close-kin analyses.

Most of the objectives of the project were met. The analyses continue to provide important information that is relevant for the understanding of Atlantic bluefin tuna biology and improves stock assessment and management of this valuable resource.

1. CONTEXT

On May 13th 2019, the consortium coordinated by Fundación AZTI-AZTI Fundazioa, formed by partners Fundación AZTI-AZTI Fundazioa, IFREMER, Universitá di Genova, National Research Institute of Far Seas Fisheries, GMIT, Texas A&M University, Universidad de Cádiz, University of Cagliari, Instituto Español de Oceanografía, with subcontracted parties IPMA, Institute of Marine Research and INRH, presented a proposal to the call for tenders on biological and genetic sampling and analysis (ICCAT-GBYP 06/2019).

This proposal was awarded and the final contract between ICCAT and the consortium represented by Fundación AZTI-AZTI Fundazioa was signed on June 13th 2019.

According to the terms of the contract, a final report (Deliverable # 5) needs to be submitted to ICCAT by 10th of April 2020, including the description of the work carried out up to this date. The present report was prepared in response to such requirement.

2. SAMPLING

Task Leader: Igaratza Fraile

Participants:

AZTI: Inma Martin, Naiara Serrano, Ainhoa Arevalo, Goreti Garcia, Haritz Arrizabalaga, Naiara Rodriguez-Ezpeleta, Natalia Diaz, Iñaki Mendibil

UCA: Jose Luis Varela, Antonio Medina

NRIFSF: Yohei Tsukahara, Tomoyuki Itoh, Shuya Nakatsuka

IEO: Enrique Rodriguez Marín, Rosa Delgado de Molina

INRH: Noureddine Abbid

IMR: Ørjan Sørensen, Adam Custer, Christine Djønne, Erling Boge, Leif Nøttestad

IPMA: Pedro Lino, Rui Coelho

The sampling conducted under this project follows a specific design, aimed primarily at contributing to knowledge on population structure and mixing. As such, the sampling conducted under this project is independent from other routine sampling activities for fisheries and fishery resources monitoring (e.g. the Data Collection Framework).

2.1. Sampling accomplished

The sampling protocols and the form to collect the data have been amended as necessary to include all new codes (e.g. areas and/or institutions). These, together with instructions, have been distributed within the consortium as well as to ICCAT, so that they are distributed to other institutions conducting biological sampling (e.g. as part of tagging activities, Regional Observer Programs, farms, etc.).

The sampling tasks have finalized successfully in most of the areas. IEO has provided otolith and genetic samples from 56 individuals from Canary Islands caught in 2019. NRIFSF collected otolith and genetic samples from 314 individuals caught by Japanese longliners in the central Atlantic Ocean in October 2018, although 124 of these have not yet arrived to AZTI and will do so once the transport can be arranged safely. All the

individuals were captured east of the 45ºW boundary. Only one YOY bluefin tuna was captured in the Strait of Gibraltar by UCA. Although efforts have been made to target this size class, YOY bluefin tuna were not available in the area. However, genetic samples of 106 medium and large bluefin tuna were collected around the Strait of Gibraltar. INRH has conducted sampling on fattened tuna in Morocco, with both otolith and muscle tissue sampled from 50 individuals. Sampling by IPMA in the Portuguese traps finalized in September. Otolith, spine and muscle were sampled from 31 individuals, 9 of "Medium" category and 22 of "Large" category.

Sampling in Norwegian waters was conducted in September 2019. Samples were taken from three Norwegian purse seine vessels, M/V "Brennholm", M/V "Orfjord" and M/V "Vibeke Helene". Samples have also been taken from bycatches in other fisheries. The number of Atlantic bluefin tuna literally catching themselves after penetrating salmon farms along the coast of Norway, seem to have increased over the last few years. A total number of 165 genetic samples, 153 spines and 26 pair of otoliths have been taken from large Atlantic bluefin tuna. Because most of the BFT are sold with heads on, it was not possible to extract the otoliths from many of the individuals. In the Bay of Biscay, 5 tuna, mostly juveniles, were sampled by AZTI during tagging events. In total, 747 bluefin tuna have been sampled by Consortium partners.

The original plan, according to the Consortium contract, was to acquire samples from 580 individuals. Thus, the current sampling status by the Consortium represents 129% of the target in terms of total number of individuals. Analyzing the objectives by strata, most areas were covered according to the sampling plan. In the Atlantic side of the Strait of Gibraltar, the target was the acquisition of 50 YOY bluefin tuna. This objective was not achieved due to the lack of small fish in this area during 2019, but instead, medium and large category bluefin tuna were sampled. In the other areas, the number of individuals caught was larger than expected.

Additional samples captured in 2018 and harvested in spring 2019 arrived from two different observers of the Regional Observer Program run by MRAG, placed at Caladeros / Tuna Graso and Balfegó. They collected samples from 50 and 151 individuals, respectively. Additional samples were taken as part of ad hoc GBYP contracts for sampling BFT adults in Western and Central Mediterranean farms TAXON has collected muscle, otolith, spine and gonads of 330 individuals around the

Balearic Sea and Sardinia. ABTL sampled 282 and 804 large individuals in the Tyrrhenian Sea and Malta, respectively. Sampling of juvenile (n=13) and medium (n=82) size bluefin tuna in the Tyrrhenian Sea was carried out by NGBFT, as well as additional sampling of 19 individuals of large size bluefin tuna sampled South of Sicily. Biological samples (otoliths, tissue for genetics) from 462 individuals captured in the Levantine Sea have been collected by Akuagroup in Turkey within the framework of GBYP growth in farm studies and are expected to arrive to AZTI soon.

The summary of individuals sampled to date is presented in Table 2.1. Altogether, a total of 2941 individuals have been sampled. These samples have been catalogued and stored together with the biological tissue bank (except those from the Levantine Sea and the second batch from Central North Atlantic that have not arrived yet due to difficulties in sending samples derived from coronavirus outbreak).

Table 2.1: Number of bluefin tuna sampled by area and size class. a) Individuals sampled by the Consortium. b) Total number of individuals sampled (including those of the Consortium plus the ones sampled under other contracts and stored by the Consortium).

a)		Size-class sampled				Responsible	Target	%
		Age 0	Juvenile	Medium	Large			
		<3 Kg	3-25 Kg	26-100 Kg	>100 Kg			
Strait of Gibraltar	Gibraltar	1		90	16	UCA	50	214
East Atlantic- West African coast	Morocco				50	AZTI (INRH)	50	100
	Canary Islands				56	IEO	50	112
Northeast Atlantic	Portugal			9	22	AZTI (IPMA)	30	103
	Bay of Biscay		4	1		AZTI	0	
Central North Atlantic	Central and North Atlantic			1	313	NRIFSF	300	105
Norwegian Sea/North Sea	Norway				184	AZTI (IMR)	100	184
TOTAL nº of individuals		**1**	**4**	**101**	**641**		**580**	**129**

b)		Size-class sampled				Responsible
		Age	Juvenile	Medium	Large	
		<3	3-25 Kg	26-101	>100	
Strait of Gibraltar	Gibraltar	1		90	16	UCA
East Atlantic- West African coast	Morocco				50	AZTI (INRH)
	Canary Islands				56	IEO
Northeast Atlantic	Portugal			9	22	AZTI (IPMA)
	Bay of Biscay		4	1		AZTI
Central North Atlantic	Central and North			1	313	NRIFSF
Norwegian Sea/North Sea	Norway				184	AZTI (IMR)
Western Mediterranean	Balear Sea				201	ROP
	Balear Sea			7	268	TAXON
	Sardinia			14	41	TAXON
	Tyrrhenian		13	82		NGBFT
	Tyrrhenian				283	ABTL
Central Mediterranean	South Sicily				19	NGBFT
	Malta				804	ABTL
Eastern Mediterranean	Levantine Sea			267	195	AKUA
TOTAL nº of individuals		**1**	**17**	**450**	**2473**	

A total of 1079 biological samples have been collected by the Consortium and incorporated to the tissue bank (322 otoliths, 154 fin spines and 603 genetic samples). Table 2.2a shows the number of otoliths, fin spines and genetic samples in each stratum.

In addition, the Consortium received samples from other teams contracted by ICCAT to conduct biological sampling in farms. Altogether (considering the samples collected by the Consortium and those that arrived from other contracts), the Consortium handled 4427 biological samples (1600 otoliths, 598 fin spines and 2229 genetic samples, Table 2.2b and Figure 2.1). Several hundreds of otoliths and tissue samples corresponding to individuals captured in the Levantine Sea are expected to arrive soon from Akuagroup.

Table 2.2: Number of samples collected by area and tissue type. a) Samples taken by the Consortium. b) Total number of samples (including those of the Consortium plus the ones taken under other contracts and stored by the Consortium).

a)		Tissue				Sampler
		Otolith	**Spine**	**Muscle/fin**	**Total**	
Strait of Gibraltar	Gibraltar	1		107	108	UCA
East Atlantic- West African coast	Morocco	50		50	100	AZTI (INRH)
	Canary Islands	55		56	111	IEO
Northeast Atlantic	Portugal			31	31	AZTI (IPMA)
	Bay of Biscay		1	4	5	AZTI
Central North Atlantic	Central and North Atlantic	190		190	380	NRIFSF
Norwegian Sea/North Sea	Norway	26	153	165	344	AZTI (IMR)
TOTAL nº of individuals		**322**	**154**	**603**	**1079**	

b)		Tissue				Sampler
		Otolith	**Spine**	**Muscle/fin**	**Total**	
Strait of Gibraltar	Gibraltar	1		107	108	UCA
East Atlantic- West African coast	Morocco	50		50	100	AZTI (INRH)
	Canary Islands	55		56	111	IEO
Northeast Atlantic	Portugal			31	31	AZTI (IPMA)
	Bay of Biscay		1	4	5	AZTI
Central North Atlantic	Central and North Atlantic	190		190	380	NRIFSF
Norwegian Sea/North Sea	Norway	26	153	165	344	AZTI (IMR)
Western Mediterranean	Balear Sea			201	201	ROP
	Balear Sea	262	275	275	812	TAXON
	Sardinia	55	55	55	165	TAXON
	Tyrrhenian	95	95	95	285	NGBFT
	Tyrrhenian	216		255	471	ABTL
Central Mediterranean	South Sicily	19	19	19	57	NGBFT
	Malta	631		726	1357	ABTL
Eastern Mediterranean	Levantine Sea	?	?	?		AKUA
TOTAL nº of individuals		**1600**	**598**	**2229**	**4427**	

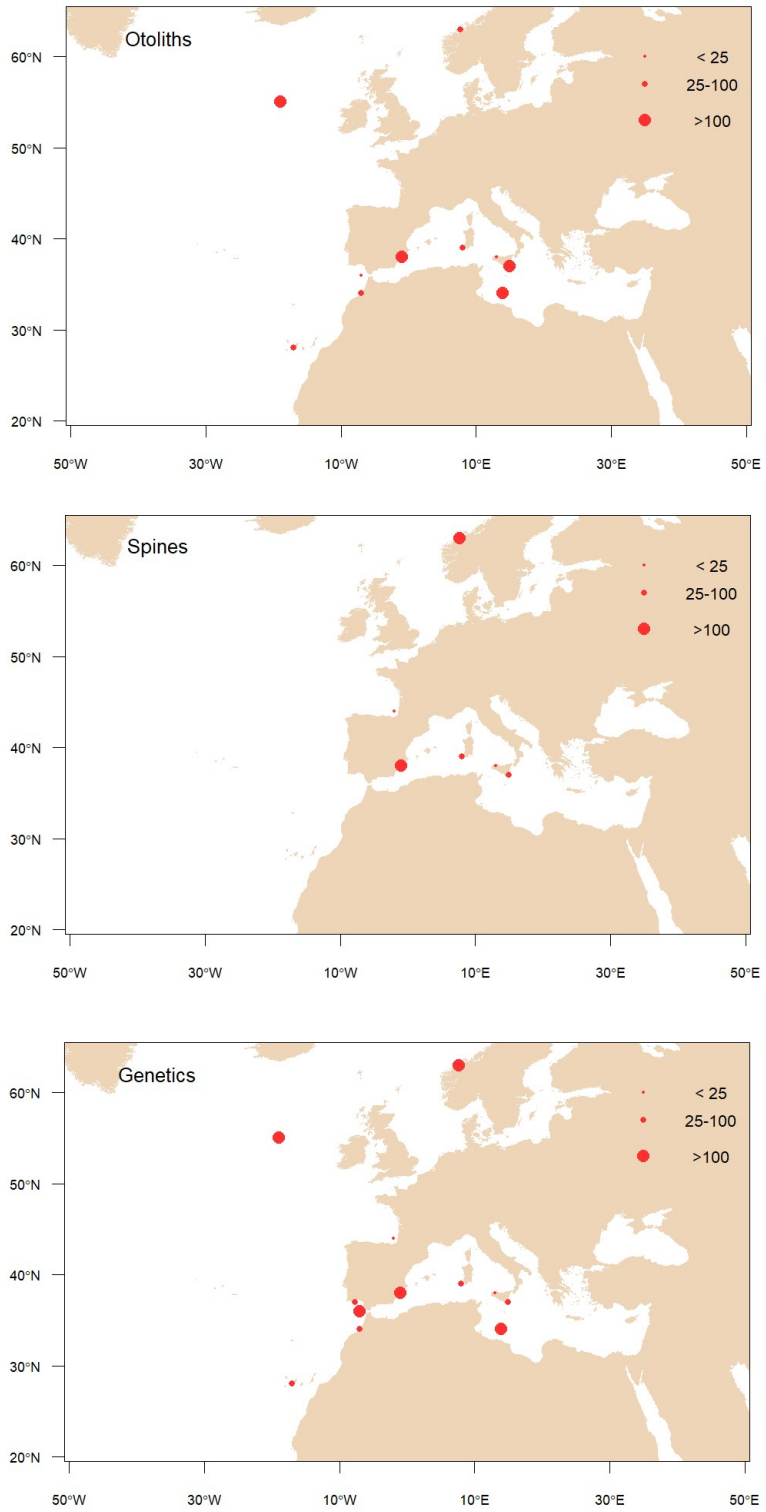

Figure 2.1: Total number of otoliths, fin spines and genetic samples collected under all GBYP contracts in Phase 9 in the Northeast Atlantic and Mediterranean, aggregated by main region (samples from Levantine sea not included yet). Positions of the dots are averages across all samples by main region.

3. GENETICS

Task Leader: Naiara Rodriguez-Ezpeleta (AZTI)

Participants: Natalia Diaz-Arce, Iñaki Mendibil, Haritz Arrizabalaga

3.1. Introduction

Previous studies supporting the presence of two populations of Atlantic Bluefin Tuna (ABFT) have allowed the development of a traceability SNP panel that assigns individuals to their stock of origin, which is very relevant for ABFT management (Rodríguez-Ezpeleta et al. 2019). Yet, more in-depth analyses have shown that the population dynamics of ABFT is more complex than a meree homing behavior to the two main spawning grounds (the Mediterranean and the Gulf of Mexico) with feeding aggregates mixing in the Atlantic. First, individuals with Mediterranean genetic background are found within the Gulf of Mexico and, second, the Slope Sea constitutes a genetically intermediate population (see Phase 8 report), which might explain why some individuals cannot be assigned to either population and why some Gulf of Mexico individuals are assigned to the Mediterranean Sea. Initially, these unassignments and misassignments were thought to be a methodological bias, but recent results suggest that they might be due to a more complex population structure in ABFT that is not considered by the genetic assignment method. Thus, in order to better understand the migration and reproductive behavior of ABFT and to develop an improved traceability panel that takes these new findings into account, additional analyses were envisaged.

To achieve this objective, three main tasks have been carried out.

Task 1 has consisted on improving the traceability tool by integrating new findings of ABFT population dynamics and on reassigning previously assigned feeding aggregates to assess differences. Two main activities were planned in relation to this task: 1) generation of new baselines and 2) reassignment of > 2000 individuals from feeding aggregates that were already included in Phase 8. Task 2 has consisted on origin assignment of newly collected ABFT samples from different locations along the Atlantic Ocean to complete the global picture of stock-mixing obtained in Phases 6 and 8. Finally, task 3 has consisted on formulating and testing hypotheses that better explain ABFT

population structure by 1) determining the origin of the Slope Sea spawning area and by 2) understanding mechanisms for maintenance of genetic differentiation despite mixing.

3.2. Material and methods

3.2.1. DNA extraction and SNP genotyping

DNA of 470 individuals from different locations and size classes was extracted and genotyped for the 96 SNP diagnostic panel (Table 3.1). DNA was extracted using the Wizard® Genomic DNA Purification kit (Promega, WI, USA) following manufacturer´s instructions for "Isolating Genomic DNA from Tissue Culture Cells and Animal Tissue". The starting material was approximately 20 mg of tissue or whole larvae and after extraction all samples were suspended in equal volumes of Milli-Q water. DNA quantity (ng/µl) was evaluated on the Qubit® 2.0 Fluorometer (Life Technologies) and DNA integrity was assessed by electrophoresis. Genotyping of the newly collected samples for the 96 SNPs in including in the traceability panel from Rodríguez-Ezpeleta et al. (2019) different locations of the North Atlantic and different age classes was performed on the BiomarkTM HD platform using Flex Six™ and 96.96 Dynamic Array IFCs, and the resulting data set was analysed with the Fluidigm Genotyping Analysis Software.

Table 3.1. Summary of genotyped samples.

Institute	Area	2013	2015	2016			2017			2018	2019	
		L	L	J	M	L	J	M	L	L	L	Total
DFO	Canada	3	45			32			26			**106**
IEO	Canarias									6		**6**
NOAA	West Atlantic			20	29	61	24	32				**166**
IMR	Norway									79		**79**
ROP	Gibraltar									1		**1**
NRIF	Central Atlantic	12							100			**112**
AZTI	Bay of Biscay										5	**5**
Total		**15**	**45**	**20**	**29**	**93**	**24**	**32**	**126**	**86**		**470**

3.2.2. Generation of genetic informed baselines

Ancestry values (Q) for each of the 463 ABFT individuals from the RAD dataset sequenced in Phases 6 and 8 including larvae, Young of the Year and adult individuals from the Gulf of Mexico, the Slope Sea and the Mediterranean spawning grounds were estimated using ADMIXTURE (Alexander, Novembre, Lange 2009) assuming two ancestral populations. These were used as a proxy for individual genome-wide genetic background assignment. Based on estimated ancestral proportions individual genetic profile was assigned as Gulf of Mexico ($Q<0.25$), Mediterranean ($Q>0.75$) or intermediate ($0.25<Q<0.75$). This information was used to generate a new baseline relocating individuals according to their genetic profile instead of capture location. Only Gulf of Mexico-like, Mediterranean-like and Mediterranean captured (assuming that samples captured in the Mediterranean show a homogeneous genetic background) individuals were included to generate the genetic-informed baseline. Assignment rate of the newly generated baseline was calculated following the same procedure described in Phase6. Assignments were performed with GENECLASS2 (Piry et al. 2004) using the Rannala and Mountain (1997) criterion (0.05 threshold) considering two (Gulf of Mexico-like and Mediterranean-like) populations as baselines. For each individual that was not involved in the 96 SNP selection process (see Phase6), assignment scores (i.e. probability of belonging to each of the baseline populations) were calculated using a leave-one-out approach using the different baselines excluding the sample being assigned for each calculation. Assignment rates were calculated considering only assignment scores > 80%.

3.2.1. Assignment of samples of unknown origin

A total of 2496 adult samples of unknown origin captured at different feeding grounds in the North Atlantic (including 2026 already included in Phases 6 and 8 and 470 newly genotyped here) were assigned with GENECLASS2 (Piry et al. 2004) using the Rannala and Mountain (1997) criterion (0.05 threshold) using the location informed or the newly generated genetic-informed baseline and considering results applying 80% threshold for assignment scores.

3.2.2. RAD-loci assembly and SNP calling

RAD-seq data from 4 Southern bluefin tuna (*Thunnus maccoyii*), 4 albacore (*Thunnus alalunga*) and 5 Pacific bluefin tuna (*Thunnus orientalis*) samples available from (Díaz-Arce et al. 2016) were analysed following the same procedure described in Phase 8 for RAD-seq raw read processing. Genotypes were added to the RAD-seq dataset used in Phase 8 that contained 535 ABFT individuals to generate a new catalogue of RAD-loci. Only samples with more than 25,000 RAD loci were kept and only SNPs contained in RAD-loci present in at least 75% of the ABFT or in 75% of the individuals from each of the other species included were kept and exported into PLINK (Purcell et al. 2007) using *populations*. The genotype table was filtered to allow minimum genotyping rates of 0.90 and 0.80 per SNP and individual, respectively. SNPs with a minimum allele frequency smaller than 0.05 within ABFT (except when the minor allele had a minimum allele frequency over 0.25 in at least one of the other species for the catalogue including the other species) and which failed Hardy Weinberg equilibrium test at $p < 0.05$ in the group composed by Mediterranean L and YoY or in that composed by Gulf of Mexico L were removed. Resulting genotype tables from both catalogues including and excluding other tuna species and including all SNPs or only the first SNP per tag were converted to *genepop*, *structure*, PLINK, *BayeScan*, *immanc*, VCF and treemix formats using populations and PGDSpider version 2.0.8.3 (Lischer, Excoffier 2012).

3.2.3. Estimation of recent migration rates

Migration rates between the Mediterranean, Slope Sea and Gulf of Mexico locations as well as individual ancestries were estimated using BayessAss v3.04 (Wilson, Rannala 2003) considering only L and YoY samples from the RAD catalog including only ABFT samples. Mixing parameters were adjusted by running tests following manual recommendations and the mixing parameters for the allele frequencies, inbreeding coefficients and migration rates were set to 0.2, 0.01 and 0.1 respectively. BayesAss was run executing 10,000,000 iterations and discarding the first 3,000,000 iterations as burn-in and setting the interval between samples of the MCMC to 100. The program was run three times using different subsets of 5,000 randomly selected SNPs.

3.2.4. Loci under selection

Loci under selection were screened from the RAD dataset including only ABFT individuals using two approaches. The reversible jump Markov chain Monte Carlo approach implemented in BAYESCAN 2.1 (Foll, Gaggiotti 2008) was applied by grouping samples per location setting default parameters of 50000 burn-in steps, 5000 iterations 10 thinning interval size and 20 pilot runs of size 5000. Candidate loci under selection with a posterior probability higher than 0.76 (considered as strong according to the Jeffery's interpretation in the software manual) and a false discovery rate (FDR) lower than 0.05 were selected. The multivariate analysis method, which does not require a prior grouping of the samples, implemented in the pcadapt R package was applied following Luu, Bazin, Blum (2017) recommendations and outlier SNPs were selected following the Benjamini-Hochberg procedure. Pairwise linkage disequilibria between all filtered SNPs from those scaffolds which contained SNPs under selection was measured using the R package LDheatmap.

3.2.5. Tests for nuclear introgression

Nuclear introgression from albacore to ABFT was tested by estimating historical relationships among species and populations using TreeMix (Prickell 2012), which estimates the maximum likelihood tree for a set of populations allowing historical gene flow events, and the *ABBA/BABA* test (Kulathinal, Stevison, Noor 2009; Green et al. 2010; Durand et al. 2011), which measures the excess of derived alleles shared by the outgroup and one tested groups (in this case, one ABFT group) compared with the derived alleles share by the outgroup and another group taken as a reference (a different ABFT group). Using the RAD dataset including other tuna species, TreeMix was run allowing from 0 to 10 migration events, obtaining increasing number of possible gene flow events and associated likelihood values. The *ABBA/BABA* test was performed on the allele frequencies of the derived allele in albacore and ABFT locations, based on the ancestral state defined by the outgroup species Southern bluefin tuna. Patterson's D statistic was calculated using R for all possible combinations of target and reference groups of ABFT, always considering albacore as the donor species.

3.2.6. Generation of new subset of SNPs for traceability

From the genotype table obtained from the RAD dataset including only ABFT samples, two new subsets of SNPs for traceability were selected. Samples were divided into three groups according to their genetic background based on estimated ancestral proportions individual genetic profile was assigned as Gulf of Mexico-like (Q<0.25), Mediterranean-like (Q>0.75) or intermediate (0.25<Q<0.75) or captured location (Gulf of Mexico or Mediterranean) and two thirds of the samples contained in each group were randomly selected and extracted for genetic based or location-based SNP subset selection. To generate both subsets SNPs were ranked by pairwise F_{ST} values and most 96 discriminative SNPs between Gulf of Mexico or Gulf of Mexico-like and Mediterranean or Mediterranean-like samples were selected using the TRES software (Kavakiotis et al. 2015) respectively for the location and genetic based SNP subsets. If more than one SNP was derived from the same assembled RAD tag only the SNP with the highest pairwise F_{ST} was kept and the next best ranked SNP was included to sum up to 96 total selected SNPs. Assignment rates of the two newly selected subsets of SNPs were calculated based on assignment of origin of those individuals that were not included during the SNP selection process.

3.3. Results and discussion

3.3.1. DNA extraction and SNP genotyping

From the 470 newly genotyped samples for the 96 SNP panel 9 samples with >10% of missing data were excluded from the final dataset which included 461 individuals at a 99.4% genotyping rate.

3.3.2. Improved baseline for origin assignment

From the 463 samples analyzed, genotypes for the 96 SNP panel were available for 352, including samples captured in the Gulf of Mexico (175), the Mediterranean Sea (164) and Slope Sea (13). In total, 69 individuals were identified as genetically intermediate and were therefore excluded, 11 samples captured in the Gulf of Mexico were relocated as Mediterranean-like and 6 and 1 samples captured in the Slope Sea were relocated as Gulf of Mexico-like and Mediterranean-like respectively. Gulf of Mexico-like (137 samples) and Mediterranean-like (151 samples) were used as baseline.

Assignment rates obtained using the genetic-informed baselines where higher than those obtained using the location-informed baseline (86 vs 82% and 86 vs 78% for the Gulf of Mexico and Mediterranean samples) (Figure 3.1). Besides, when using the genetic-informed baseline lower proportions of unassigned samples were obtained. Therefore, relocation of Mediterranean-like samples captured in the Gulf of Mexico improve the reference definition of the Gulf of Mexico-like group allele frequencies, improving their assignment rates.

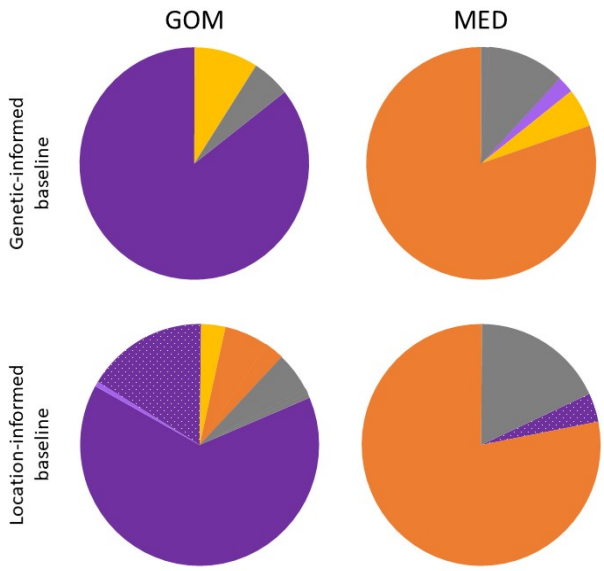

Figure 3.1. Assignment rates of Gulf of Mexico-like or Gulf of Mexico (GOM) and Mediterranean-like or Mediterranean (MED) samples using genetic background (top) or

location (bottom) respectively as reference for baseline generation and assignment rate calculation. Purple and orange represent GOM-assigned and MED-assigned samples, light purple and light orange represent respectively GOM-assigned and MED-assigned samples of alternative location or genetic background and dotted purple filling represent Gulf of Mexico or Gulf of Mexico-like samples of genetic background (bottom).

3.3.3. Comparing assignment of feeding aggregate samples using a location informed or a genetic-informed baseline

Individual origin assignment of a total of 2,487 samples captured at different feeding grounds along the Atlantic (2,024 genotyped in Phase6 and Phase 8 + 461 newly genotyped) was performed using the 96 SNP traceability panel developed in Phase 6 and the location-informed baseline generated in Phase 6 or the newly generated genetic-informed baseline (Figure 3.2).

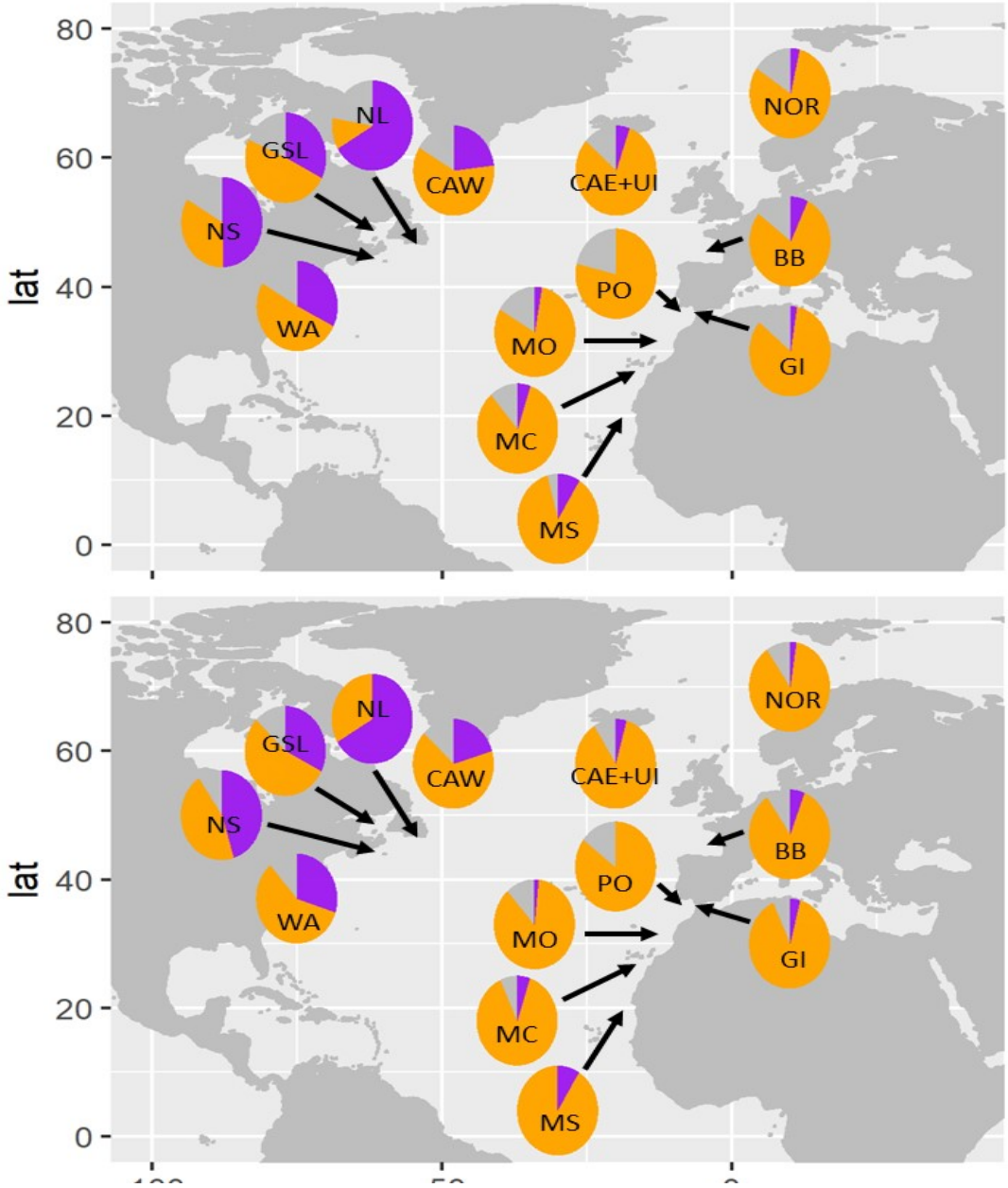

Figure 3.2. Percentage of samples belonging to the Gulf of Mexico and the Mediterranean Sea assessed using the 96 SNP traceability panel and the location-informed baseline developed in Phase 6 (above) or the newly generated genetic-informed baseline (below) at different feeding grounds along the North Atlantic: Norway (NOR), Bay of Biscay (BB), Portugal (PO), Strait of Gibraltar (GI), Morocco (MO), Canarias (MC), Mauritania (MS), Central Atlantic (east of 45°W, CAE), Central Atlantic (west of 45°W, CAW), Newfoundland (NL), Gulf of Saint Lawrence (GSL), Nova Scotia (NS), West Atlantic (WA).

Addition of the newly genotyped samples completing the mixing map along the North Atlantic Ocean confirmed previously observed patterns, revealing strong mixing of eastern and western genetic origin individuals in the west Atlantic. Indeed, the Mediterranean genetic profile was majoritarian at every sampled location except for Nova Scotia (NS) and Newfoundland (NL).

In general, using the genetic-informed baseline, a high proportion of the previously unassigned samples are re-assigned as Mediterranean-like (Figure 3.2 and Table 3.2) suggesting that better resolution to assign Mediterranean-origin samples is obtained. Besides, high proportions of samples previously assigned as Gulf of Mexico are unassigned when using the genetic-informed baseline, suggesting that they could be false Gulf of Mexico positives corrected by improving reference genetic variation ranges for both genetic backgrounds in the baseline. No individual that was previously assigned as Mediterranean was assigned as Gulf of Mexico-like and vice versa.

Table 3.2. Summary of number of samples from feeding aggregates genotyped during Phase 6, Phase 8 and newly genotyped samples for the 96 SNP traceability panel developed in Phase 6 that are assigned as Mediterranean or Mediterranean-like (MED), as Gulf of Mexico or Gulf of Mexico-like (GOM) or unassigned using the location or genetic-informed baselines. Lower values indicate the number of individuals caught in western (left) and eastern (right) locations.

Genetic → Location ↓	MED	GOM	Unassigned
MED	**1823** (346; 1477)	0 (0;0)	1 (0;1)
GOM	0 (0;0)	**254** **(192;63)**	33 (18;15)
Unassigned	161 (50;111)	4 (1;3)	**211** **(61;150)**

3.3.4. New subsets of SNP for traceability

Two different subsets of SNPs that best discriminated between genetic and location-based groups respectively were selected from the RAD-seq ABFT dataset which contains 463 samples and 19,291 SNPs. Assignment rates of these two SNP subsets calculated using respective individual subsets that were excluded during SNP selection show very low proportions of unassigned samples.

Assignment rates using the genetic-informed and the location-informed baselines were respectively 60 and 87.5% for the Mediterranean Sea samples and in both cases 85% for the Gulf of Mexico samples (Figure 3.3). While assignment rates of Gulf of Mexico samples were kept high, the assignment rates of the Mediterranean samples improved with respect to the previously developed 96 SNP panel. Unexpectedly, better assignment rates were obtained when SNPs were selected considering capture location. These promising preliminary results suggest that the existing SNP panel could be improved by selecting a new subset of SNPs. Testing this potential improvement would require increasing the number of genotyped reference samples of known origin for these subsets of SNPs and assignment rate recalculation.

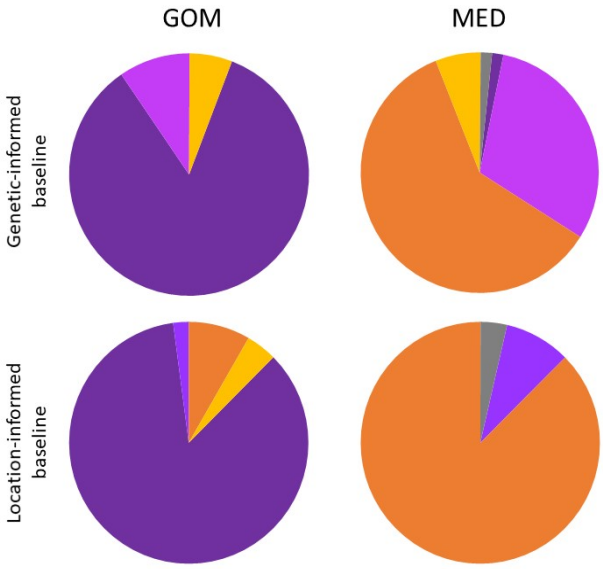

Figure 3.3 Assignment rates of Gulf of Mexico-like or Gulf of Mexico (GOM) and Mediterranean-like and Mediterranean (MED) samples using two different subsets of 96 SNPs selected based on genetic background (top) or on captured location (bottom). Purple and orange represent GOM-assigned and MED-assigned samples, and light purple and light orange represent respectively GOM-assigned and MED-assigned with alternative location (top) or genetic background (bottom).

Interestingly, both SNP subsets selected based on genetic profile or capture location revealed cryptic structuring related with a structural variant (Figure 3.4) further studied when analysing signatures of natural selection in section 1.3.5. Understanding of the potential implications of this genomic region in local adaptability is required to assess their validity for traceability.

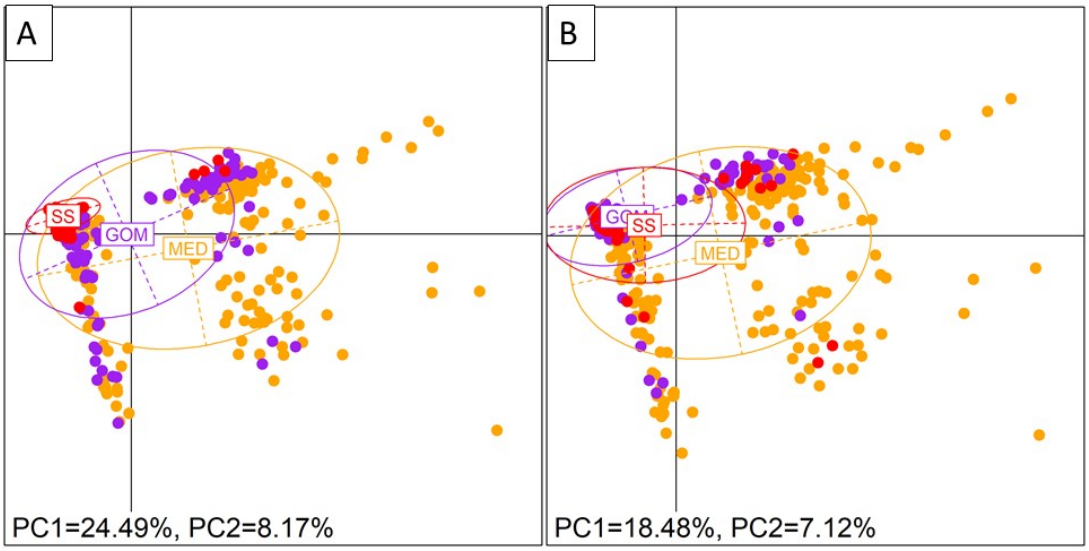

Figure 3.4. Principal Component Analysis (PCA) performed using the selected subsets of 96 SNPs for traceability based on genetic profile of the samples (A) and capture location (B). Dots represent reference samples from the Gulf of Mexico (GOM), the Mediterranean Sea (MED) and the Slope Sea (SS).

3.3.5. Origin and role of the Slope Sea in the ABFT populations connectivity

F3-admixture tests support an admixed composition of the SS from the Mediterranean Sea and the Gulf of Mexico (Figure 3.5A), suggesting that either the Slope Sea originated through admixture of both populations or that Slope Sea originated after split from one of the other two populations but received or receives genetic inflow from the other through secondary contact after divergence. Proportion of individuals at each location that are migrants from other source location estimated by BayesAss v3.04 support strong contemporary migration from the Mediterranean Sea into the Slope Sea and the Gulf of Mexico spawning grounds (Figure 3.5B).

The heterogeneous genetic profile of the Slope Sea, compatible with the three possible F1 parental pair combinations between Mediterranean and Gulf of Mexico individuals, indicates in one hand that strong contemporary genetic in-flow could be occurring in this population preventing genetic variation from stabilization. On the other hand, it hampers identifying the origin of Mediterranean genetic component incorporated into the Gulf of Mexico population or assessing the origin of the Mediterranean-like adult individuals found in the Gulf of Mexico, as Mediterranean genetic background can be found in both the Mediterranean and the Slope Sea populations. Results on electronic tagging revealed how some adult individuals visiting either Gulf of Mexico and Mediterranean spawning grounds can also visit the recently discovered Slope Sea spawning area (Richardson et al.2016), supporting the capability of adult individuals from both populations of spawning in the Slope Sea enabling trans-Atlantic gene-flow through interbreeding in the Slope Sea spawning ground.

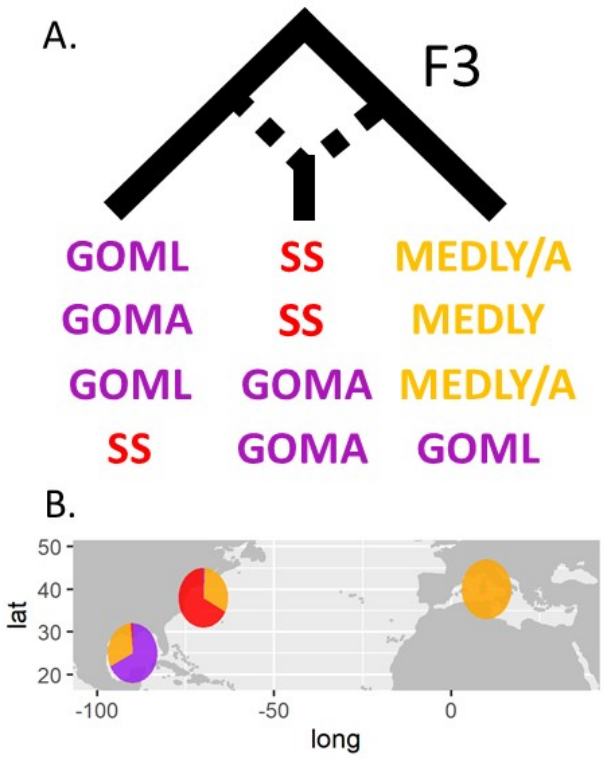

Figure 3.5. Genetic and demographic connectivity between the three ABFT spawning grounds. A. Combination tests for which F3-statistic provided with statistically significant (Z< -1.96) negative values, indicating genetic admixture origin of a target population (central branch) from other two source populations (side branches). B. Per-location recent in-migration rates measured as proportion of individuals at each location that are migrants from the other two source locations (pie-charts) estimated by BayesAss.

3.3.6. Mechanisms for the maintenance of stock structure despite observed mixing at spawning site and season

Some of the results obtained about population structure of ABFT suggest relatively high ongoing inter-population migration. Gene-flow, as the ultimate consequence of migration when it involves incorporation of immigrant alleles into the recipient population, acts diluting genetic differentiation between populations. Indeed, low F_{ST} values between populations, like those found in this study, are common among fish marine species which typically show large population sizes, high rates of dispersal and wide-ranging distributions. Moreover, when these characteristics are met, demographically very low number of migrants could dilute the signal of genetic differentiation (Lowe, Allendorf 2010; Gagnaire et al. 2015). As local adaptation can maintain genetic differentiation despite high gene-flow (Dionne et al. 2008; Tigano, Friesen 2016) we screened for signatures of natural selection in the genome of ABFT that could help understanding the extent of genetic connectivity between populations (Mariani, Bekkevold 2014; Gagnaire et al. 2015). Besides, genomic signature of inter-species genomic introgression event between albacore tuna and ABFT was analyzed, as introgression events could be an important source for rapid adaptive processes.

3.3.6.1. Genomic signatures of natural selection

Outlier loci potentially under selection consistently revealed strong structuring that does not correspond to the three sampled locations (Figure 3.6A, 3.6B). The found cryptic structuring was equivalent between analyses as shown by PCA coordinate correlations (Figures 3.6C, 3.6D), all analyses showing strong grouping along the first PC. In both analyses, the 10% SNPs with the highest loading plots of the first and second PC consistently mapped to the same two (BKCK01000075 and BKCK01000111) and four (BKCK01000076, BKCK01000100, BKCK01000161 and BKCK01000173) reference scaffolds from the Pacific bluefin tuna genome respectively. Among all scaffolds containing outlier SNPs two scaffold pairs were found to be under high linkage-disequilibrium: the first 750Kb region of scaffold BKCK01000075 (where the SNP under selection are located) and scaffold BKCK01000111 (linkage group 1), and scaffolds BKCK01000161 and BKCK01000173 (linkage group 2) (Figures 3.6E,3.6F). Samples within clusters along the PC1, which are those driven by the linkage group 1 identified based on x axis coordinate (Figure 3.6A) exhibited different average heterozygosity values for SNPs derived from the linkage group 1, being individuals from

the central group (group 2 in Figure 3.7) more heterozygous than the other two (Figure 3.7).

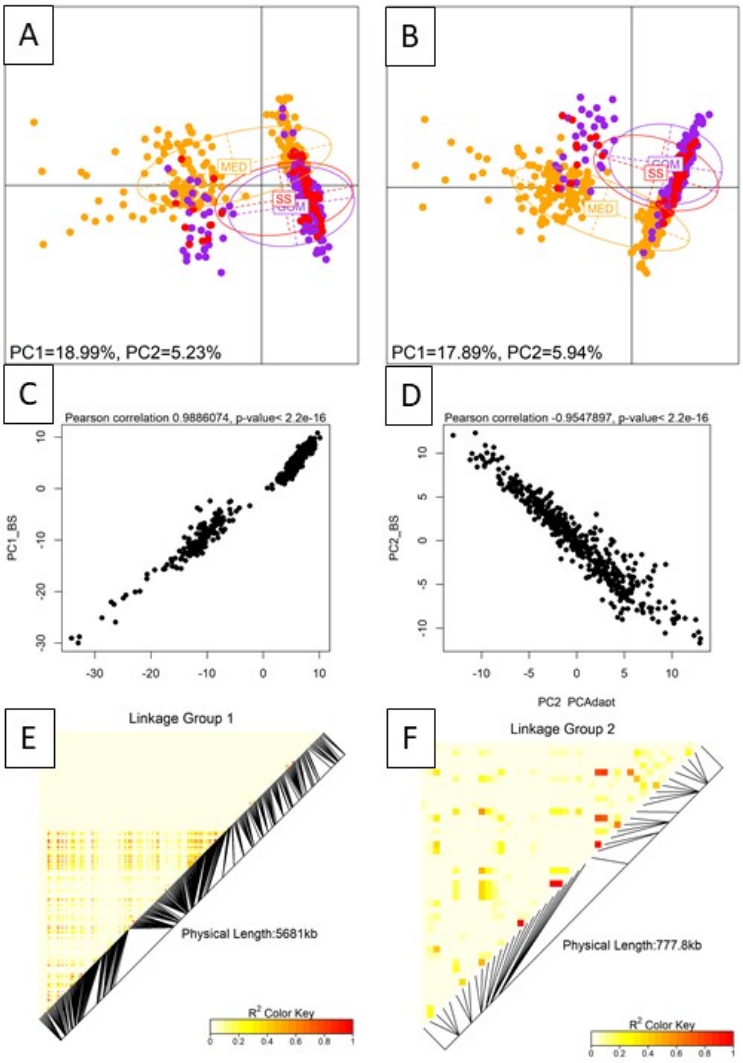

Figure 3.6. PCA performed using outlier SNPs selected by PCAdapt (A) and BayeScan (B). (C) and (D) show coordinate correlation for PC1 and PC2 respectively from PCA's performed using SNPs selected using both methods. (D) and (F) represent pairwise linkage disequilibrium between SNPs from linkage groups 1 and 2 respectively.

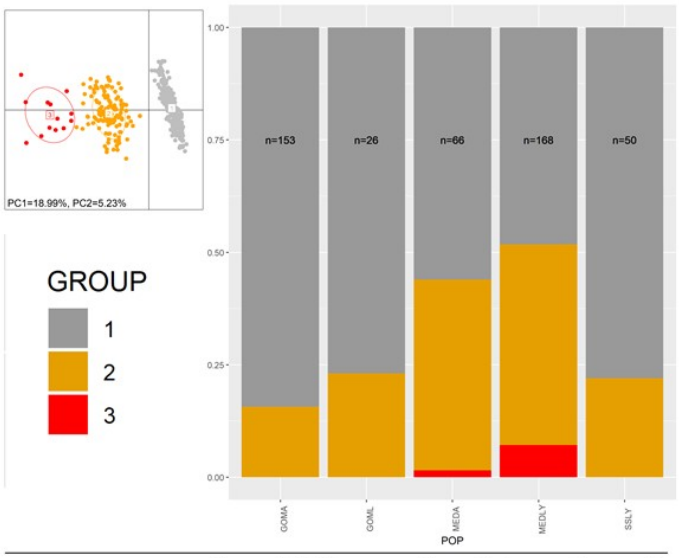

		He - all SNPs		He - Linkage Group 1	
GROUP	n	X	SD.	X	SD.
1	306	0.240	0.015	0.124	0.033
2	144	0.242	0.013	0.512	0.080
3	13	0.238	0.015	0.266	0.059

Figure 3.7. A. Proportion of individuals from each location and age class that belong to the three different clusters differentiated by SNPs derived from linkage group 1 along the first axis of the PCA performed using outlier loci. B. Average and standard deviation of heterozygosity values within each defined ground when using all filtered SNPs or only SNPs from linkage group 1.

The observed clear-cut grouping pattern, the high measures of linkage disequilibrium, and different heterozygosity proportions between groups suggest that that this structuring is the consequence of different versions of a chromosomal inversion located in the linkage group 1 (Barth et al. 2019; Puncher et al. 2019). The approximate size of linkage group 1 is ~2.6Mb, falling within the common range size for chromosomal inversions found in other studies (130Kb to 100 Mb (Wellenreuther, Bernatchez 2018)). Instead, we found no evidence suggesting that linkage group 2 could represent a chromosomal inversion. Alternatively, recombination rates can drop within certain chromosomic regions such as near centromeres, causing high linkage-disequilibrium. The proportions of samples within each group segregated by haplotypes of the linkage group 1, presumably carrying different versions of the inversion, differed between locations (Figure 3.7).

PCA performed using only neutral markers still show genetic differentiation and produced a similar pattern to that obtained with the whole dataset (Figure 3.8). While local adaptation contributes maintaining population structuring, this result confirms that the genetic differentiation between the two distinct genetic backgrounds observed in ABFT populations is also the result of stochastic processes, like mutation and genetic drift (Mariani, Bekkevold 2014) implying long-term reproductive isolation of both genetic components.

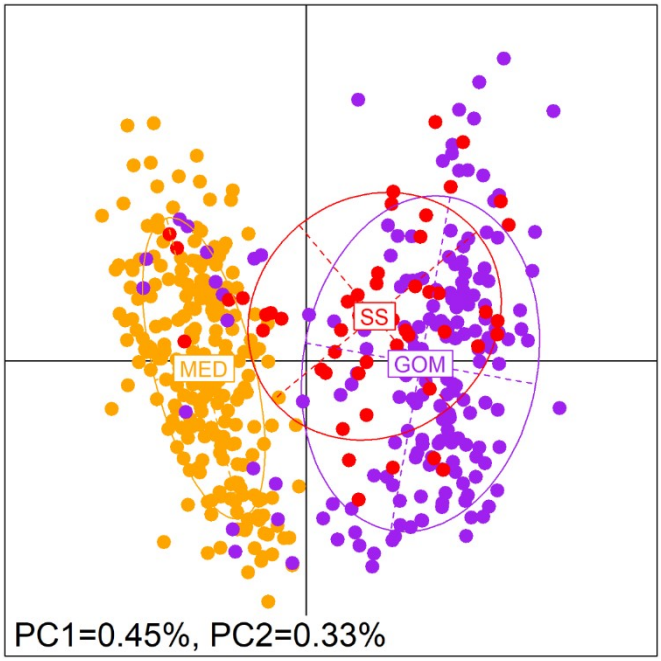

Figure 3.8 PCA performed using only neutral SNPs, excluding all those outlier SNPs detected by either PCAdapt or BayeScan

3.3.6.2. Introgression from albacore

The phylogenetic tree estimated by TreeMix (Figure 3.9A) was coherent with the expected topology (Díaz-Arce et al. 2016). The two most likely estimated gene flow events occurred between albacore and the Mediterranean ABFT L+YoY and adult groups (Figure 3.9A). Accordingly, D statistic values estimated for each group pair combination of ABFT samples using ABBA/BABA tests reveal an excess of albacore alleles shared with the Slope Sea and the Mediterranean, and to a lesser extent with the Gulf of Mexico (Figure 3.9B). These results show for the first time the printing of

nuclear introgression from albacore into ABFT. Considering TreeMix and ABBA/BABA test results together, signature of introgression is stronger in the Mediterranean, lower in the Slope Sea and the least in the Gulf of Mexico. Therefore, most likely, introgression likely occurred in the Mediterranean or Slope Sea ancestral populations. Contemplating the results on genetic connectivity patterns and the complete absence of printing of nuclear introgression in the Gulf of Mexico, introgression most likely occurred in the Mediterranean Sea and introgressed haplotypes were subsequently transmitted to the Slope Sea.

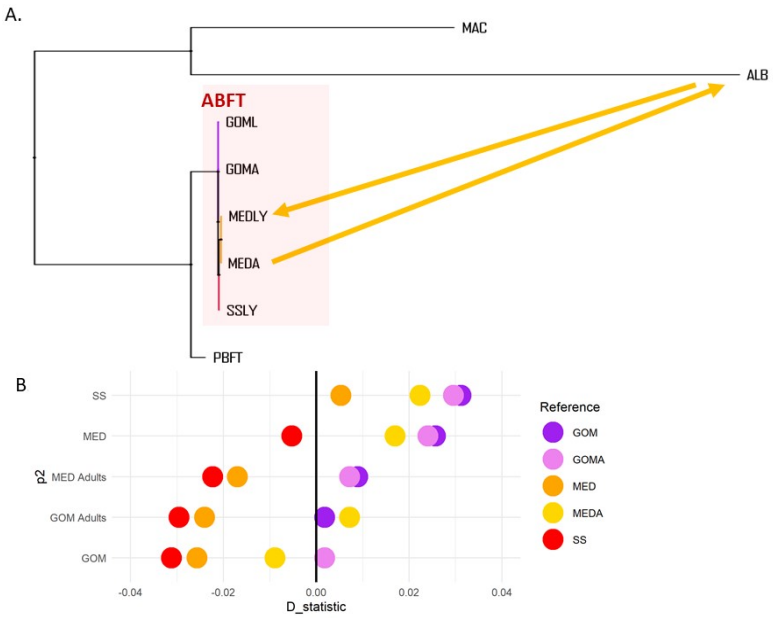

Figure 3.9. Nuclear introgression from albacore into ABFT. A. Phylogenetic tree estimated by TreeMix allowing two migration events (yellow arrow). B. D statistic values estimated from the ABBA/BABA test used to detect introgression from albacore to different target (rows) using different reference (colors) locations (adults in separated groups) of ABFT. Southern bluefin tuna allele frequencies were used to define the ancestral state of each SNP.

The heterogeneous strength of signature of introgression in the different populations in one hand may contribute to differentiation between Mediterranean Sea and Gulf of Mexico genetic components and in the other hand consists in another lead to understand genetic connectivity between ABFT populations.

3.3.6.3. Origin of the linkage groups

PCA performed using 291 SNPs and 83 SNPs extracted from the linkage group 1 and linkage group 2 respectively (Figure 3.10) grouped ABFT samples following the previously observed pattern. When using linkage group 1 SNPs Pacific bluefin tuna samples cluster with the majoritarian ABFT group while albacore samples are grouped near to the minoritarian ABFT group. When using linkage group 2 SNPs albacore individuals are more variable but closer to the MED samples, while Pacific bluefin tuna does not clearly cluster with any ABFT population. Southern bluefin tuna, included in this catalogue as an outgroup appears in general as genetically more distant (Figure 3.10). Likewise, ABBA/BABA test performed using these SNPs provides with much higher D-statistic values indicating introgression from albacore into the Mediterranean and Slope Sea populations in these regions of the genome (Figure 3.10) compared to values obtained when using the whole dataset (Figure 3.9). These results show than the identified linkage groups detected by searching for genomic signatures of natural selection in ABFT populations are related to a past introgression event from albacore tuna. ABBA/BABA test performed removing all SNPs from those scaffolds in which highest 10% loading plots for the first two PC were much lower but still show higher levels of introgression in the SS and MED compared to the GOM (Figure 3.11).

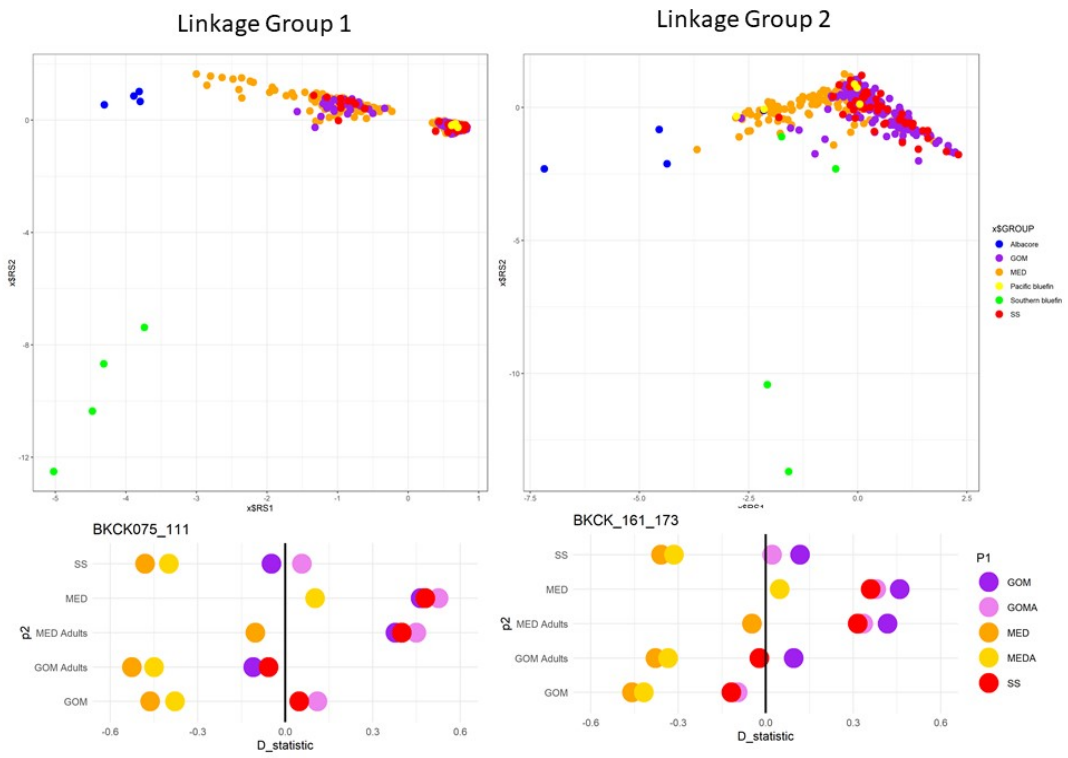

Figure 3.10. Analysis performed using 291 SNPs from linkage group 1 (left) and 83 SNPs from linkage group 2 extracted from the reference mapped catalog dataset which includes other Thunnus species. A. PCA. B. Results of ABBA/BABA test: along the y axis are target groups and colors represent reference groups. The higher the D-statistic, the more introgressed is the target group respect to the reference group. In all the tests Southern bluefin tuna and albacore tuna were used as outgroup and donor respectively.

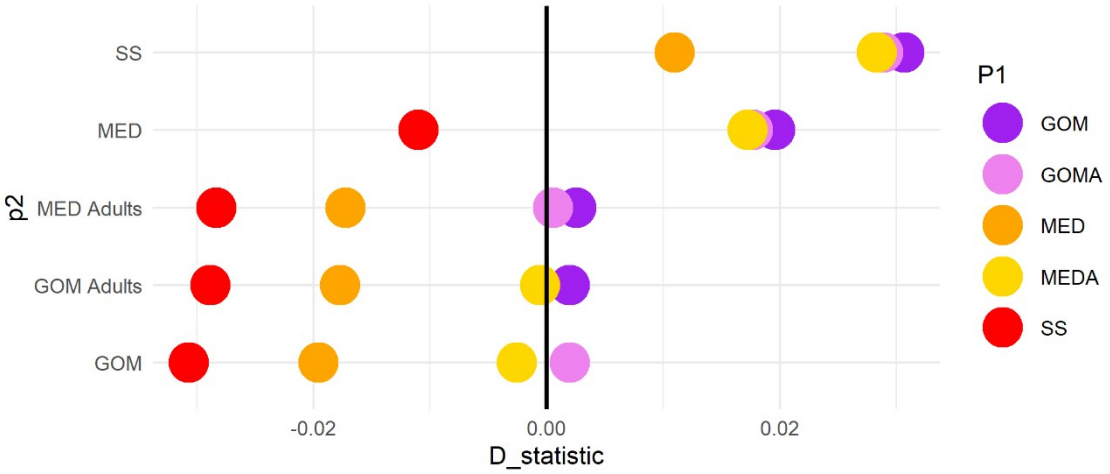

Figure 3.11. ABBA/BABA test performed using all filtered SNPs extracted from the reference mapped catalog dataset which includes other T. species after excluding those located in scaffolds in which highest loading plot SNPs were found. Along the y axis are target groups and colors represent reference groups. The higher the D-statistic, the more introgressed is the target group respect to the reference group. In all the tests Southern bluefin tuna and albacore tuna were used as outgroup and donor respectively.

3.4. Conclusions

- Current knowledge of population structure of ABFT suggest a more complex connectivity scenario than two reproductively isolated populations (Gulf of Mexico and Mediterranean Sea) that mix for feeding in the Atlantic since:
    - individuals with Mediterranean genetic background are observed in the Gulf of Mexico, but not the other way around, and
    - the Slope Sea is composed of individuals of Mediterranean, Gulf of Mexico and intermediate genetic background, supporting the idea that this region is a mixed spawning ground.

- Despite demonstrated gene flow from the Mediterranean to the Gulf of Mexico, genetic differentiation is maintained between the two sides of the Atlantic. This can be due to:
    - prevalence of a signature of local adaptation acquired from an introgression event from albacore tuna in the Mediterranean ABFT, or
    - long-term isolation of both populations followed by a recently increased migration rate towards the West.

- Previous SNP traceability tool resulted in a proportion (10% of Gulf of Mexico and 2% of Mediterranean) of miss-assigned individuals. This could be due to:
    - an inherent error in the method (due to a small discriminative power of the SNPs selected or to a baseline not reflecting the complete range of genetic variation), or
    - presence of Mediterranean-like individuals in the Gulf of Mexico, or
    - confounding factors due to the existence of a third genetic component.

- New strategies to improve the SNP-based traceability tool have included using genetic instead of location-informed baselines, and selection of a new subset of SNPs based on a larger reference dataset considering genetic or location-informed assignment of samples. We found that:
    - genetic-informed baselines improve assignment rates of Gulf of Mexico and Mediterranean samples especially by decreasing the number of unassigned individuals, and
    - new subset of SNPs using location information to assign samples to origin result in a slightly improved assignment compared to the previous assignment panel.

- Assignment of feeding aggregates to genetic or location of origin are similar, although there are differences, and confirm previous findings:
    - genetic based assignments result in less unassigned samples, which are mostly assigned as Mediterranean
    - western locations have a higher degree of mixing

3.5. Future work and management implications

Future work should concentrate on:

- understanding the role of local adaptation and connectivity of ABFT in relation to stressors such as climate change or fishing pressures, as it is likely that the introgression from albacore and/or the expansion towards a new spawning ground are responses to impacts; this can be due by performing additional analyses on the existing datasets, but particularly by analysing temporal replicates and if possible, including old samples
- understanding the genetic background (and presence of signatures of selection) in the feeding aggregates to determine correlation between long range migrations and presence of a given genetic marker
- understanding changes in absolute and effective population sizes of each of the stocks in order to anticipate future resilience and adaptive potential of the species
- improving the traceability panel with alternative strategies (e.g. generating genetic baselines based exclusively on larvae, develop ways to identify and integrate a third "intermediate" genetic background into the baselines, etc…).

The work presented here has management and conservation implications:

- the current mixed stock model does not acknowledge that individuals from both stocks can interbreed and the consequences of doing so should be evaluated
- it is not clear what is the contribution of the individuals born in the Slope Sea to each of the two main stocks as there is no way to differentiate them genetically
- the current SNP traceability tool, despite being based in oversimplified assumptions, performs adequately, although the alternative based on a genetic-informed baseline reduces the number of unassigned individuals
- we thus recommend the use of the current SNP panel either based on the location informed or genetics informed baselines, which despite potential miss-assigned and unassigned samples, provides a much better estimation of catch composition than using capture location.

References

World Health Organization: Global Strategy for dengue prevention and control, 2012–2020. WHO report 2012 (reference number WHO/HTM/NTD/VEM/2012.5). Geneva, Switzerland. Retrieved from http://www.who.int/denguecontrol/9789241504034/en.

Alexander, DH, J Novembre, K Lange. 2009. Fast model-based estimation of ancestry in unrelated individuals. Genome research.

Barth, JMI, D Villegas-Ríos, C Freitas, et al. 2019. Disentangling structural genomic and behavioural barriers in a sea of connectivity. Molecular Ecology 28:1394-1411.

Block, BA, SLH Teo, A Walli, A Boustany, MJW Stokesbury, CJ Farwell, KC Weng, H Dewar, TD Williams. 2005. Electronic tagging and population structure of Atlantic bluefin tuna. Nature 434:1121-1127.

Díaz-Arce, N, H Arrizabalaga, H Murua, X Irigoien, N Rodríguez-Ezpeleta. 2016. RAD-seq derived genome-wide nuclear markers resolve the phylogeny of tunas. Molecular Phylogenetics and Evolution 102:202-207.

Dionne, M, F Caron, JJ Dodson, L Bernatchez. 2008. Landscape genetics and hierarchical genetic structure in Atlantic salmon: the interaction of gene flow and local adaptation. Molecular Ecology 17:2382-2396.

Durand, EY, N Patterson, D Reich, M Slatkin. 2011. Testing for ancient admixture between closely related populations. Molecular Biology and Evolution 28:2239-2252.

Foll, M, O Gaggiotti. 2008. A genome-scan method to identify selected loci appropriate for both dominant and codominant markers: a Bayesian perspective. Genetics 180:977-993.

Gagnaire, P-A, T Broquet, D Aurelle, F Viard, A Souissi, F Bonhomme, S Arnaud-Haond, N Bierne. 2015. Using neutral, selected, and hitchhiker loci to assess connectivity of marine populations in the genomic era. Evolutionary Applications 8:769-786.

Green, RE, J Krause, AW Briggs, T Maricic, U Stenzel, M Kircher, N Patterson, H Li, W Zhai, MH-Y Fritz. 2010. A draft sequence of the Neandertal genome. science 328:710-722.

Kavakiotis, I, A Triantafyllidis, D Ntelidou, P Alexandri, H-J Megens, RPMA Crooijmans, MAM Groenen, G Tsoumakas, I Vlahavas. 2015. TRES: Identification of Discriminatory and Informative SNPs from Population Genomic Data. Journal of Heredity 106:672-676.

Kulathinal, RJ, LS Stevison, MA Noor. 2009. The genomics of speciation in Drosophila: diversity, divergence, and introgression estimated using low-coverage genome sequencing. PLoS genetics 5:e1000550.

Lischer, HE, L Excoffier. 2012. PGDSpider: an automated data conversion tool for connecting population genetics and genomics programs. Bioinformatics 28:298-299.

Lowe, WH, FW Allendorf. 2010. What can genetics tell us about population connectivity? Molecular Ecology 19:3038-3051.

Luu, K, E Bazin, MGB Blum. 2017. pcadapt: an R package to perform genome scans for selection based on principal component analysis. Molecular Ecology Resources 17:67-77.

Mariani, S, D Bekkevold. 2014. Chapter Fourteen - The Nuclear Genome: Neutral and Adaptive Markers in Fisheries Science. In: SX Cadrin, LA Kerr, S Mariani, editors. Stock Identification Methods (Second Edition). San Diego: Academic Press. p. 297-327.

Piry, S, A Alapetite, J-M Cornuet, D Paetkau, L Baudouin, A Estoup. 2004. GENECLASS2: A Software for Genetic Assignment and First-Generation Migrant Detection. Journal of Heredity 95:536-539.

Puncher, GN, S Rowe, GA Rose, NM Leblanc, GJ Parent, Y Wang, SA Pavey. 2019. Chromosomal inversions in the Atlantic cod genome: Implications for management of Canada's Northern cod stock. Fisheries Research 216:29-40.

Purcell, S, B Neale, K Todd-Brown, et al. 2007. PLINK: a tool set for whole-genome association and population-based linkage analyses. American Journal of Human Genetics 81:559-575.

Rodríguez-Ezpeleta, N, N Díaz-Arce, JF Walter III, et al. 2019. Determining natal origin for improved management of Atlantic bluefin tuna. Frontiers in Ecology and the Environment 17:439-444.

Tigano, A, VL Friesen. 2016. Genomics of local adaptation with gene flow. Molecular Ecology 25:2144-2164.

Wellenreuther, M, L Bernatchez. 2018. Eco-Evolutionary Genomics of Chromosomal Inversions. Trends in Ecology & Evolution 33:427-440.

Wilson, GA, B Rannala. 2003. Bayesian Inference of Recent Migration Rates Using Multilocus Genotypes. Genetics 163:1177-1191.

4. OTOLITH MICROCHEMISTRY

Task Leader: Igaratza Fraile (AZTI), Deirdre Brophy (GMIT) & Jay Rooker (TAMU)

Participants:

AZTI: Haritz Arrizabalaga

GMIT: Elizabeth Tray, Roxanne Duncan

NordSIM: Martin Whitehouse, Heejin Jeon, Kerstin Linden

4.1. Determining nursery origin of bluefin tuna captured in the potential mixing zones

4.1.1. Introduction

The results from previous phases suggested that western origin contributions were negligible in the Mediterranean Sea, Bay of Biscay and Strait of Gibraltar, but mixing rates could be considerable, in some years, in the central North Atlantic, Canary Islands and western coast of Morocco. To further assess the spatial and temporal variability of mixing proportions, 129 otoliths collected in the central North Atlantic in 2016 were analyzed for stable carbon and oxygen isotopes ($\delta^{13}C$ and $\delta^{18}O$).

4.1.2. Material and Methods

In this section, we investigate the origin of bluefin tuna collected in the central North Atlantic Ocean (east and west of 45ºW), using stable $\delta^{13}C$ and $\delta^{18}O$ isotopes in otoliths. Samples utilized for this study (N=129) were collected from September to November 2016 by Japanese longliners operating in the central North Atlantic Ocean (Figure 4.1).

Otolith handling followed the protocols previously described in Rooker et al. (2008). Briefly, following extraction by GBYP participants, sagittal otoliths of bluefin tuna were cleaned of excess tissue with nitric acid (1%) and deionized water. One sagittal otolith from each bluefin tuna specimen was embedded in Struers epoxy resin (EpoFix) and sectioned using a low speed ISOMET saw to obtain 1.5 mm transverse sections that included the core. Following attachment to a sample plate, the portion of the otolith

core corresponding to approximately the yearling periods of bluefin tuna was milled from the otolith section using a New Wave Research MicroMill system. A two-vector drill path based upon otolith measurements of several yearling bluefin tuna was created and used as the standard template to isolate core material following Rooker et al. (2008). The pre-programmed drill path was made using a 500 µm diameter drill bit and 15 passes each at a depth of 50 µm was used to obtain core material from the otolith. Powdered core material was transferred to silver capsules and later analyzed for $\delta^{13}C$ and $\delta^{18}O$ on an automated carbonate preparation device (KIEL-III) coupled to a gas-ratio mass spectrometer (Finnigan MAT 252). Stable $\delta^{13}C$ and $\delta^{18}O$ isotopes are reported relative to the PeeDee belemnite (PDB) scale after comparison to an in-house laboratory standard calibrated to PDB.

Figure 4.1: Sample distribution. Otoliths were collected by Japanese longliners in 2016 in two regions of the central North Atlantic.

Stable isotope signals of mixed stocks were compared with yearling samples from Mediterranean and Gulf of Mexico nurseries revised in GBYP-Phase 3 and presented in

Rooker et al. (2014). HISEA software (Millar 1990) was used to generate direct maximum likelihood estimates (MLE) of mixed-stock proportions in each of the mixing zones. HISEA computes the likelihood of fish coming from a nursery area with characterized isotopic signature. MLE estimator is defined as the composition that maximizes the likelihood of the entire mixed fishery sample (Millar 1990). Uncertainty in estimation is addressed by re-sampling the baseline data 500 times with replacement and bootstrapping the mix data (n=1000).

4.1.3. Results and Discussion

$\delta^{13}C$ and $\delta^{18}O$ were measured in the otolith cores of bluefin tuna from the central North Atlantic and compared to baseline populations from the Mediterranean Sea and Gulf of Mexico (Figure 4.2).

Otolith $\delta^{18}O$ values corresponded well with those measured in yearling otoliths from the eastern and western nurseries, whereas $\delta^{13}C$ values measured in adult bluefin tuna otoliths from the central North Atlantic were, in general, slightly enriched compared to baseline samples. The enrichment of $\delta^{13}C$ has been previously reported in previous phases of the project, and we think the reason for such enrichment lies in the metabolism of the fish. The carbon forming the otolith aragonite is derived from a mixture of carbon from dissolved inorganic carbon in the surrounding seawater and carbon released from respiration of the diet. The relative proportion of respired carbon compared to DIC carbon in the blood (and therefore in the endolymph surrounding the otolith) is in turn proportional to metabolic rate. Since $\delta^{13}C$ values of these two carbon sources are very different, fluctuations in fish metabolic rate influence the otolith $\delta^{13}C$ value, with higher metabolic rates producing more depleted otolith $\delta^{13}C$ values.

Mixed-stock analyses using MLE procedure indicated that catches in 2016 were comprised largely of the Mediterranean population both east and west of the 45ºW management boundary (Table 4.1). Mixing rate estimates in the western North Atlantic using this methodology varied considerably in preceding years, with catches in 2011 dominated by the Mediterranean population, and in 2012 and 2013 dominated by the Gulf of Mexico population (Figure 4.3). From 2014 to 2016, catches have been largely dominated by the Mediterranean population. East of 45ºW, catches were usually dominated by the Mediterranean population, although in 2013 a substantial contribution of western migrants was found. The last results from 2016 confirm that

mixing of the two populations occurs at variable rate, but Mediterranean bluefin tuna may be the principal contributors to the Japanese fishery operating in the central North Atlantic.

Management of Atlantic bluefin tuna has traditionally been based on separate stock assessments east and west of the 45°W stock boundary, assuming that the effects of mixing are negligible. However, otolith chemistry results west of 45ºW suggest that the area west of 45°W stock boundary in the central North Atlantic may also be sustained by the eastern stock. Therefore, it is crucial for stock evaluation to characterize stock composition and the degree to which each area is influenced by the mixing of the two stocks, since it has large implications for the sustainable management of the species.

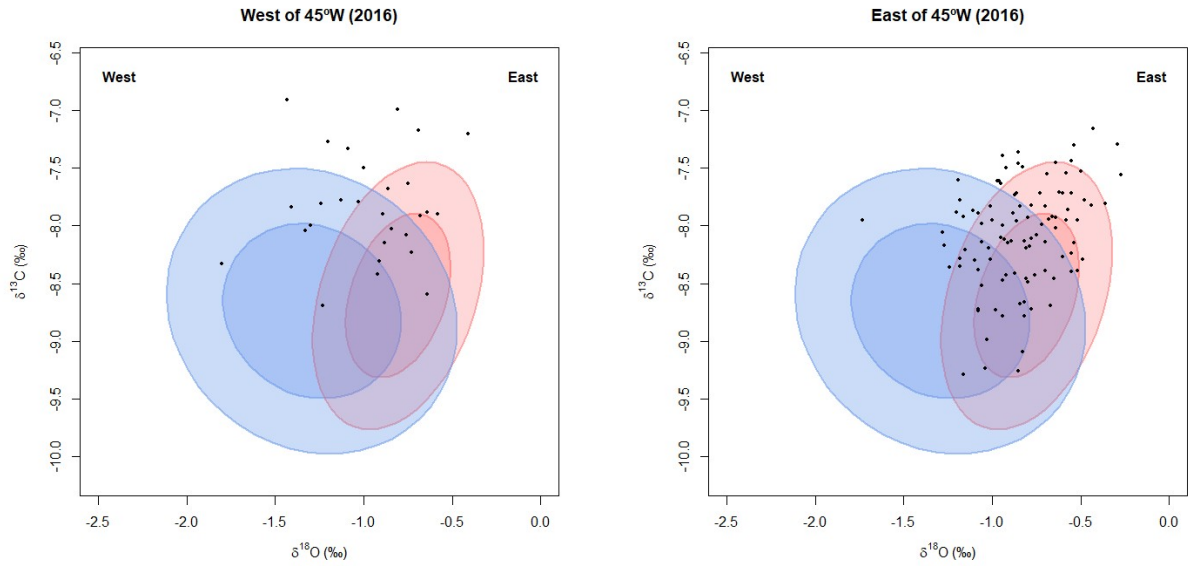

Figure 4.2: Confidence ellipses (1 and 2 SD or ca. 68% and 95% of sample) for otolith δ13C and δ18O values of yearling bluefin tuna from the east (red) and west (blue) nurseries along with the isotopic values (black) for otolith cores of bluefin tuna collected by the Japanese fleet in 2016 east (N=101) and west (N=28) of the 45ºW boundary.

Figure 4.3: Interannual variation of the mixing proportions east and west of the 45ºW boundary estimated by Maximum Likelihood Estimator (HISEA program).

Table 4.1: Maximum-likelihood estimates of the origin of bluefin tuna from the central North Atlantic (east and west of the 45ºW boundary) analyzed under the current contract. Estimates are given as percentages. The mixed-stock analysis (HISEA program) was run under bootstrap mode with 1000 runs to obtain standard deviations around estimated percentages (± %).

	Mixing proportions west of 45ºW					**Mixing proportions east of 45ºW**			
Year	**West**	**East**	**SD**	N		**West**	**East**	**SD**	**N**
2016	21%	79%	2%	28		9%	99%	5%	101

4.2. Individual origin assignment

4.2.1. Introduction

Samples analyzed in Task 1 were also assigned to origin individually, with associated levels of probability. The identification of individual origin is needed for at least two main reasons: the construction of stock-age-length-keys, and the comparison/improvement of individual assignments based on different types of markers (i.e. genetic, otolith shape and stable isotopes). Moreover, it allows to table the results according to any stratification that might be used during the stock assessment or MSE process.

4.2.2. Material and Methods

During the current project, 129 individual bluefin from the central North Atlantic (west of 45ºW, N=28; east of 45ºW, N=101) were assigned to their natal origin (Gulf of Mexico or Mediterranean Sea).

$\delta^{13}C$ and $\delta^{18}O$ values of bluefin tuna otoliths were statistically analyzed and individuals were assigned to source populations with associated levels of probability. Among the classification methods tested with the baseline dataset, it has been shown that Quadratic Discriminant Function Analysis (QDFA) performs the best attaining the highest classification accuracy (Fraile et al. 2015). Thus, QDFA was used to provide posterior probabilities for each pair of $\delta^{13}C$ and $\delta^{18}O$ values.

4.2.3. Results and Discussion

Individual origin assignments based on QDFA suggest that population mixing occurs in all studied regions at variable rates (Table 4.2). Individual origin assignment was performed using the yearling baseline revised in GBYP-Phase 3 and the adult baseline samples of spawner groups presented in GBYP-Phase 8. Overall, mixing proportions using QDFA using either yearling or adult baseline yield higher western contributions than MLE. However, considering the confidence intervals around those averages (i.e. mean±2*s.d), the results are generally concordant.

From the 129 individuals analyzed for otolith stable isotopic composition, 55 were genetically identified during Phase 8. Otolith chemistry and genetic analyses

corresponded well in identifying the origin of bluefin tuna from the Mediterranean Sea. 37 individuals were identified as Mediterranean origin using otolith chemistry, and only 1 of them was genetically assigned to be of western origin. Instead, 12 fish were identified of western origin based on otolith chemistry, and only 5 of them were confirmed with genetics. Six individuals were unclassified with otolith chemistry, which were mostly of Mediterranean origin based on genetics. This analysis supports previous conclusions that using individual origin assignment with otolith chemistry may overestimate mixing proportions in the central North Atlantic.

Table 4.2: Proportions of eastern and western contributions in the central North Atlantic (east and west of the 45ºW boundary) based on individual origin assignment approach. Results based on yearling and spawning adult reference samples were compared. Quadratic Discriminant Function Analysis was used to estimate individual origin.

	Mixing proportions west of 45ºW				**Mixing proportions east of 45ºW**			
Year	**West**	**East**	N		**West**	**East**	**N**	**BASELINE**
2016	43%	57%	28		18%	82%	101	Yearling
2016	36%	64%	28		20%	80%	101	Adult

4.3. Discrimination of nursery areas within the Mediterranean Sea by trace element and stable isotope composition in young-of-the-year bluefin tuna

4.3.1. Introduction

The results from previous phases suggested that trace element composition might allow discriminating the Atlantic bluefin tuna from different spawning areas of the Mediterranean Sea. In 2011 and 2013, signatures of YOY from the eastern Mediterranean were distinct to those captured in the central and western basins. Moreover, in 2013, distinction between the Balearic Sea, Ionian Sea and Tyrrhenian Sea was possible. However, juvenile bluefin tuna from the Bay of Biscay did not match any of the signatures from the main nursery areas. In order to broaden our understanding of the relation between otolith elemental chemistry and bluefin tuna ecology the work on otolith chemistry within the Mediterranean Sea was expanded. On one hand, the collection of reference samples was enlarged to ensure that nursery regions are well represented by the reference otoliths. On the other hand, additional juvenile bluefin tuna from the Bay of Biscay, Strait of Gibraltar, Sardinia and Sicily were analyzed and compared to reference otolith's signatures.

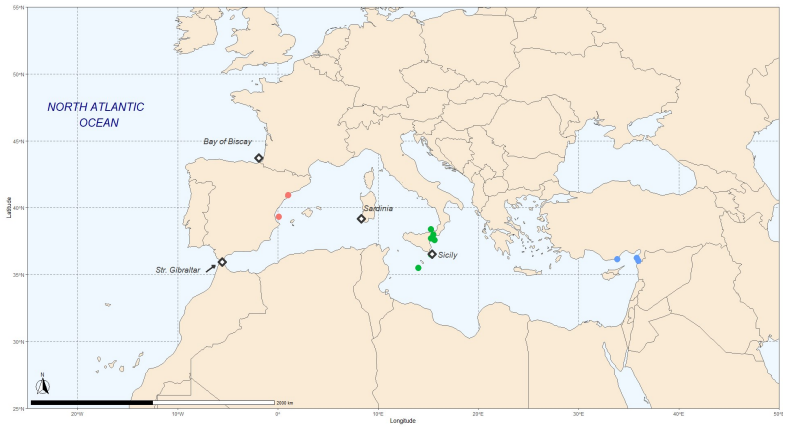

Figure 4.4: Sampling locations of young-of-the-year (age-0) and juvenile (age 1+) bluefin tuna (Thunnus thynnus) in the three main nursery areas of the Mediterranean Sea and adjacent waters. Age-0 individuals were captured in the western (red), central (green) and eastern (blue) Mediterranean Sea, whereas juveniles of the same cohorts (diamonds) were captured in the Bay of Biscay, Strait of Gibraltar, Sardinia and Sicily.

4.3.2. Material and Methods

Young-of-the-year (YOY) bluefin tuna used in this study were collected in 2011 and 2013 in the different spawning grounds within the Mediterranean Sea (Figure 4.4). Strait fork length (SFL) of every individual was measured to the nearest cm. YOY bluefin tuna from the different nurseries captured over a wide temporal range were selected to ensure a good representation of the nursery area. Juvenile bluefin tuna were captured in the Bay of Biscay, Strait of Gibraltar and waters around Sardinia and Sicily. Age of the juvenile tuna was calculated by otolith direct age estimates or age-length key (Cort 1991). The year of birth (cohort) was back-calculated using age and capture date (summary data on Table 4.3).

Sagittae otoliths were extracted from each YOY and juvenile fish using fine-tipped forceps, cleaned of excess tissue with nitric acid (1%) and deionized water and placed in plastic vials until further processing. Trace element and stable isotopic measurements were performed on the same otolith.

For microchemistry analyses, whole otoliths were embedded in a mix of Araldite epoxy GY502 and hardener HY956 in a 5:1 weight ratio. After a block was removed from the mold, otolith cores from each bluefin tuna specimen were identified and marked under a light microscope. Then, otolith blocks were sanded until the core was exposed (Figure 4.5A) and polished using sandpaper of multiple grits. After polishing, otoliths were triple rinsed Milli-Q water and dried under a laminar air flow prior to the laser ablation-ICP-MS analysis.

Table 4.3: Otoliths used for nursery discrimination and origin estimates within the Mediterranean Sea. Western, central and eastern Mediterranean otoliths were used as reference samples, whereas shaded cells correspond to juvenile-adolescent bluefin tuna used for origin estimation

Area	Capture Dates	Cohort	Size range (SFL)
Western Med.	11-28 September 2011	2011	24-36 cm
	15 September – 7 November 2013	2013	27-46 cm
Central Med.	23-24 October 2011	2011	35-41 cm
	10 September – 23 October 2013	2013	17-43 cm
Eastern Med.	10-20 August 2011	2011	27-35 cm
	27 July – 16 September 2013	2013	18-43 cm
Bay of Biscay	12 July 2012-28 August 2013	2011	58-97 cm
Strait of Gibraltar	11 September 2017-10 January 2018	2013	120-142 cm
Sardinia	May 2015- 18 June 2017	2013	101-140 cm
Sicily	27 October 2017 – 20 November 2018	2013	124-147 cm

Otolith samples were analyzed with an IR 1030 nm femtosecond laser (Alfamet-Novalase, France) in conjunction with an Elan DRC II (Perkin Elmer) located at the Institut des Sciences Analytiques et de Physico-Chimie pour l'Environnement et les Matériaux (IPREM), Pau, France. A rectangle of 250 µm x 200 µm was ablated in the first inflexion point of the otolith and results over a whole ablated surface were analyzed for trace element concentration to get the signature of the post-larval live stage (Figure 4.5B). This allows avoiding possible perturbations resulting from the contamination introduced by the Crystalbond throughout micro-cracks often occurring around the core, as well as incorporation of elements due to maternal transfer. A pre-ablation step was implemented to minimize potential surface contamination (rectangle of 300 µm x 250 µm). We analyzed two glass reference materials (NIST 612 and NIST 610; National Institute of Standards and Technology, USA) and aragonite reference material, FEBS-1 (National Research Council, Canada) as an internal standard to monitor the instrument drift and maintain analytical precision. Nine isotopes (Li^{7}, Mg^{24}, Ca^{43}, Mn^{55}, Fe^{56}, Cu^{63}, Zn^{66}, Sr^{88} and Ba^{138}) were measured in each otolith by the LA-ICP-MS system. All the

reference materials were measured at the beginning, middle and the end of each session for calibration and drift correction. Ca^{43} was used as an internal standard for each ablation to check for variation in ablation yield. The concentration of otolith Ca^{43} was assumed to be constant at 388.000 µg Ca g-1 otolith. The data processing proceeds by identifying the background and signal windows for each measurement. Each measurement is defined here as the acquisition of data from one complete rectangle. The background signal is defined as the period during which only the carrier gas composition is measured, prior to the laser firing. The background signal was used to calculate the limit of detection (LOD) which was calculated as the mean background level plus 3 times standard deviation respectively. Concentrations below LOD were not included in the statistical analysis.

Once trace element analyses were completed, stable isotope analyses were performed on the same otolith following a similar procedure described in Task 1. Embedded otolith blocks were first attached to a microscope slide and then to a sample plate using thermostatic glue (Crystalbond). The portion of the otolith core corresponding to approximately the first two to three month of live of bluefin tuna was milled from the otolith section using a New Wave Research MicroMill system. A two-vector drill path based upon otolith measurements of several yearling bluefin tuna was created and used as the standard template to isolate core material. The pre-programmed drill path was made using a 300 µm diameter drill bit and 10 passes each at a depth of 50 µm was used to obtain core material from the otolith. Powdered core material was transferred to plastic vials and later analyzed for $\delta^{13}C$ and $\delta^{18}O$ on an automated carbonate preparation device (KIEL-III) coupled to a gas-ratio mass spectrometer (Finnigan MAT 252). Stable $\delta^{13}C$ and $\delta^{18}O$ isotopes are reported relative to the PeeDee belemnite (PDB) scale after comparison to an in-house laboratory standard calibrated to PDB.

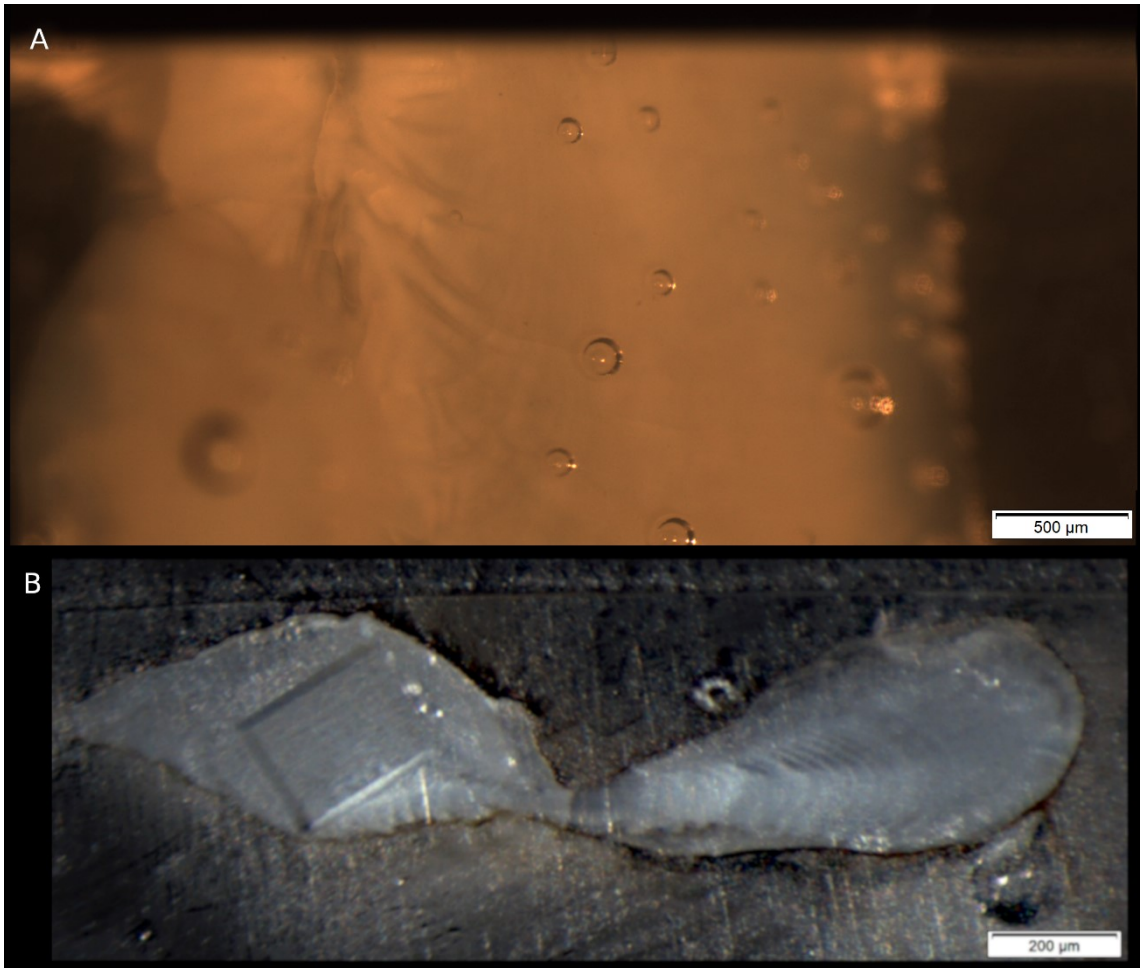

Figure 4.5: A) Example of an otolith of a juvenile bluefin tuna polished until the core is exposed. B) Example of an otolith section of YOY bluefin tuna from the western Mediterranean Sea captured in 2013 showing the pre-ablation and ablation squares analyzed by LA-ICPMS. The integrated trace element concentration of the ablation period corresponds to the post-larvae period (approximately 18-50 days after hatching) based on direct daily ageing.

Statistical analyses were performed in R. Normality and homogeneity of variance (homoscedasticity) were examined by fitting trace element data to a linear model using sampling area as an explanatory variable. The normal Q-Q plots were used to examine whether the residuals were normally distributed, and Scale-Location plots were used to check homoscedasticity. When necessary, data were transformed using Tukey's Ladder of Powers transformation to ensure normality. Homoscedasticity among groups was verified using a Fligner test. To detect basin-scale differences in the elemental fingerprint we performed a one-way analysis of variance (ANOVA) or a Welch's ANOVA

(for heteroscedasticity) to determine which elements contributed to separation among areas.

Multivariate statistics were used to determine which areas differed significantly in their multi-elemental signature. Pairwise-PERMANOVA test was used for comparisons, using Euclidean distance as resemblance measure and Benjamini–Hochberg p-value correction. A Principal Component Analysis was applied to otolith trace elemental concentrations to illustrate the affinity of the elements and to determine which elements account for most of the variability in the data.

At the time of writing this report stable isotopic analyses were not completed due to the impact of disruptions caused by COVID-19 on the project team and collaborating laboratories. Hereunder, preliminary results based on trace element will be presented, but given the relevance of carbon and oxygen stable isotopes in the discrimination of nursery areas within the Mediterranean Sea, caution must be taken interpreting these results.

4.3.3. Results and Discussion

From all the elements analyzed concentrations of Cu and Fe were close to the analytical limit of the equipment and were excluded from the posterior analyses. Moreover, Fe concentrations were found to be very high in the Araldite resin, and therefore high values of Fe together with visual analyses of the otoliths after the ablation were used to discard samples with potential resin contamination.

Multielemental signature of YOY bluefin tuna otoliths was significantly different among the nursery areas in 2011 but not in 2013. In samples captured in 2011 differences were mainly found in the Eastern Mediterranean Sea, around the Levantine Sea (PERMANOVA test p-value < 0.05), but differences between the central and western Mediterranean basins were not statistically significant. Elemental signature difference was driven by Li, Mg, Mn, Sr and Ba concentrations (Figure 4.6). Li concentration in the Eastern Mediterranean Sea were lower than those measured in the central and western areas, whereas Mg, Mn, Sr and Ba concentration were found to be higher in the eastern basin.

In order to visualize the discrimination capacity among the three nursery areas on a two-dimensional axis a PCA was performed using otolith elemental concentration of YOY bluefin tuna from these three regions (Figure 4.7). The first two axis of the PCA explained 59% and 62% of the variation in the data in 2011 and 2013 respectively. In 2011, the eastern Mediterranean reveals a different fingerprint mostly derived from Sr and Ba (dimension-1), but the fingerprint of central and western Mediterranean is basically identical. This confirms our ability to discriminate bluefin tuna from the eastern Mediterranean Sea from the other two sources, but the incapability to discriminate bluefin tuna originated in the western and central Mediterranean Sea. This could be explained if the YOY bluefin tuna at the age of 18-50 days (corresponds to the analyzed otolith portion) have already moved between the western and central Mediterranean Sea. Alternatively, it could also be due to the fact that the physicochemical properties of the seawater in these two nursery areas were not distinct enough to imprint a distinctive signature in the otoliths. The PCA of YOY bluefin tuna from 2013 does not show a clear separation among nursery areas (Figure 4.7). This is in concordance with PERMANOVA test, which demonstrated that differences among nursery areas were not statistically significant. The similarity of elemental concentrations among the three areas hampers our ability to estimate the origin of bluefin tuna from the 2013 cohort.

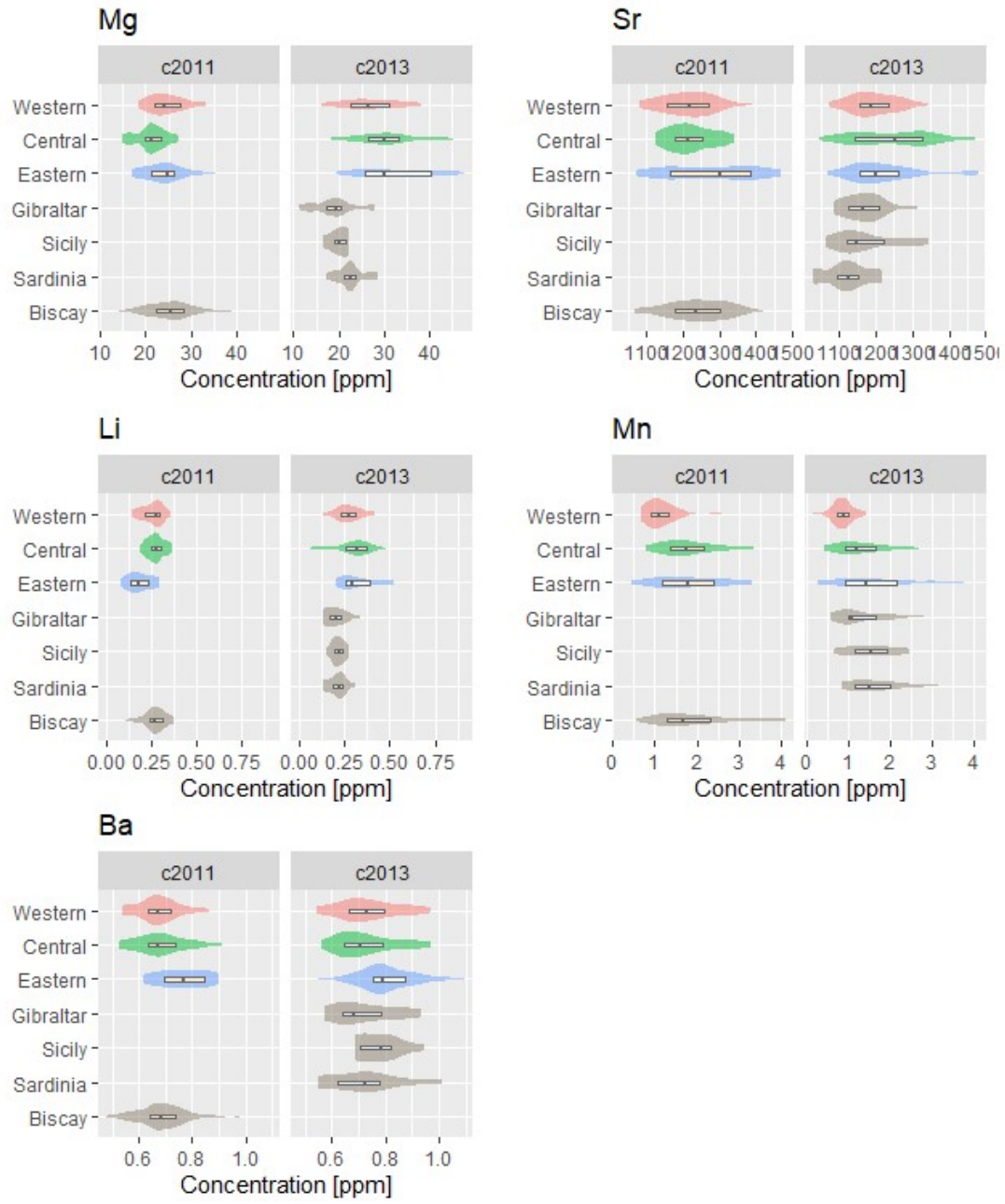

Figure 4.6: Trace element concentration in otoliths of YOY bluefin tuna captured in the western (salmon), central (green) and eastern (blue) Mediterranean Sea in 2011 and 2013. Concentrations of juvenile bluefin tuna captured in several locations of the Mediterranean Sea (around Sicily and Sardinia) and Atlantic Ocean (Strait of Gibraltar and the Bay of Biscay) from 2011 and 2013 cohorts are shown in grey.

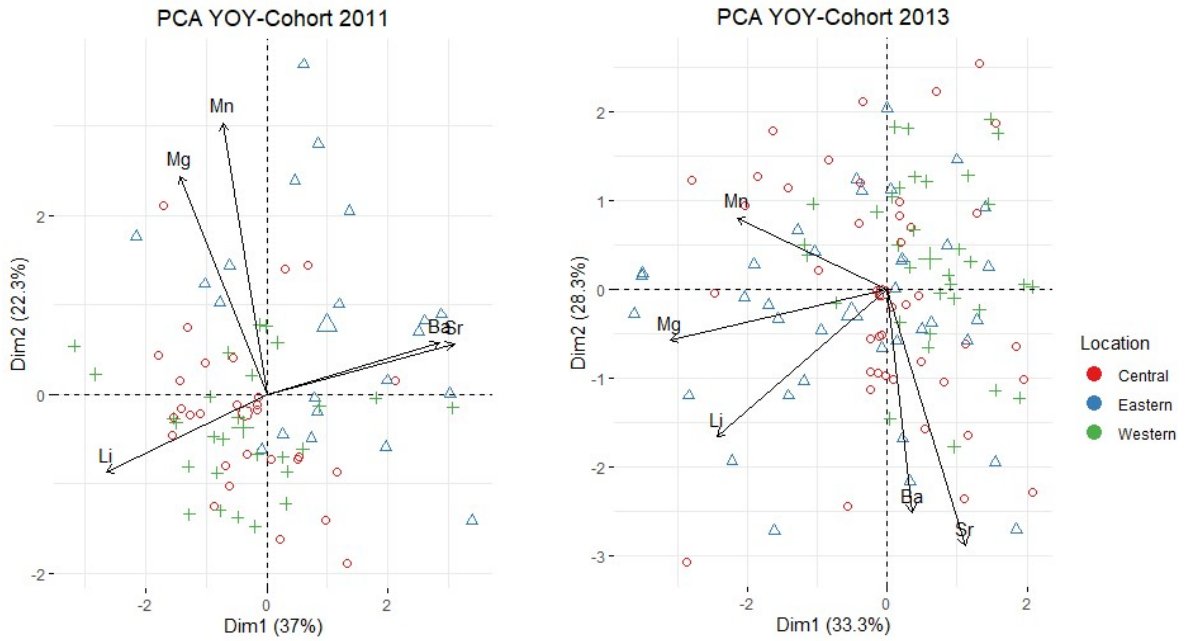

Figure 4.7: Principal Component Analysis of the elemental fingerprints in otoliths of YOY bluefin tuna captured in 2011 (left) and 2013 (right).

On a second step, a PCA was produced including YOY and juvenile-adolescent bluefin tuna from the same cohort. This allowed a visual comparison of fingerprints of the nursery areas with those from feeding areas and/or migratory corridors. In 2011, the variables that contributed the most to the PCA were Mg, Mn and Li in the X-axis and Sr and Ba in the Y-axis (Figure 4.8, lower panels). The discrimination of the eastern Mediterranean nursery area from the other two was driven mainly driven by the y-axis, that is, by Sr and Ba concentrations. Juvenile (age 1+) bluefin tuna captured in the Bay of Biscay in summer 2012 were compared with nursery signatures, but we found no clear association with neither eastern or central-western Mediterranean signatures. The mean PCA coordinates of the Bay of Biscay aggregation were closer to the central-western signature, but the degree of dispersal was higher than that found in the western-central nursery. This could be explained by the fact that the bluefin tuna aggregations in the Bay of Biscay may be composed of tuna from different nursery areas.

In 2013, the variables that contributed the most to the X-axis of the PCA were again Li and Mg, whereas Sr, Mn and Ba were the main contributors of the Y-axis. Differences in composition among the three nursery areas were small, and using trace elements only

separation was not achieved. However, the signature of juvenile and adolescent bluefin tuna inhabiting in the Strait of Gibraltar, Sardinia and Sicily was found to be different from the three nursery areas sampled. One of the explanations could be the existence of nursery areas not included in this analysis.

However, and given the sensitivity of the analyses to the $\delta^{13}C$ and $\delta^{18}O$ not included in the current analysis, these results must be interpreted carefully.

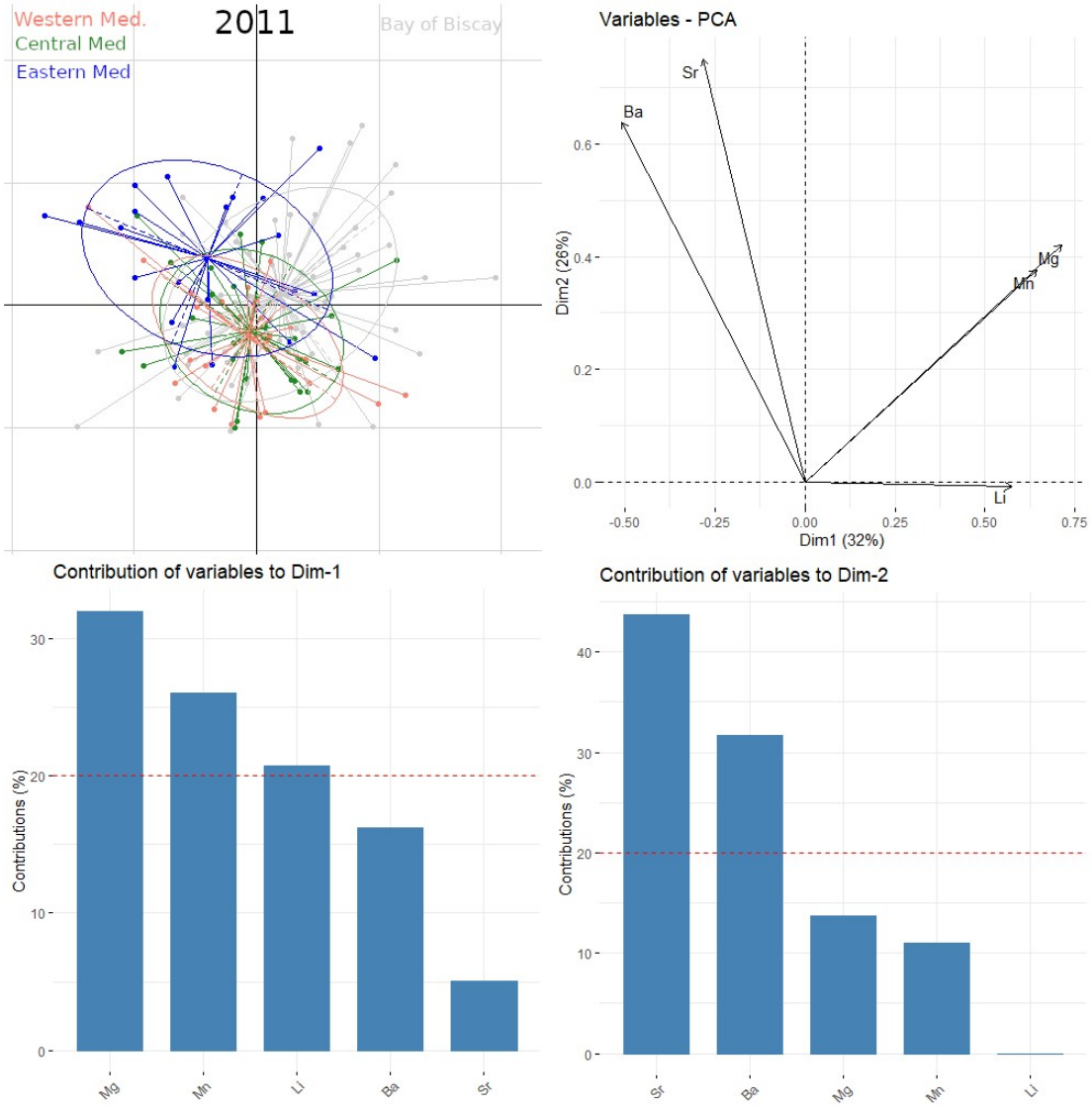

Figure 4.7: Principal Component Analysis of the elemental fingerprints in otoliths of YOY bluefin tuna captured in 2011 and juvenile (age 1+) bluefin tuna from the 2011 cohort captured in the Bay of Biscay (upper panels). Relative contribution of each element to the first two dimensions is shown in the lower panels.

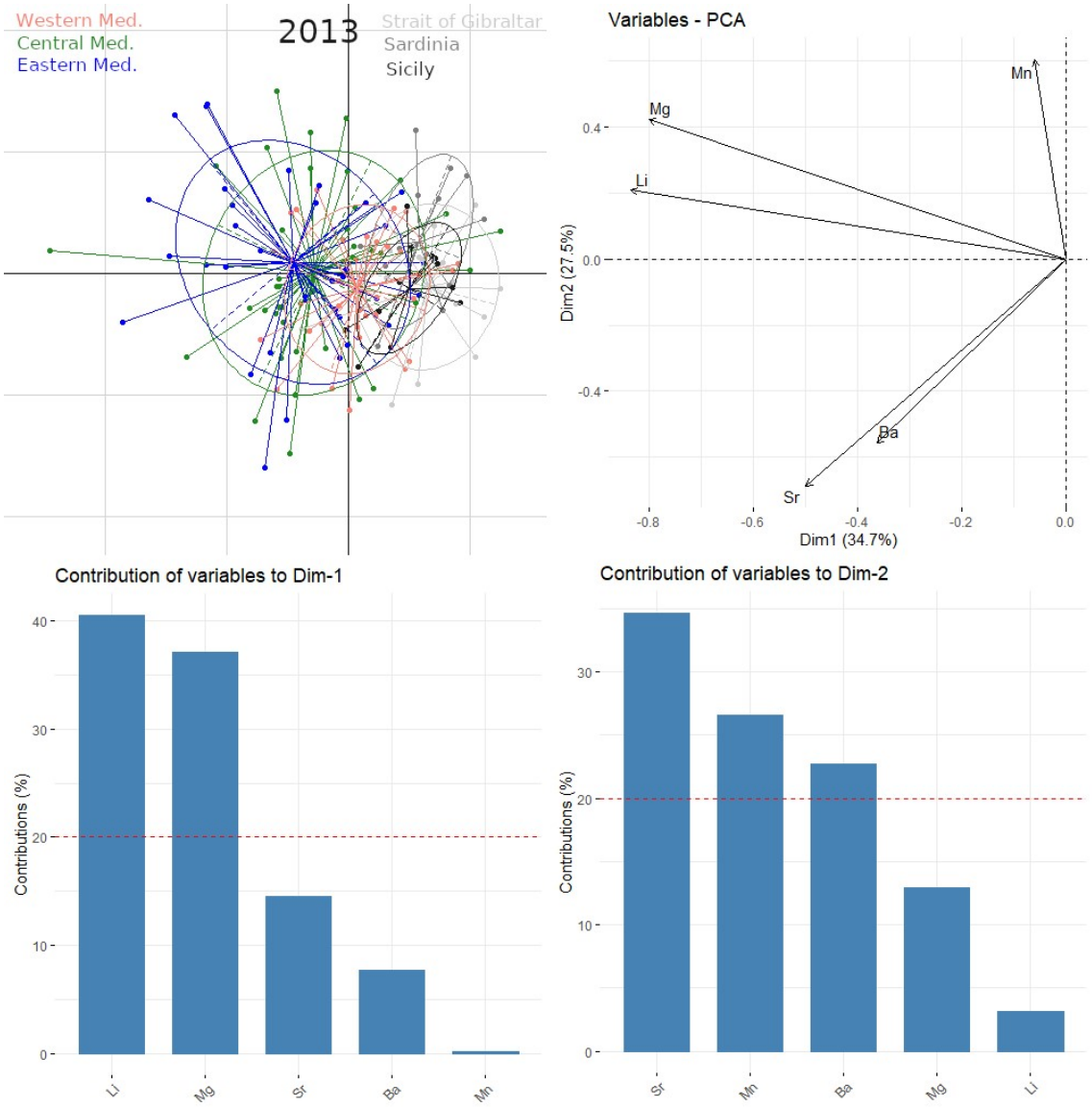

Figure 4.8: Principal Component Analysis of the elemental fingerprints in otoliths of YOY bluefin tuna captured in 2013 and juvenile (age 2 to 5) bluefin tuna from the 2013 cohort captured in the Strait of Gibraltar, waters around Sardinia and Sicily (upper panels). Relative contribution of each element to the first two dimensions is shown in the lower panels.

4.4. Otolith oxygen isotopes measured by high-precision secondary ion mass spectrometry (SIMS) reflect movements between the Mediterranean Sea and the Atlantic Ocean

4.4.1. Introduction

Due to geographical variation in temperature and water chemistry, bluefin tuna from nursery areas in the western and eastern Atlantic can be distinguished based on otolith stable isotopes (Rooker et al. 2008a). Currently, stable isotope signatures in the portion of the otolith representing the first year of life are used to discriminate between the eastern and western stocks, assuming that there is little movement of bluefin away from the main spawning areas in the first year (Rooker et al. 2014). The analytical approach used is isotope ratio mass spectrometry which requires the otolith material to be reduced to a powder using a fine drill (micromill) prior to analysis. The method can distinguish between yearlings from the western and eastern Atlantic with a high rate of accuracy and also has a high resolving power for discriminating between adults from the main spawning areas in the Gulf of Mexico and the Mediterranean (GBYP Phase 8 final report). However, due to the requirement to micromill the sample, the IRMS approach has a coarse temporal resolution and is not suitable for investigating fine scale movements of fish between areas.

Thanks to recent analytical advances, it is now possible to measure stable isotopes in otoliths with very high spatial resolution using secondary ion mass spectrometry (SIMS) (Matta et al. 2013). With this technique a sectioned polished sample is analyzed using a narrow beam which can measure stable isotope ratios in spots as small as 10μm diameter and as close together as 30μm. By combining stable isotope data with available maps of oxygen isotopes ($\delta^{18}O$) in seawater and temperature it is possible to derive a probabilistic estimate of a fish's location at a given point in time (the isoscape approach, Trueman et al. 2012). SIMS therefore offers the opportunity to reconstruct movements of bluefin during the first year of life (when the fish are too small to tag) and to investigate current hypotheses relating to the existence of resident and migratory components within the Mediterranean (Aranda et al. 2013, Arrizabalaga et al. 2019). Ultimately, this could help to resolve discrepancies between otolith core stable isotope

signatures and genetics, by establishing if individuals of uncertain origin moved away from their spawning area early in life or originated from a third spawning component.

This task involves a pilot SIMS analysis of otoliths from young of the year and adult bluefin tuna as a first step in the development of an isoscape approach to investigating early movements of bluefin. The analysis was focused on four groups of fish: young of the year from the East Atlantic and Mediterranean ($\delta^{18}O$ measured along core to edge transects); adults held captive at tuna farms in the Mediterranean for three years ($\delta^{18}O$ measured at the otolith edge, corresponding to 2-3 years of recent growth); free moving adults collected from various sites in the Mediterranean ($\delta^{18}O$ measured at the otolith edge, corresponding to 2-3 years of recent growth); adults of disputed origin that had been assigned to the GOM using otolith core stable isotope signatures and to the Med based on genetics ($\delta^{18}O$ measured along core to edge transects). $\delta^{18}O$ profiles were compared across the four groups and to estimated ranges of otolith $\delta^{18}O$ based on sea surface temperature and ocean $\delta^{18}O$ predictions. The potential to use $\delta^{18}O$ profiles to reconstruct environmental histories and to infer temperature histories and migration patterns is evaluated.

Objectives:

- To use SIMS to obtain highly resolved profiles of $\delta^{18}O$ across otolith growth trajectories in bluefin tuna
- To evaluate the feasibility of using an isoscape approach to reconstruct early movements of bluefin tuna
- To compare $\delta^{18}O$ otolith profiles between young-of-the-year collected within and outside (e.g Gulf of Cadiz) of the Mediterranean to establish the timing of movement
- To characterize Mediterranean "residency" using $\delta^{18}O$ otolith profiles from farmed fish held within the Mediterranean for >3 years and compare to profiles of free-moving adults in the Mediterranean.

- To describe $\delta^{18}O$ profiles in otoliths of bluefin which are not clearly identified as of western or eastern origin and evaluate the evidence that:
    - These fish belong to a third spawning component
    - These fish originate from either of the two main spawning areas but migrate during the first year of life

4.4.2. Methods

Otolith selection and preparation for SIMS analysis

Otoliths were selected from the GBYP tissue bank held by AZTI (Figure 4.9). A total of 35 were prepared for SIMS analysis: YOY Atlantic = 7; YOY Med = 7; Mediterranean free moving = 7; Mediterranean farmed = 9; Disputed origin = 5 (Table 4.4). Otoliths were prepared according to protocols described in Rooker et al. (2008b). Briefly, following extraction, sagittal otoliths of bluefin tuna were cleaned of excess tissue with nitric acid (1%) and deionized water. One sagittal otolith from each individual was embedded in Struers epoxy resin (EpoFix) and sectioned on the transverse plane using a low speed ISOMET saw to obtain 1.5 mm transverse sections that included the core. In preparation for SIMS analysis, sections were polished to expose a smooth surface and attached to a 60mm diameter epoxy block custom made for the SIMS chamber.

Table 4.4: Summary of fish and otolith chemistry measurements

Group	Length (cm) mean (min-max)	Otolith $\delta^{18}O$ mean (min-max)	Sampling years
Disputed origin	146 (45-233)	-2.98 (-6.16- -0.17)	2013-2015
Med farmed	153 (145-162)	-2.29 (-4.12- -0.61)	2016
Med free	160 (138-191)	-3.08 (-5.65 - -0.14	2015-2017
YOY Atl	30 (26-34)	-3.40 (-4.76 - -2.03)	2015, 2017
YOY Med	37 (24-49)	-3.11 (-4.88 - -1.18)	2017

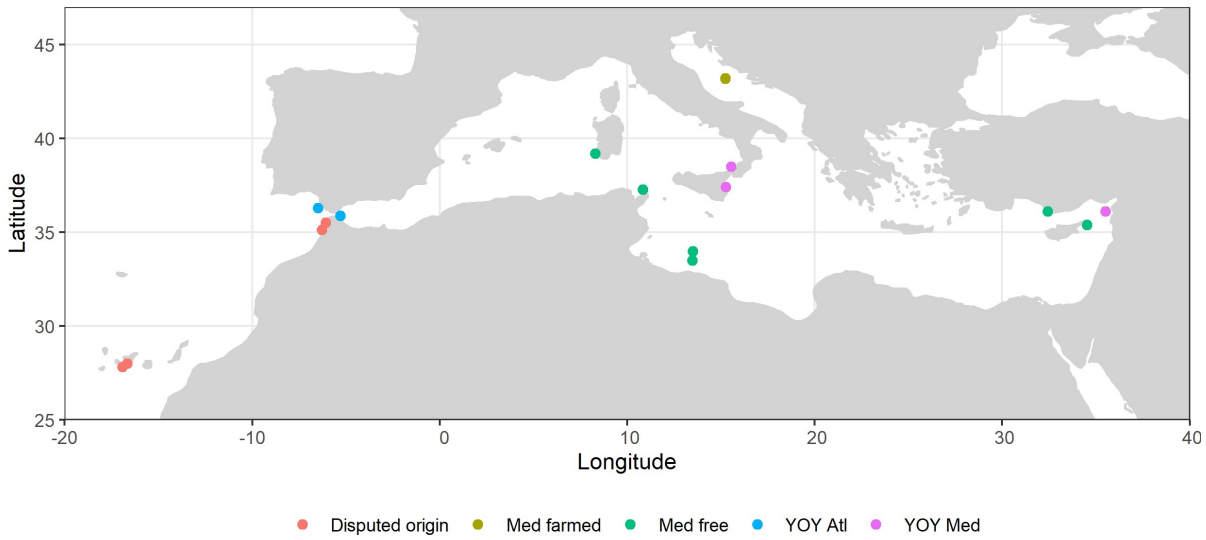

Figure 4.9*: Map of the sampling locations.*

SIMS analysis

Otoliths were analysed at the Nordsim-laboratory in the Swedish Museum of Natural History in Stockholm, Sweden. The instrument used for the analysis was a CAMECA IMS 1280 ion microprobe. Samples were recast with grains of a calcite standard and repolished using 3µm and 1µm diamond solutions. To facilitate navigation during analysis, a tiled image of each mount was generated using the Olympus cellSens software. The mounts were coated with a layer of gold before analysis in the ion microprobe machine.

Oxygen isotope measurements were taken from 10µm spots with a distance of 40-80 µm between spots (centre to centre). Sample analyses were performed in blocks of 6, bracketed by two analyses of the standards. The results were reported in per mil (‰) relative to the Pee Dee belemnite (PDB) standard with a mean reproducibility of ± 0.13‰. On each otolith from the YOY and disputed origin groups a transect from the core to the edge was analysed. On the otoliths from the Mediterranean groups (farmed and free moving), a transect of 1500 µm length starting from the edge was analysed, in order to capture the previous 2-3 years of otolith growth approximately.

Relating oxygen stable isotope signatures to water chemistry

The isotopic composition of oxygen in otoliths ($\delta^{18}O_{oto}$) is linearly related to the isotopic composition ($\delta^{18}O_w$) and temperature (T) of the seawater in which the fish resides through the fractionation equation:

$$\delta^{18}O_{oto} - \delta^{18}O_w = \gamma T + \beta.$$

By coupling an empirically derived fractionation equation with estimates of δ^{18}Ow and sea surface temperature (SST) it is possible to use otolith oxygen isotope ratios as geolocators, although the successful application of this approach is somewhat limited by uncertainties surrounding small scale variation in δ^{18}Ow and species specific variation in the fractionation equation (Trueman et al. 2012).

A 1°X1° grid of δ^{18}Ow was obtained from the dataset published by LeGrand and Schmidt (2006). Estimates of SST at the time and location of sampling were obtained from the MET Office Hadley Centre Observations dataset (https://www.metoffice.gov.uk/hadobs/hadisst/).

4.4.3. Results and Discussion

SIMS δ^{18}O otolith measurements

The SIMS δ^{18}O otolith measurements ranged from -6.16 to -0.16. Values were markedly lower than previously reported estimates obtained from Atlantic bluefin tuna otoliths using IRMS (-2.3 to 0.02; Brophy et al in review). Similar discrepancies between SIMS and IRMS measurements were observed in an analysis of cod otoliths (Helser et al. 2018). They may arise because protein and hydrous components are removed from the otolith material by acid digestion prior to IRMS or due to differences in the bicarbonate standards that are used in each type of analysis. For cod otoliths, the relationship between the two types of measurements is described by the regression equation:

$$\delta^{18}O \text{ IRMS} = 0.4773\ \delta^{18}O \text{ SIMS} + 0.483 \qquad \text{(Helser et al. 2018)}$$

Using this conversion, the range of $\delta^{18}O$ otolith measurements obtained using SIMS in this study would convert to an equivalent of -2.5 to 0.41 for an IRMS analysis.

Estimated relationship between otolith $\delta^{18}O$ and water chemistry

The most robust approach to deriving a field based fractionation equation for Atlantic bluefin tuna would be to relate otolith $\delta^{18}O$ values to $\delta^{18}O$ measurements from the rearing water of fish held in pens. If both measurements were obtained at regular intervals during the year, seasonal changes in water temperature and otolith $\delta^{18}O$ could be used to estimate the fractionation coefficients. In this case, no field measurements of water chemistry were available, so modelled estimates from the available ocean $\delta^{18}O$ and SST datasets were used.

The Mediterranean farmed samples were all collected at the same time (January 2016), so seasonal changes in otolith $\delta^{18}O$ could not be observed directly. However, SIMS otolith transects from two fish showed a clear seasonal signal with $\delta^{18}O$ measurements decreasing along the first three points from the edge (as water temperatures increased) and then increasing (Figure 4.10). Through interpolation of these data, otolith $\delta^{18}O$ was estimated at regular intervals from the time of sampling (January) to the time of the annual maximum in SST (August). These estimates were related to mean SST at the farm location at the same time intervals. A fractionation equation was then estimated using the linear model:

$$P.\delta^{18}O_{oto} - P.\delta^{18}O_{w} = \gamma T + \beta.$$

Where P.δ18Ooto represents the interpolated estimates of otolith $\delta^{18}O$ from the two farmed individuals, P.δ18Ow is the estimate of $\delta^{18}O$ in the water based on the gridded dataset of Le Grande and Schmidt (2006) and T represents the interpolated estimates of SST at the sampling location corresponding to the P.δ^{18}Ooto measurements.

The derived fractionation equation was used to predict $\delta^{18}O$oto values for each month of the year within several regions:

- Putative spawning and larval drift areas (Gulf of Mexico, Slope Sea, central Mediterranean, eastern Mediterranean, Western Mediterranean)
- The location where the Mediterranean farmed individuals were held

- The grid square in which the Mediterranean free moving individuals were captured

This provided ranges of predicted otolith $\delta^{18}O$ signatures against which the observed values could be compared for the purpose of evaluating movement scenarios.

The fractionation equation presented here requires considerable refinement before its accuracy can be evaluated. It should be estimated based on a larger number of individuals and ideally using real-time observations of $\delta^{18}O$ in the water and the otolith. The uncertainty around the model parameters also needs to be estimated. It is included here largely to demonstrate how the isoscape approach could be implemented through further development.

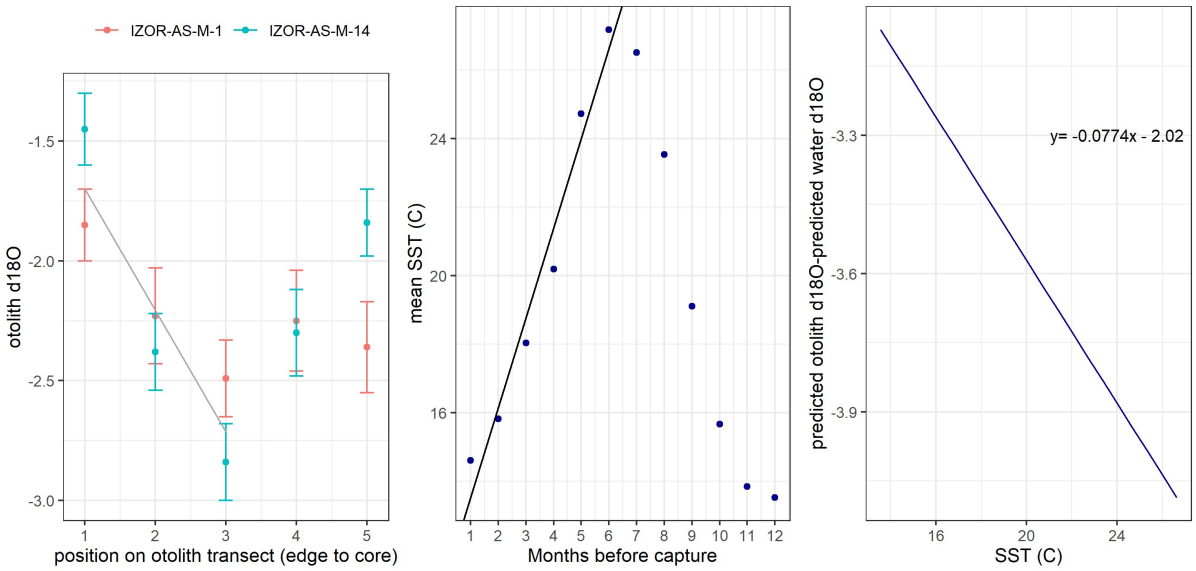

Figure 4.10: Seasonal patterns in otolith $\delta^{18}O$ as observed in otoliths of two fish from the Mediterranean farmed group (left panel). The grey trendline is the regression used to predict otolith $\delta^{18}O$ at regular intervals between the temperature minimum (January) and maximum (August), which are evident in the plot of mean monthly SST estimates at the sampling location (middle panel; black line shows the temperature trend from January to August). The fractionation equation which was derived from the estimates of otolith $\delta^{18}O$, SST and water $\delta^{18}O$ is shown in the right panel.

Individual variability in $\delta^{18}O$

High levels of variability in otolith measurements of $\delta^{18}O$ were observed in the Mediterranean free moving group which included individuals from across a wide geographical area (Figure 4.11). There was also a high level of variability across otolith transects from the disputed origin group which could reflect their migration away from the main spawning areas. In general, individual variability in $\delta^{18}O$ was greater across the otolith transect (whole lifetime signature) than at the otolith edge (recent environment signature). Nonetheless, there was still a notable degree of variability in $\delta^{18}O$ at the otolith edge among individuals from the same sampling location, even for the Mediterranean farmed group which had been held in pens for three years prior to capture and had therefore been exposed to the same conditions. For the Mediterranean farmed group, $\delta^{18}O$ measurements at the otolith edge ranged from -1.19 to -2.99. This corresponds to a water temperature range of 7° to 30 °C based on the fractionation relationship described above. Mean monthly SST in the grid square where the farm was located ranged from 14.6 °C in January 2016 to 27.2°C in August 2015. A number of factors could contribute to the observed variability in $\delta^{18}O$ at the otolith edge. Fish with relatively high $\delta^{18}O$ values at the otolith edge may have displayed a behavioural preference for cooler deeper waters. Due to possible erosion of the otolith edge during otolith preparation, some edge measurements may represent conditions several months before sampling, during the previous summer. This could explain lower than average $\delta^{18}O$ values at the otolith edge. Finally, $\delta^{18}O$ in otoliths can vary due to individual variation in the physiological response to temperature (Darnaude et al. 2014). These sources of variation decrease the accuracy with which environmental histories can be reconstructed using otolith $\delta^{18}O$.

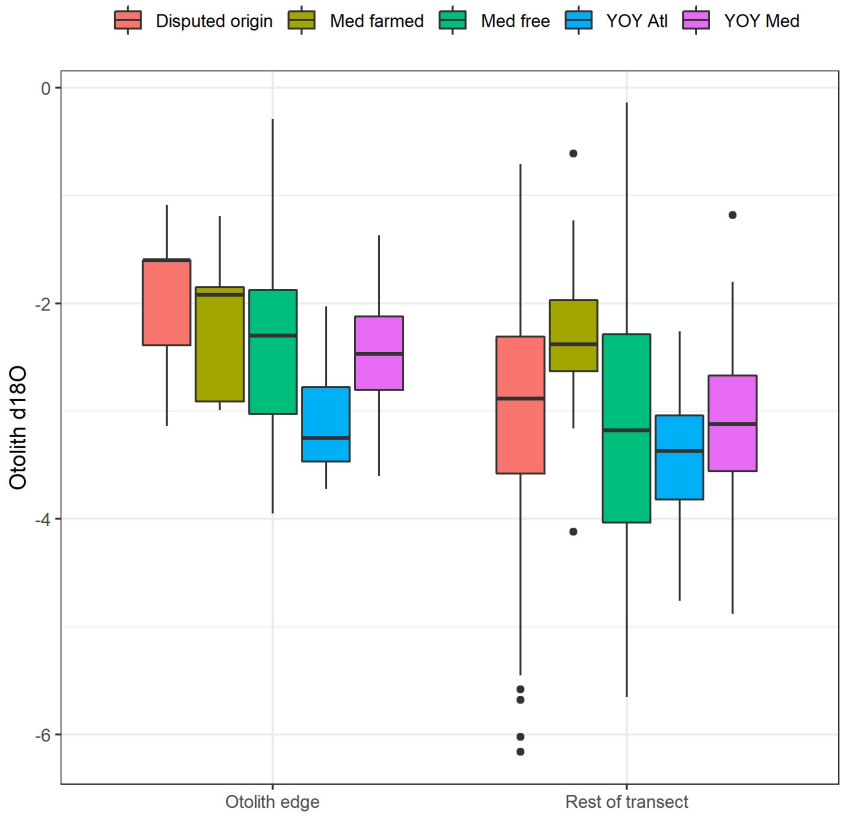

Figure 4.11: Variation in otolith measurements of $\delta^{18}O$ across individuals in each group.

Comparison of farmed and free moving fish in the Mediterranean

Most of the $\delta^{18}O$ measurements from the farmed fish stayed within the range of the monthly predicted values (Figures 4.12 and 4.13). In some fish, an annual cycle in $\delta^{18}O$ was apparent, reflecting seasonal changes in water temperature (e.g. IZOR-AS-M-14). In one fish (IZOR-MS-M-2), the values were above the predictions for most of the transect, demonstrating the influence of individual physiological variation on otolith $\delta^{18}O$ (Figure 4.12).

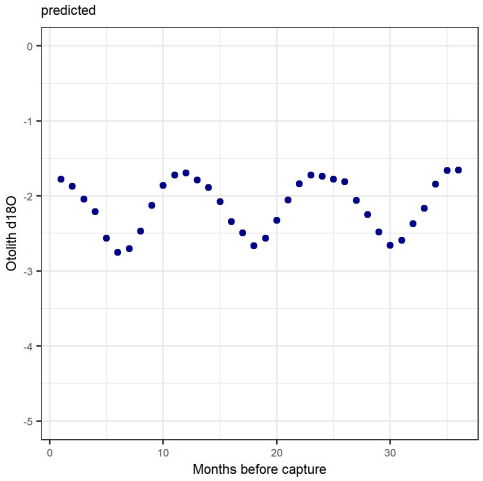

Figure 4.12: Predicted annual cycle in $\delta^{18}O$ in otoliths from the Mediterranean farmed group.

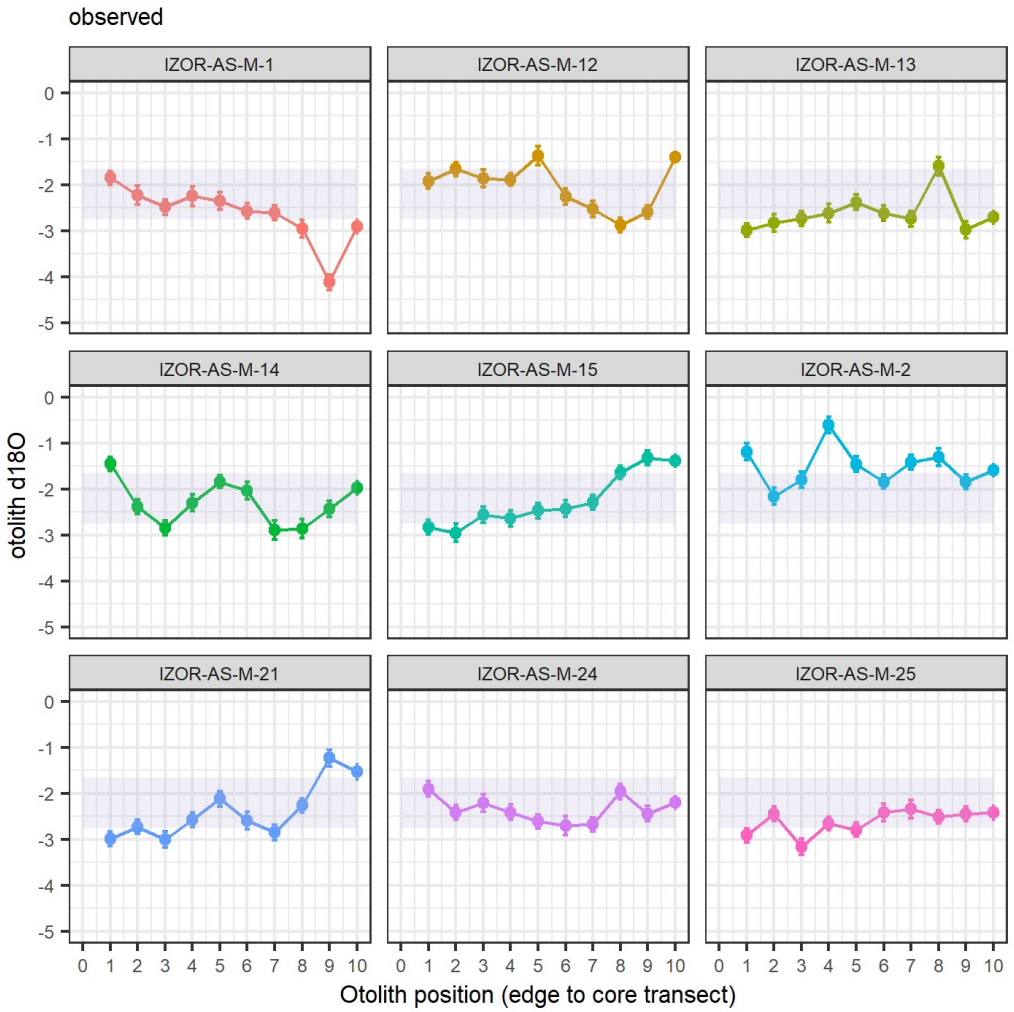

Figure 4.13: Observed $\delta^{18}O$ measurements from SIMS transects of 1.5mm length, taken from the edge towards the core of otoliths from the Mediterranean farmed group. The limits of the predicted values (Figure 4.12) are shaded in grey.

In the free moving fish from the Mediterranean, $\delta^{18}O$ values across the transect showed a lot more variability with some fish showing substantial variation from the predicted values (Figure 4.14). Some profiles suggested residency close to the sampling location (e.g. ISTA-LS-M-181), while others indicated that the fish had spent a considerable period in a different water mass (e.g. FMAP-MA-L-179).

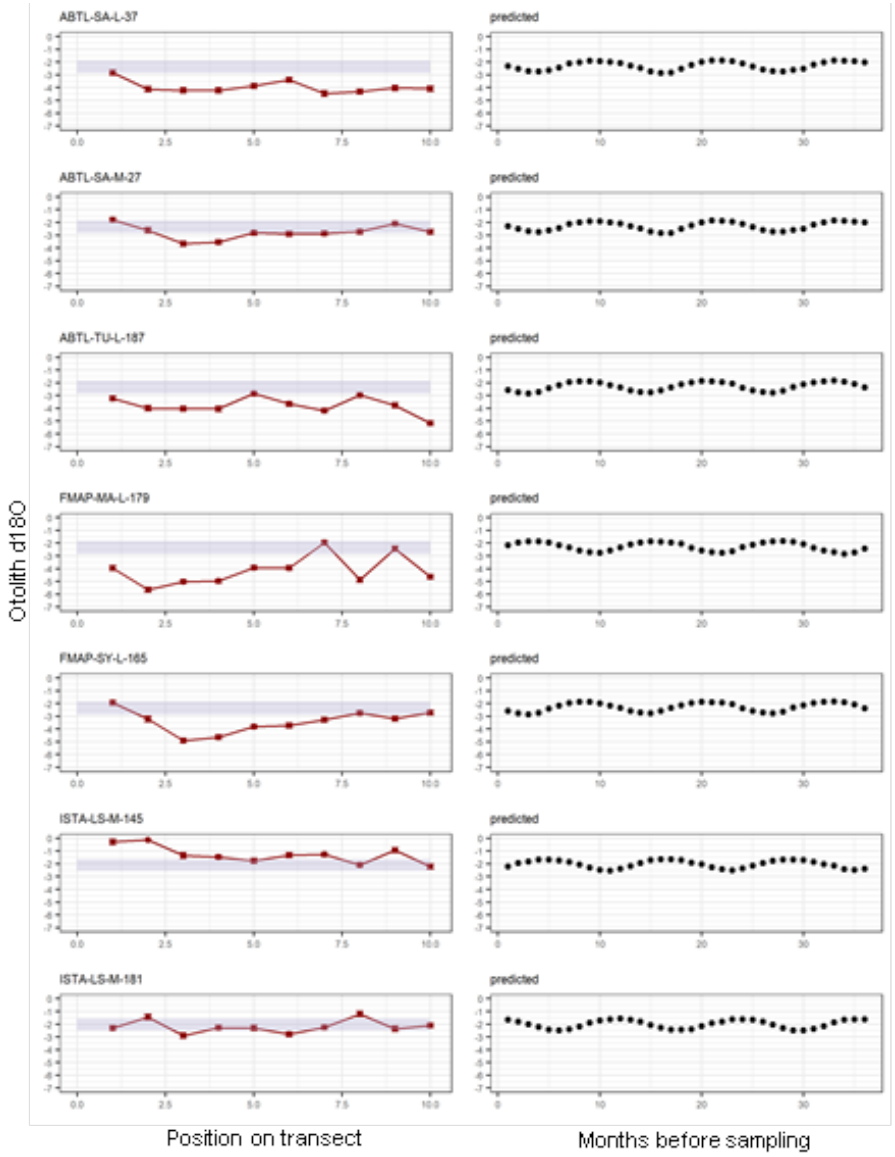

Figure 4.14: Observed $\delta^{18}O$ measurements from SIMS transects of 1.5mm length, taken from the edge towards the core of otoliths from the Mediterranean free moving group (left hand panels), alongside the predicted $\delta^{18}O$ values in the otoliths based on residency at the sampling location. The limits of the predicted values are shaded in grey.

Predicted otolith $\delta^{18}O$ values for putative spawning and larval drift areas

Predicted levels of $\delta^{18}O$ in the otolith varied across the five putative spawning and larval drift areas and showed an annual cycle (Figure 4.15). As expected, fish spending their larval phase in the Mediterranean are predicted to have the highest levels of otolith $\delta^{18}O$ values, while those in the Gulf of Mexico would have the lowest values. Predictions for the Slope Sea area are highly variable and intermediate between the Mediterranean and Gulf of Mexico.

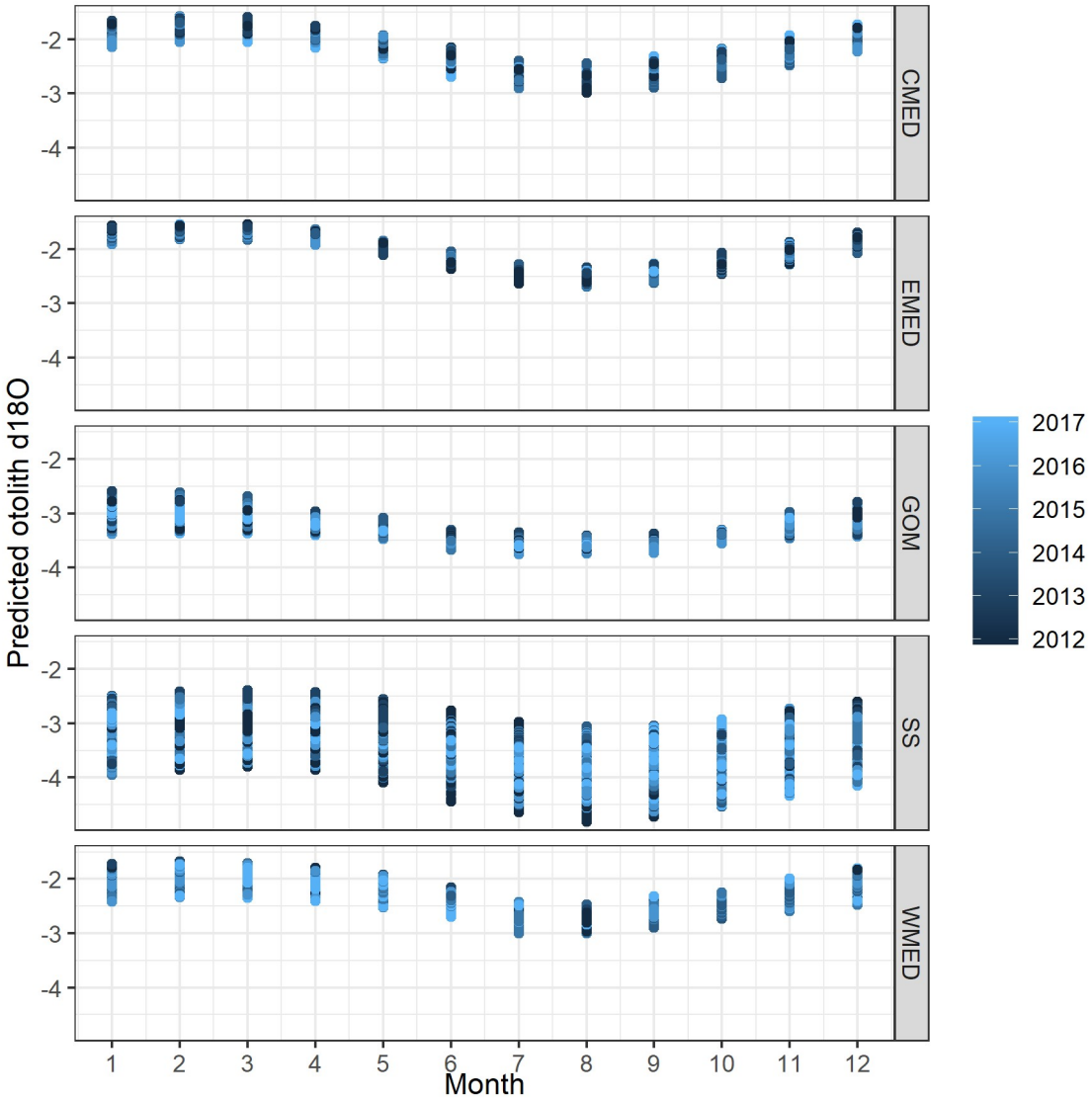

Figure 4.15: Predicted otolith $\delta^{18}O$ values for each month across putative spawning and larval drift areas.

Core to edge δ18O profiles in young of the year

There were no clear differences between the $\delta^{18}O$ otolith profiles from Mediterranean and Atlantic young of the year (Figure 4.16). However, profiles varied considerably between individuals within each group, indicating a variety of environmental histories. The three fish collected in October showed a clear increase in $\delta^{18}O$ towards the end of the transect which is consistent with seasonal cooling. At the beginning of the transect, some individuals showed relatively little variability in $\delta^{18}O$ (e.g. NECT-SI-0-2) which may indicate retention within an area of homogenous water chemistry, while others showed a steady increase from the core towards the edge (e.g. NECT-SI-0-6), indicative of movement through different water masses. Several individuals had $\delta^{18}O$ values at the otolith core <-3, which are not consistent with predictions for the Mediterranean during the early growth period (May-October). However, it should be borne in mind that the predictions are based on the estimated temperature - $\delta^{18}O$ relationship for adult fish and may not be appropriate for the larval growth period.

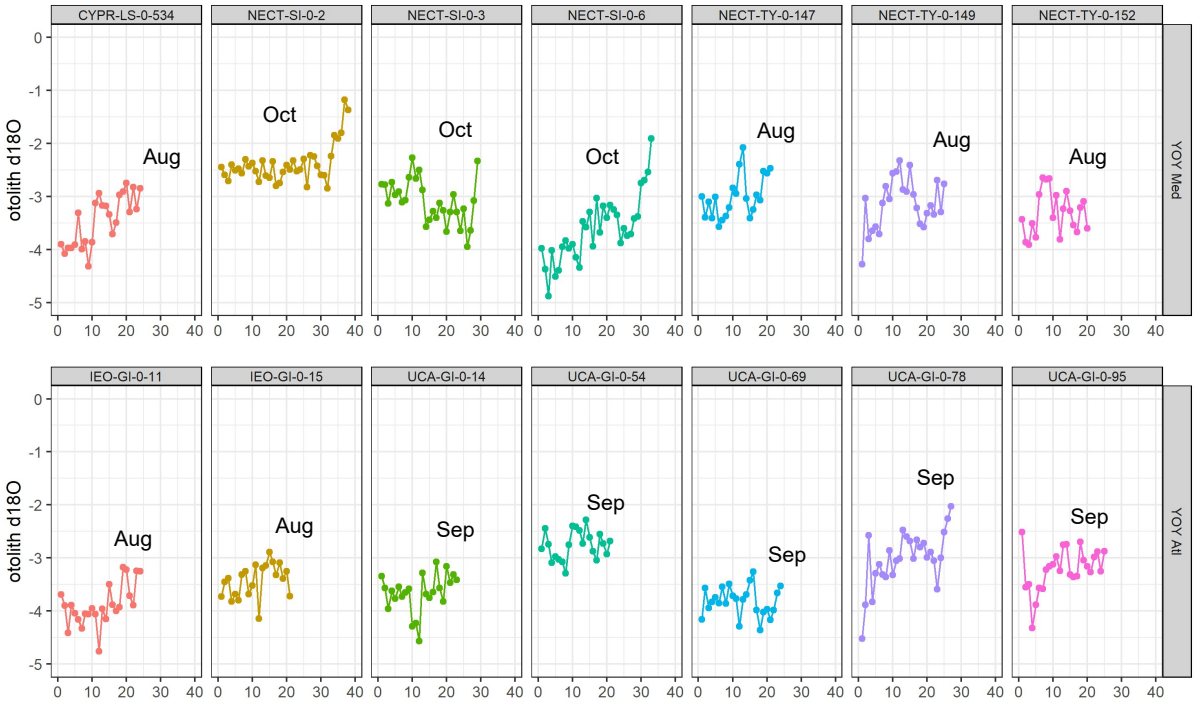

Figure 4.16: Core to edge $\delta^{18}O$ profiles in otoliths from young of the year collected in the Mediterranean (YOY Med) and eastern Atlantic (YOY Atl). The month of collection is indicated on each plot.

Core to edge $\delta^{18}O$ profiles in adults of disputed spawning origin

The five individuals included in the disputed origin group had been previously assigned to the Gulf of Mexico population based on stable isotope signatures in the core of the otolith (first 12 months of life) and to the Mediterranean population based on their genetics. The stable isotope measurements had been taken using micromilling and IRMS; $\delta^{18}O$ values were lower than the typical values reported for the Mediterranean baseline populations (Brophy et al in review). Surprisingly, for three of these individuals, the mean SIMS $\delta^{18}O$ values at the otolith core (within ~120µm of the core) were well above the range of values observed in the Mediterranean and Atlantic young of the year and were much closer to the predictions for the Mediterranean than the Gulf of Mexico (Figure *4.17*). The remaining two individuals had low levels of $\delta^{18}O$ in the otolith core, but levels overlapped with some of the Mediterranean young of the year.

The core to edge transects showed two contrasting patterns; in three individuals the $\delta^{18}O$ decreased at the start of the transect while in two individuals they increased (Figure *4.18*). After this initial growth period individuals showed fluctuating levels of δ18O, with clear annual signals evident in the later part of the transects. In some individuals, δ18O stayed above -3.5 for the entire life cycle (e.g. INRH-MO-L-229), while in others δ18O periodically decreased to below -5 (e.g. INRH-MO-L-277). This may indicate eastern Atlantic/Mediterranean residency and trans-Atlantic migration respectively.

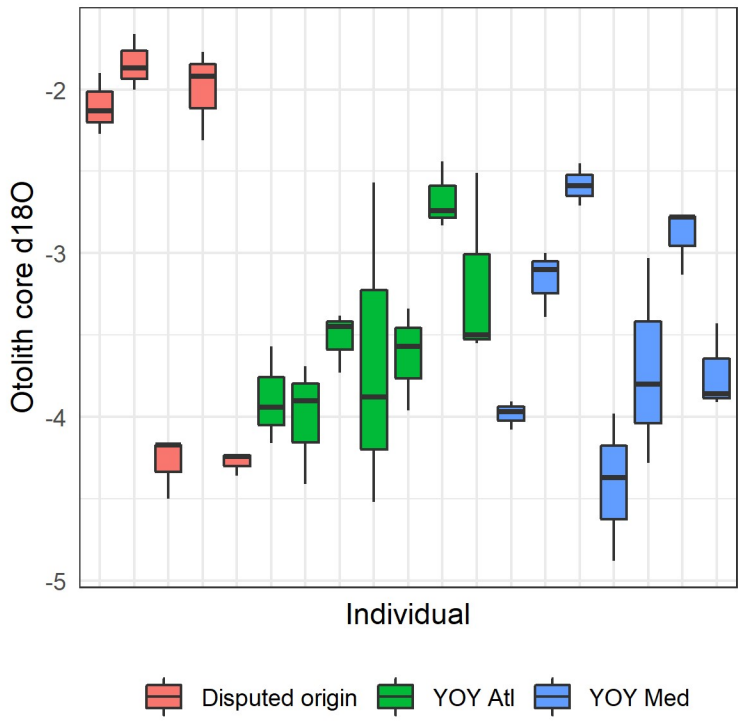

Figure 4.17: $\delta^{18}O$ levels at the otolith core (first 3 measurements, 0-120µm from the core).

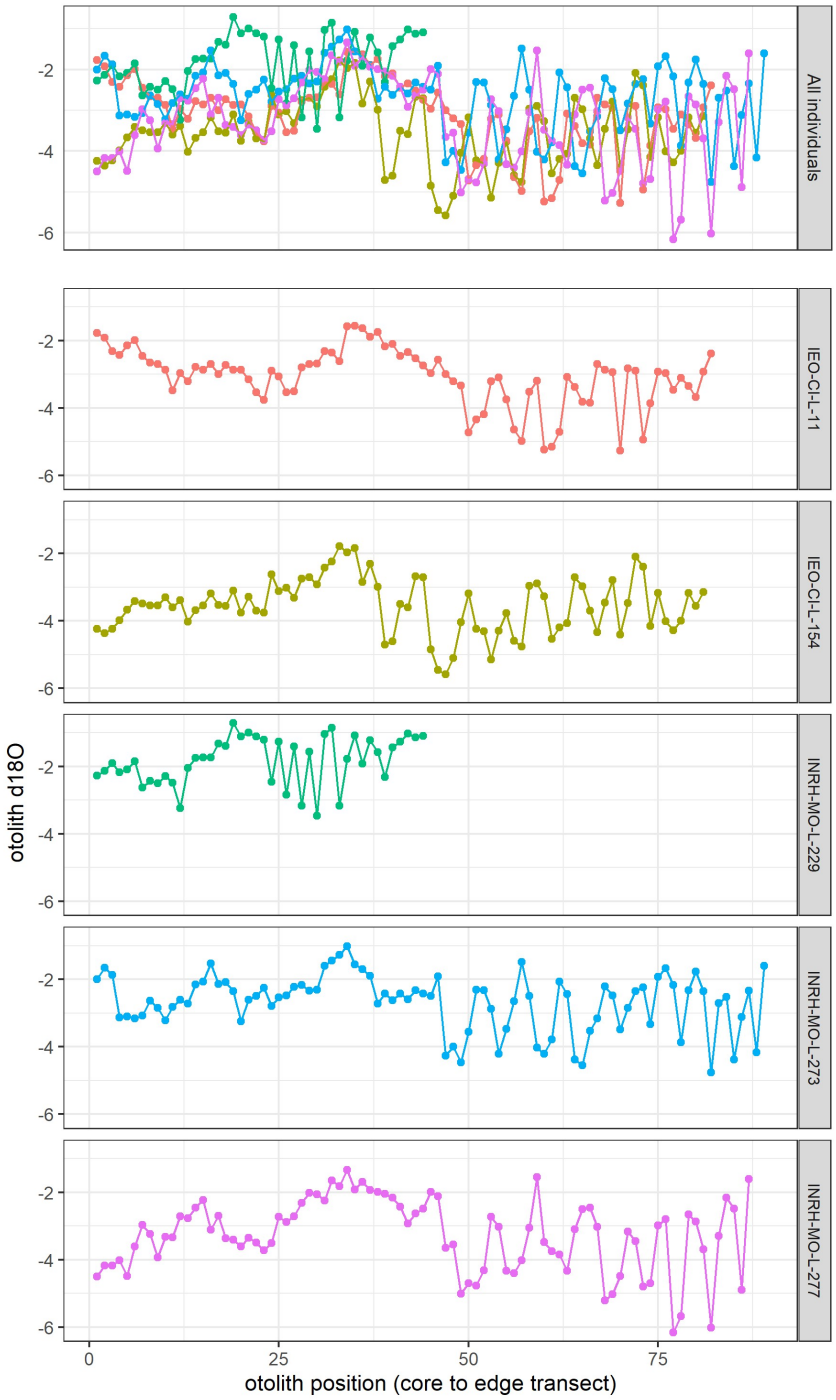

Figure 4.18: Core to edge $\delta^{18}O$ profiles in otoliths from fish of disputed natal origin (assigned to the GOM using IRMS measurements of stable isotopes and to the Mediterranean using genetics).

4.4.4. Conclusions

- The SIMS analysis has provided highly resolved estimates of $\delta^{18}O$ along otolith growth transects
- Additional work is needed to provide a robust and fully validated field based fractionation equation for Atlantic bluefin tuna; this could be achieved through repeated sampling of otoliths and water at tuna farms.
- The framework presented here can be used to support the reconstruction of environmental histories and to infer temperature histories and migration patterns
- $\delta^{18}O$ signatures in individuals from the same environment showed considerable variability which will reduce the accuracy of such reconstructions
- The approach is particularly useful for comparing relative patterns in δ18O profiles between individuals
- Comparison of $\delta^{18}O$ profiles shows substantial variability in environmental histories during the first few months of life
- The results support the hypothesis that some individuals are retained within homogenous water masses during early life, while others are exposed to wide variation in water chemistry

References

Aranda, G., F. J. Abascal, J. L. Varela, and A. Medina. 2013. Spawning behaviour and post-spawning migration patterns of atlantic bluefin tuna (Thunnus thynnus) ascertained from satellite archival tags. PLoS One 8:e76445.

Arrizabalaga, H., Arregui, I., Medina, A., Rodríguez-Ezpeleta, N., Fromentin, J.-M. and Fraile, I. (2019) Life History and Migrations of Mediterranean Bluefin Tuna In: The Future of Bluefin Tunas: Ecology, Fisheries Management, and Conservation.B. Block (ed.) Johns Hopkins University Press, pp. 67-93.

Brophy, D, Rodríguez-Ezpeleta, N, Fraile, I and Arrizabalaga, H. in review. Combining genetic markers with stable isotopes in otoliths reveals complexity in the stock structure of Atlantic bluefin tuna (Thunnus thynnus). Submitted to Scientific Reports.

Darnaude, A. M., A. Sturrock, C. N. Trueman, D. Mouillot, Eimf, S. E. Campana, and E. Hunter. 2014. Listening In on the Past: What Can Otolith δ18O Values Really Tell Us about the Environmental History of Fishes? PLoS One 9:e108539.

Helser, T. E., C. R. Kastelle, J. L. McKay, I. J. Orland, R. Kozdon, and J. W. Valley. 2018. Evaluation of micromilling/conventional isotope ratio mass spectrometry and secondary ion mass spectrometry of δ18O values in fish otoliths for sclerochronology. Rapid Communications in Mass Spectrometry 32:1781-1790.

LeGrande, A. N., and G. A. Schmidt. 2006. Global gridded data set of the oxygen isotopic composition in seawater. Geophysical Research Letters 33.

Matta, M. E., I. J. Orland, T. Ushikubo, T. E. Helser, B. A. Black, and J. W. Valley. 2013. Otolith oxygen isotopes measured by high-precision secondary ion mass spectrometry reflect life history of a yellowfin sole (Limanda aspera). Rapid Communications in Mass Spectrometry 27:691-699.

Rooker, J. R., H. Arrizabalaga, I. Fraile, D. H. Secor, D. L. Dettman, N. Abid, P. Addis, S. Deguara, F. S. Karakulak, A. Kimoto, O. Sakai, D. Macias, and M. N. Santos. 2014. Crossing the line:

migratory and homing behaviors of Atlantic bluefin tuna. Marine Ecology Progress Series 504:265-276.

Rooker, J. R., D. H. Secor, G. De Metrio, R. Schloesser, B. A. Block, and J. D. Neilson. 2008a. Natal Homing and Connectivity in Atlantic Bluefin Tuna Populations. Science 322:742-744.

Rooker, J. R., D. H. Secor, G. DeMetrio, A. J. Kaufman, A. B. Rios, and V. Ticina. 2008b. Evidence of trans-Atlantic movement and natal homing of bluefin tuna from stable isotopes in otoliths. Marine Ecology Progress Series 368:231-239.

Trueman, C. N., K. M. MacKenzie, and M. R. Palmer. 2012. Identifying migrations in marine fishes through stable-isotope analysis. Journal of Fish Biology 81:826-847.

5. CALIBRATION OF FISH AGEING SERVICES OTOLITH AGE ESTIMATES AND CREATION OF AN OTOLITH REFERENCE COLLECTION.

Task leader: Enrique Rodriguez-Marin (IEO)

Participants:
AZTI: Patricia L. Luque
IEO: Pablo Quelle
NMFS: Robert Allman
SABS: Dheeraj S. Busawon
UNICA: Piero Addis, Andrea Bellodi
UNIGE: Fulvio Garibaldi

5.1. Introduction

The ICCAT GBYP and national programs have invested a considerable effort in sampling calcified structures of Atlantic bluefin tuna (*Thunnus thynnus*, ABFT) and in the age estimation of this species from otoliths and the first radius of the first dorsal fin (spine). Direct ageing allows for good estimates of age composition of the catches enabling good cohort tracking of catch-at-age. This is why, since 2017, the "bluefin tuna Species Group" is trying to use the direct ageing method to obtain the catch at age matrix used in the population assessment (Anon. 2017).

Methodology standardization of age interpretation from ABFT calcified structures, addressing intra and inter laboratory consistent readings, has been a priority within the GBYP (Busawon et al., 2020). With this purpose, an international workshop on ABFT direct ageing was held at the beginning of 2019 (Rodriguez-Marin et al., 2020). This recent GBYP workshop had the participation of most of researchers currently involved in direct ageing of ABFT. In addition, a scientist from the Fish Ageing Services (FAS), with extensive experience in the field of fish ageing, as well the GBYP coordinator, were

also involved. The workshop reviewed the current protocols for otolith preparation and age reading criteria, which allows for standardized ageing methodology for future studies.

The Fish Ageing Services laboratory (FAS) was contracted by ICCAT GBYP in Phase 7 to provide age estimates from 2000 Atlantic bluefin tuna otolith samples. With the objective of ensuring that age readings provided by FAS follow the ICCAT reviewed reading protocol (Rodriguez-Marin et al., 2020), a sub-sample calibration exercise was planned. An additional objective was to create a new reference collection from the aged samples.

5.2. Material and methods

Six research centers participated in this calibration, four from Europe (AZTI - Tecnalia, University of Genova, UNIGE; University of Cagliari, UNICA; and Instituto Español de Oceanografía, IEO), one from United States of America (Panama City Laboratory, National Marine Fisheries Service, NMFS) and another from Canada (St. Andrews Biological Station, SABS). All agers have experience in direct ageing of Atlantic bluefin tuna using otoliths and contribute with age-length data to the assessment of this species. The calibration exercise consisted of participants reading a sub-sample of 10% of the otoliths previously aged by FAS, to determine a measure of inter-laboratory precision. A total of 223 otoliths were used for this calibration, the sample selection attempted to be representative of the set of 2000 otoliths read by FAS and to include the entire range of set sizes. The size range of the bluefin tunas analyzed included samples of straight fork length from 27 to 268 cm (Figure 5.1). Otolith section preparations were imaged and two sets, physical otolith sections and digital images, were used in the age estimation precision analysis. This enabled the participation of all research centers, as images are easier to share, and allows, to a limited extent, the comparison between both sets of readings. Additionally, physical sections and digital images will be used to build a reference collection using the consensus age obtained from readings.

A reading form was provided and the following information was recorded for each sample: number of annual bands (opaque), ventral arm edge type (wide translucent, narrow translucent or opaque), edge confidence (1= no confident; 2= confident in completeness and not with the type and 3= confident), readability code (1= pattern

present-no meaning, 2= pattern present-unsure with age estimate, 3= good pattern present-slightly unsure in some areas, 4= good pattern-confident with age estimate), reading date and notes with observations about the sample.

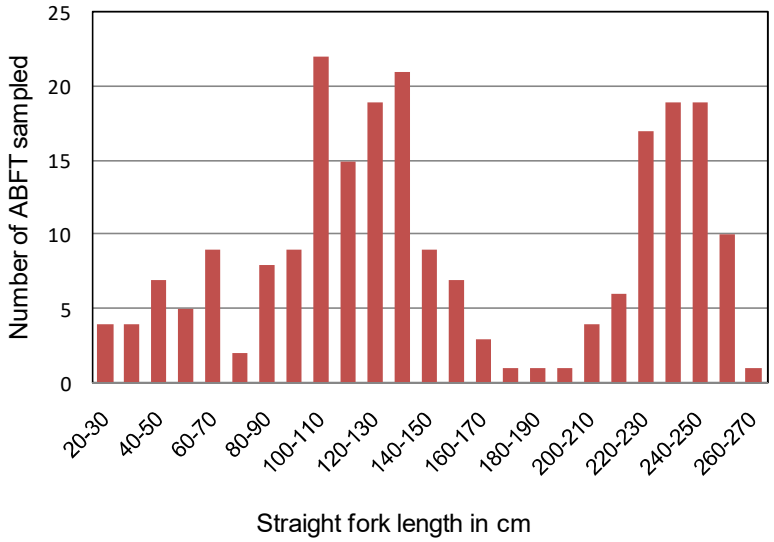

Figure 5.1. Length distribution of analyzed specimens by 10 cm size bin.

According to the reviewed protocol (Rodriguez-Marin et al., 2020), age estimates consisted in the counting of opaque bands using transmitted light. The otolith sections, were read twice. A third and final age reading was completed if the two age estimations differ by 2 or more years, to produce the final age estimate. The 3rd and final age estimate was done with knowledge of the first two readings. All readings were performed blindly without knowledge of fish size or catch date.

The readings from each reader and laboratory were compared with FAS readings. At the IEO laboratory the aging was based on two readers, each of which read once the whole data set, using the most experienced reader for the third reading when ages were different by more than one year. At the UNICA University two readers made independent estimates of age, each reader taking two readings of the whole data set. Three modal readings have also been used: "Mode Experts" (Mode_E) for the readings of all laboratories including the readings of both physical otolith sections and digital images; "Mode Picture" (Mode_P) for laboratories that have read with digital images and "Mode Live" (Mode_L) for laboratories that have read using physical otolith sections.

FAS used live readings and in the rest of the laboratories the reading mode is indicated at the end of the name (lab. name_L for live and lab. name_P for pictures). Precision was estimated through Coefficient of Variation (CV), Average Percent Error (APE), Evans-Hoenig and Bowker symmetry tests, age bias plots and age difference distributions between readers (Campana et al., 1995; McBride, 2015). FSA, R package version 0.8.20 (Ogle 2018) was used for the analysis.

5.3. Results and discussion

Diagnosis of paired age agreement was obtained by readers and readers mode (Table 5.1). CV values were close to 10, which is the precision level required for production ageing. However, this value was slightly exceeded in 4 comparisons. The precision between FAS and modal values show that the set of experts have acceptable precision compared to FAS. The symmetry tests showed bias in four cases regardless of the type of method used, physical sections or digital images, highlighting the labs UNIGE and NMFS, which showed bias in both tests of symmetry. The mean readability and edge type confidence by each reader compared with FAS showed high values, above the average of each scale (Table 5.1). The percentage of coincidence with FAS readings in the type of edge assigned was also analyzed, obtaining acceptable results, since there are three possible options. The greatest coincidence in the edge type was obtained with the IEO and both laboratories used physical sections (Table 5.1).

Table 5.1. Diagnosis of paired age agreement for all data (n = 223). Precision indices: CV = Coefficient of Variation, APE = Average Percent Error, Evans-Hoenig and Bowker symmetry tests, symmetry bias (, ** = significant differences in one or both symmetry tests, p < 0.01), mean readability score, mean edge type confidence and edge type agreement with FAS readings. Readers acronyms are explained in material and methods section.*

Readers comparison	CV	APE	Evans-Hoenig	Bowker	Symmetry bias	Mean Readability	Mean Edge type Confidence	Edge type agreement with FAS (%)
FAS-Mode_E	6,31	4,46	0,3698	0,0114				
FAS-Mode_L	8,21	5,80	0,2548	0,0239				
FAS-Mode_P	8,22	5,82	0,0266	0,0938				
Mode_P-Mode_L	10,31	7,29	0,4332	0,1694				
FAS-IEO_L	8,18	5,78	0,2861	0,0283		2,75	2,36	42,15
FAS-AZTI_L	12,65	8,94	0,0130	0,0008	*	2,67	2,16	33,63
FAS-UNICA_2_P	9,16	6,48	0,0109	0,1030		3,09	2,65	35,43
FAS-UNICA_1_P	10,43	7,37	0,2512	0,0475		3,09	2,59	36,77
FAS-SABS_P	10,61	7,50	0,0655	0,0031	*	2,57	2,37	37,67
FAS-UNIGEN_P	9,55	6,75	0,0004	0,0052	* *	3,1	2,66	34,53
FAS-NOAA_P	7,93	5,61	0,0000	0,0006	* *	2,89	1,82	35,87

Although tests of symmetry showed no bias between FAS and Modal readings (Table 5.1), age bias plots indicate a slight bias as age increases (13+), with FAS age estimates being lower by one year than "Mode Experts" and "Mode Live" (Figure 5.2). Furthermore, this bias was apparent at an earlier age (10+) with “Mode Picture”.

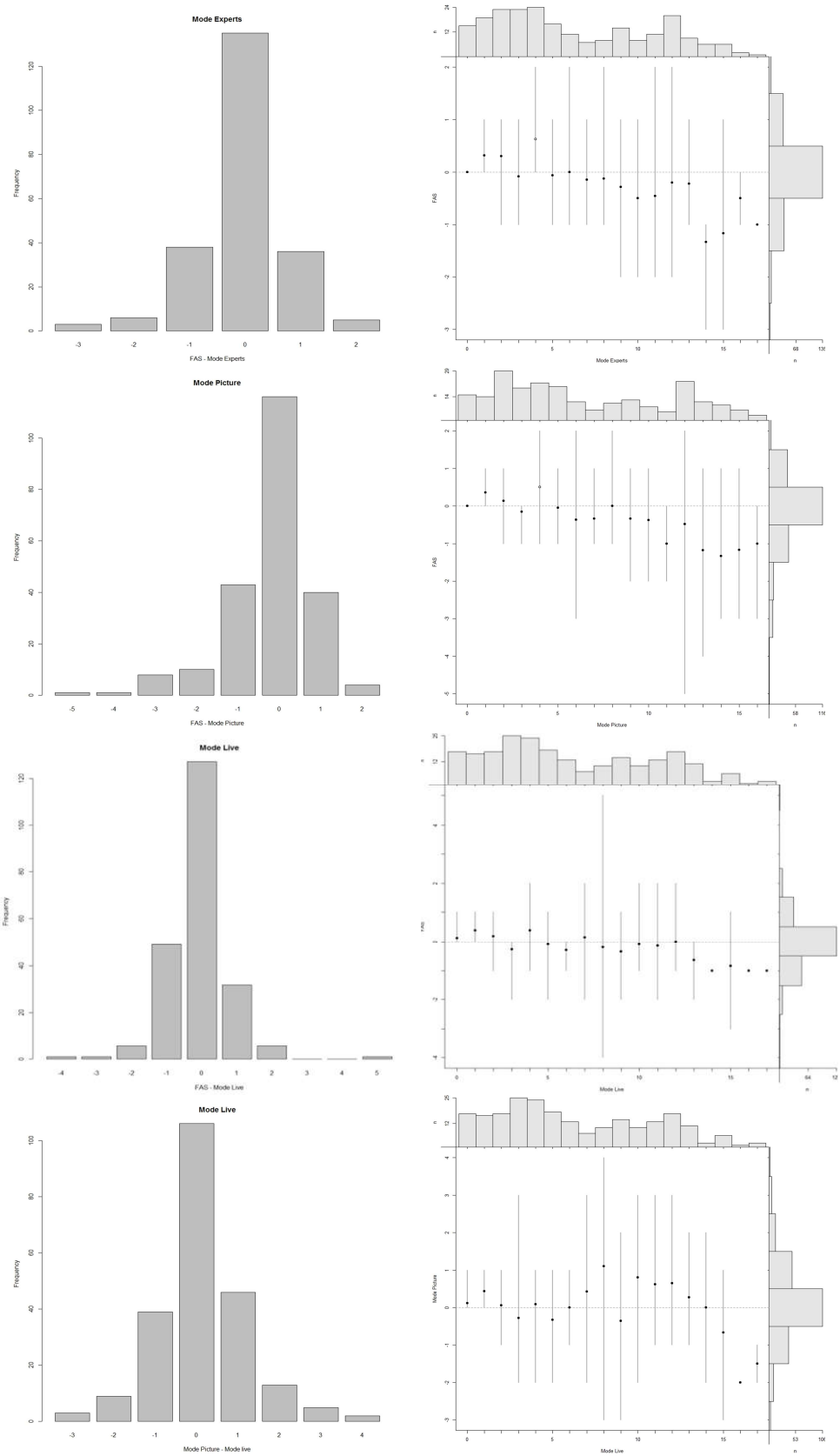

Figure 5.2. Age difference distributions and age bias plots between readers-lab. The number of samples per age class appears at the top of the bias plots.

Reading analysis showed that the following laboratories IEO_L, UNICA_2_P, UNICA_1_P and SABS_P provided similar results to FAS, although these labs tended to count more annual band for older specimens (13+) (Figure 5.3 and 5.4). Similarly, AZTI and UNIGE also had higher annual band counts compared to FAS. On the other hand, NMFS showed an opposite trend with lower annual band counts compared to FAS.

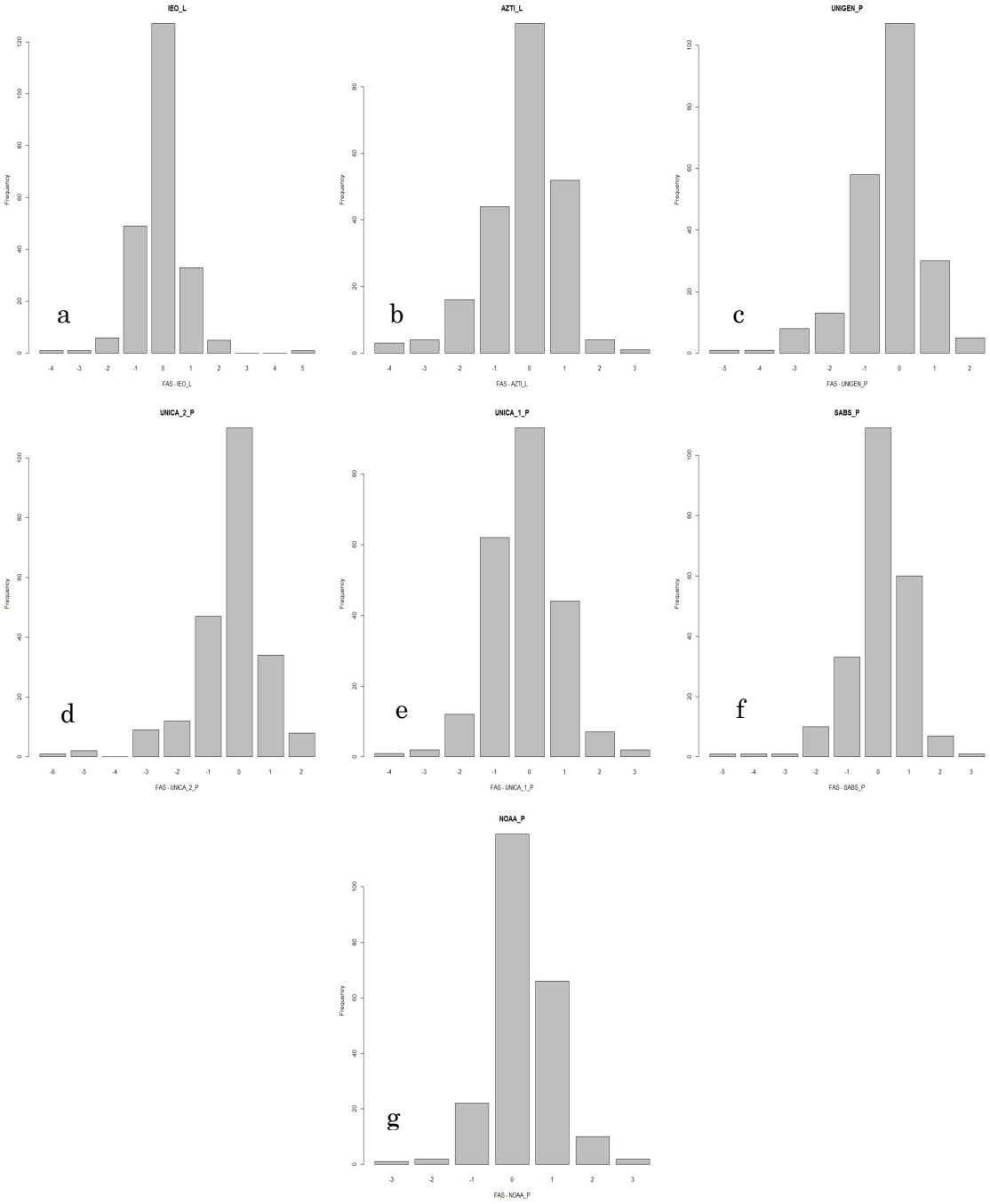

Figure 5.3. Age difference distributions between FAS and each reader-lab. a = IEO_L, b = AZTI_L, c = UNIGEN_P, d = UNICA_2_P, e = UNICA_1_P, f = SABS_P and g = NMFS_P.

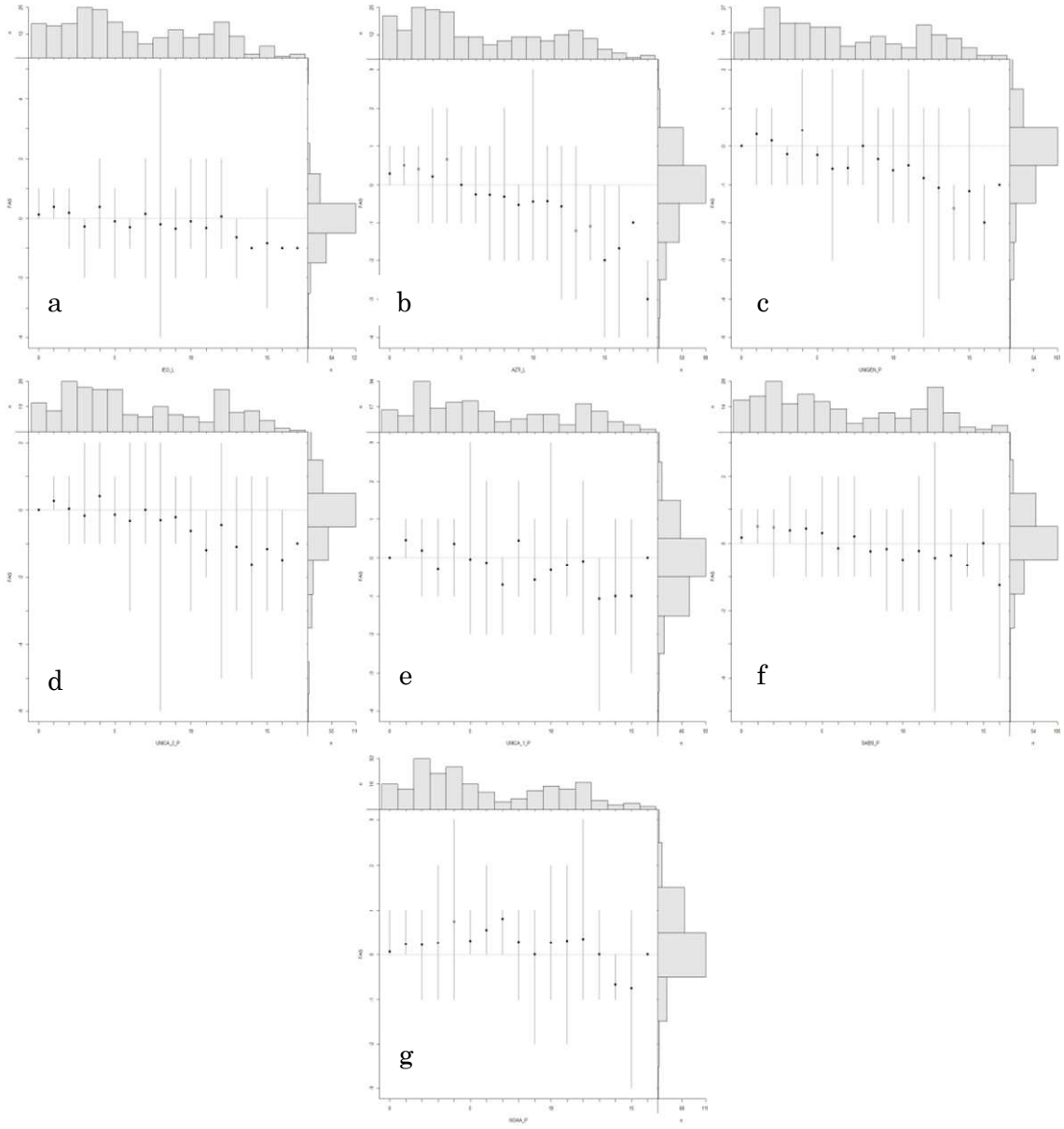

Figure 5.4. Age bias graphs (FAS age minus reader-lab. age). The number of samples per age class appears at the top of the graph. X-axis for figures: a = IEO_L, b = AZTI_L, c = UNIGEN_P, d = UNICA_2_P, e = UNICA_1_P, f = SABS_P and g = NMFS_P. Y axis: FAS.

To determine the possible reason for the lower number of opaque bands counted by FAS laboratory in older specimens (counting different structures, false annulus or edge type interpretation), a detailed inspection of FAS annotated images was performed. This bias seems to be due to the fact that this laboratory counts the bands in a different area of the otolith ventral arm than the rest of the laboratories. FAS lab counts on the external

margin of the ventral arm, while the other labs do so in the area between the sulcus margin and the ventral groove. Furthermore, they used the dorsal arm to corroborate or even read age, when this dorsal arm produces an underestimation of age and it was the ventral arm which was used in band count to validate age inferences of ABFT (Neilson and Campana, 2008). An erroneous count of false annual bands by FAS does not appear to occur, although in some cases the first annual band is counted higher with respect to the first inflection than the other readers. Possibly the lack of a reference scale in FAS readings affects in this regard. The interpretation of the edge of the otolith influences all readers, regardless of the laboratory of origin.

The annotated images of NMFS lab were also analyzed to try to discern the lowest band count compared to FAS and other labs. The difference from FAS is less than 0.5 bands at almost all ages. This seems to be because NMFS lab sometimes uses the external margin of the otolith ventral arm to count or corroborate the number of bands identified in the agreed reading area and located between the sulcus margin and the ventral groove. Furthermore, NMFS lab sometimes interprets the pattern of the first 6-8 years with fewer bands than other labs, including possible misidentification of the first band and the pattern of deposition of the first 5 annual bands. The identification of the first annual band is decisive in detecting the pattern of gradual decrease in the distance between the first annual bands. (Rodriguez-Marin et al., 2019).

The transverse bands that indicate the years in the ventral arm of the otolith, cover the entire width of the arm until the age of 4 years. From these 4 years the bands begin to be not easily identifiable along the entire width of the arm, because their curvature and the discontinuity of their path make it difficult to match the band count of both sides of the arm. For this reason, it is important to use the same reading area inside the ventral arm. FAS's use of the external margin produces systematically smaller annual band count in 1 year than ICCAT readers, starting from 10-13 years, and this discrepancy can increase in older specimens. This difference, although small, may be significant because, for example, with FAS counting procedure, the very abundant cohort of 2003 may appear as the one of 2004. From these results, it would be necessary for FAS laboratory to reread the samples of specimens older than 10 years, within the ICCAT GBYP Phase 7 contract, using the area close to the sulcus margin of the ventral arm.

The participation of a scientist from FAS in the international GBYP workshop on ABFT direct aging conducted at the beginning of 2019, allow to use a common reading criterion for the readings of other new 2000 otoliths commissioned by GBYP in Phase 9 to this ageing laboratory. The reading of these otoliths from both GBYP phases, after an age quality control, will allow to have 4000 values of length at age to be considered for the next stock assessment.

Tile plots for edge type assignment and confidence showed some small similarity between laboratories (Figure 5.5 and Figure 5.6). The tile plot of the readability code generally showed good confidence with the readings, although the readings based on pictures seem to reflect a better quality compared to the readings based on live samples (Table 5.1 and Figure 5.7).

A potential source of bias could be the light type, since most labs, except FAS and NMFS, use reflected light and readers from these labs reported difficulties in reading due to light type change. However, this is likely to be a minor factor as ageing exercises have shown no significant light type effect on age interpretation (Rodriguez-Marin et al., 2014). What seems clear is that readers showed better agreement on edge type using transmitted light instead of reflected, since it allowed to reach a 53% of agreement in the type of marginal edge between "Mode Experts" and FAS. This being the reason argued by the participants of the 2019 workshop on ABFT direct aging to recommend the change of type of light in the age reading procedure (Rodriguez-Marin et al., 2020). Another factor that could have influenced the difficulty of reading the live samples is the absence of a reference scale, whereas the traditional method of reading has so far been based on images with reference scale.

To obtain the reference collection, the samples have been examined according to their readability code and whether it was necessary to carry out a 3rd reading. Samples that had at least three readers, including both live and images readings, with the worst readability code (1) or that would have required a third reading due to differences greater than 2 bands between the first and second reading, have been removed (4 samples).

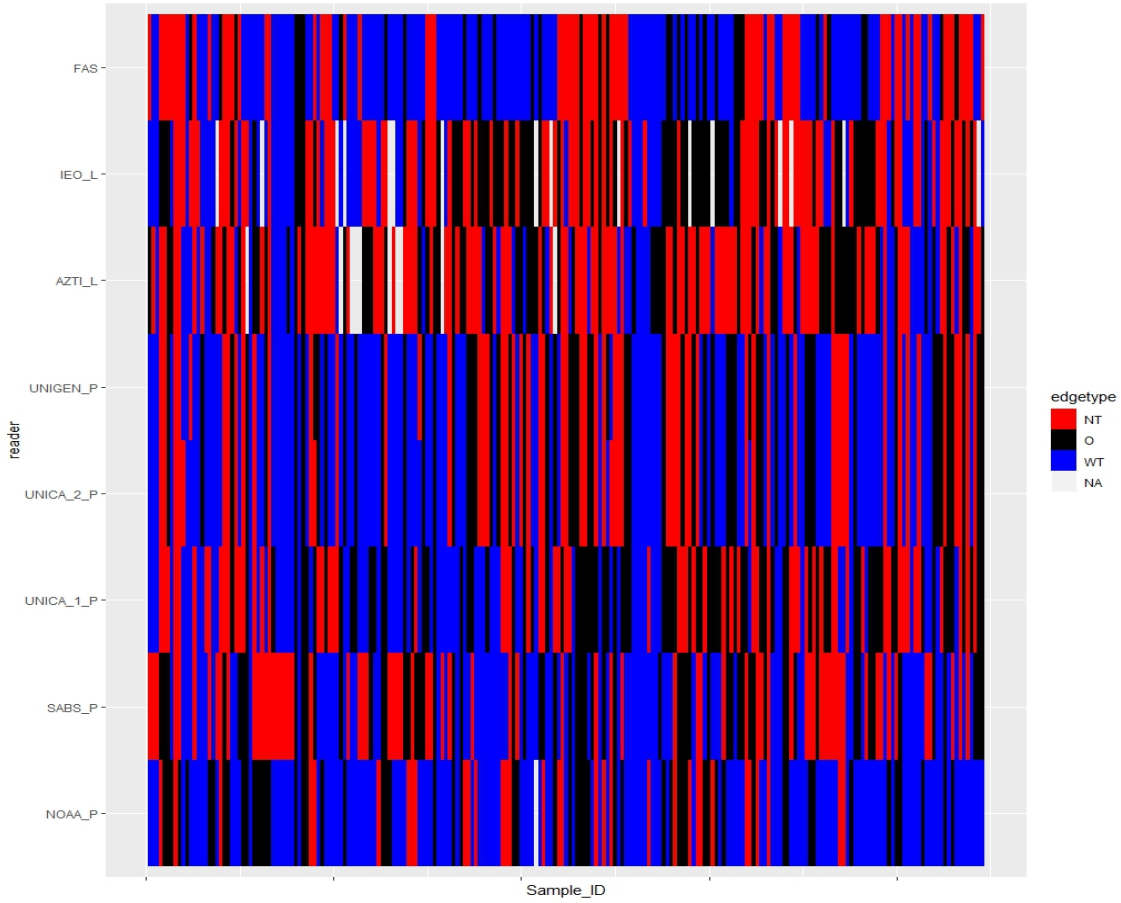

Figure 5.5. Tile plot showing otolith edge type assignment (NT= narrow translucent, Opaque= O, WT= wide translucent, NA= missing data) by sample for each reader-lab.

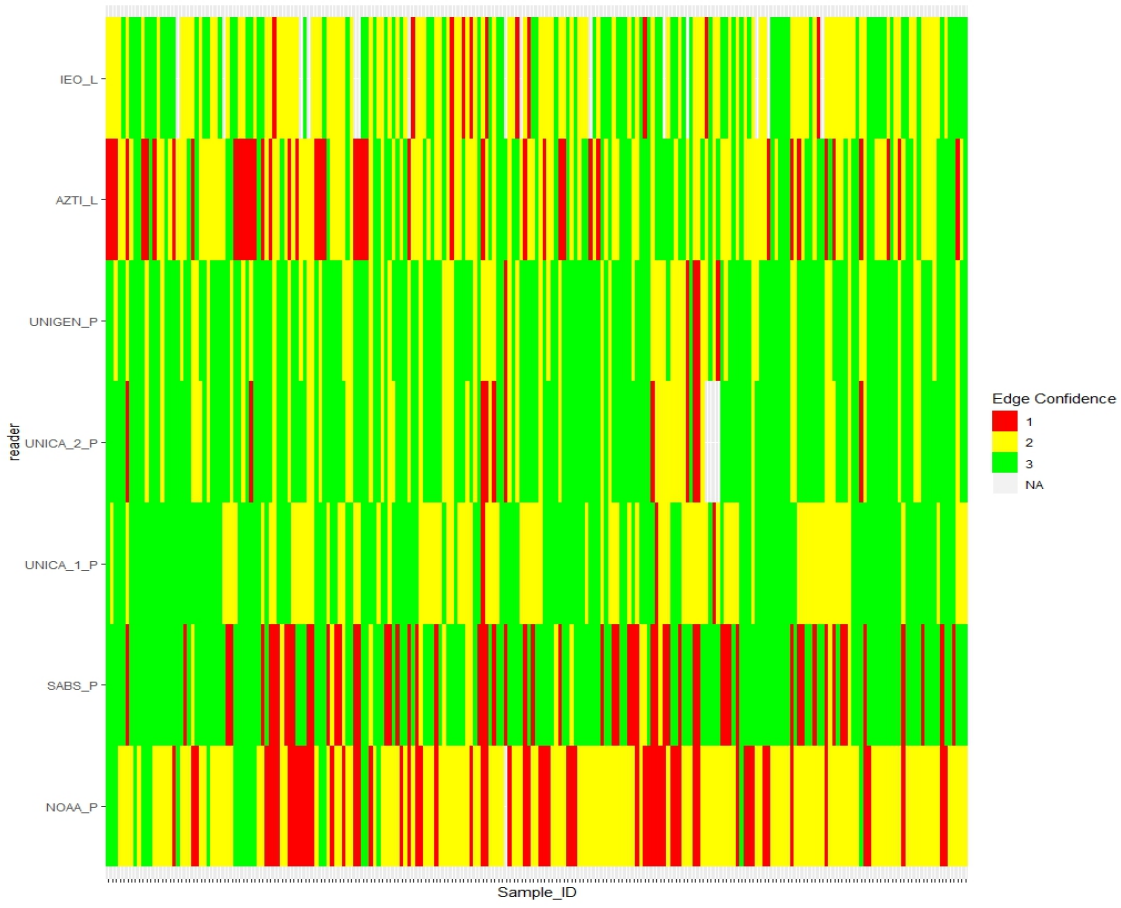

Figure 5.6. Tile plot showing otolith edge type confidence (1= no confident; 2= confident in completeness and not with the type and 3= confident) by sample for each reader-lab.

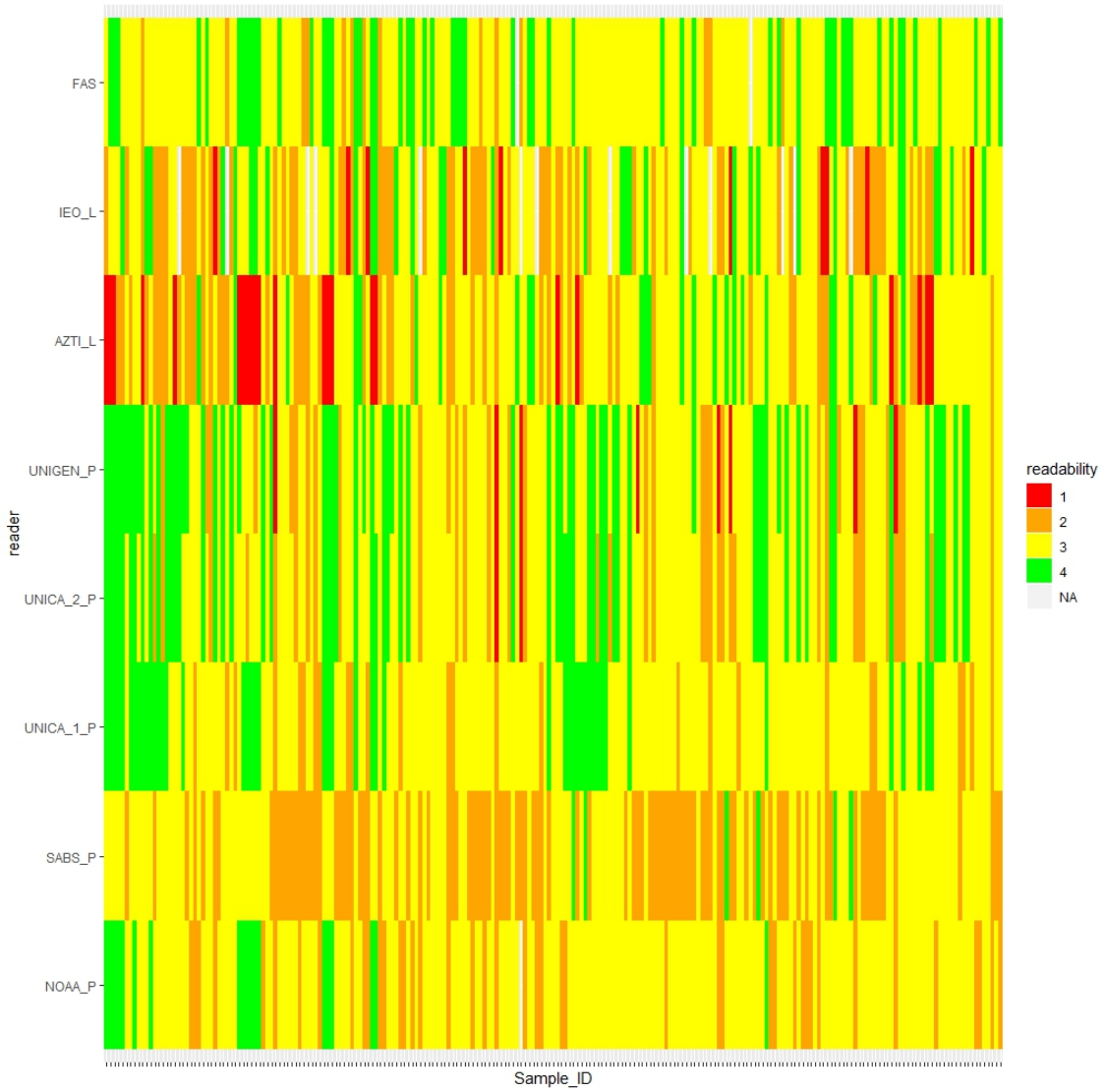

Figure 5.7. Tile plot showing otolith readability code (1= pattern present-no meaning, 2= pattern present-unsure with age estimate, 3= good pattern present-slightly unsure in some areas, 4= good pattern-confident with age estimate) by sample for each reader-lab.

5.4. Conclusions

The findings show that the band count is similar between FAS and the group of laboratories involved in direct ageing of Atlantic bluefin tuna otoliths. This is reflected by an acceptable precision between both readings. However, there is a one-year bias in the count of bands in older specimens, starting from 1-13 years of age, with a lower count by FAS compared to the rest of the laboratories. This bias seems to be due to the fact that FAS counts the bands in a different area of the ventral arm of the otolith than other laboratories. This counting discrepancy, although small is significant and it would

be necessary for FAS laboratory to reread the samples of specimens older than 10 years using the area close to the sulcus margin of the ventral arm. A reference scale helps identifying the first annual band and consequently the following first annual bands. Given these results, a new reference collection with consensus ages and following the ICCAT reviewed reading protocol will be created.

References

Anonymous. 2017. Report of the 2017 ICCAT bluefin stock assessment meeting (Madrid, July 2017). SCRS/2017/010.

Busawon, D.S., Addis, P., Allman, R., Bellodi, A., Garibaldi, F., Ishihara, T., Karakulak, S., Luque, P.L., Quelle P. Rodriguez-Marin, E. 2020. Evaluation of Atlantic bluefin tuna otolith ageing protocols. Collect. Vol. Sci. Pap. ICCAT, 76(2): 147-171.

Campana, S.E.; Annand, M.C.; Mcmillan, J.I. 1995. Graphical and statistical methods for determining the consisteny of age determinations. Transactions of the American Fishery Society. 124:131-138.

McBride. R.S. 2015. Diagnosis of paired age agreement: a simulation of accuracy and precision effects. ICES J Mar Sci; doi:10.1093/icesjms/fsv047.

Neilson, J. D. and Campana S. E. 2008. A validated description of age and growth of western Atlantic bluefin tuna (Thunnus thynnus). Canadian Journal of Fisheries and Aquatic Science 65: 1523-1527.

Ogle, D.H. 2018. FSA: Fisheries Stock Analysis. R package version 0.8.20.

Rodriguez-Marin E., Di Natale A., Quelle P., Ruiz M., Allman R. , Bellodi A., Busawon D., Farley J., Garibaldi F., Ishihara T., Koob E., Lanteri L., Luque P.L., Marcone A., Megalofonou P., Milatou N., Pacicco A., Russo E., Sardenne F., Stagioni M., Tserpes G. and Vittori S. 2014. Report of the age calibration exchange within the Atlantic Wide Research Programme for bluefin tuna (GBYP). ICCAT Standing Committee on Research and Statistics Documents SCRS/2014/150

Rodriguez-Marin E., Quelle P., Addis P., Alemany F., Bellodi A., Busawon D., Carnevali O., Cort J.L., Di Natale A., Farley J., Garibaldi F., Karakulak S., Krusic-Golub K., Luque P.L., and Ruiz M. 2020. Report of the ICCAT GBYP international workshop on Atlantic bluefin tuna growth. Collect. Vol. Sci. Pap. ICCAT, 76(2): 616-649

Rodriguez-Marin E., Quelle, P., Busawon, D., and Hanke, A. 2019. New protocol to avoid bias in otolith readings of Atlantic bluefin tuna juveniles. Collect. Vol. Sci. Pap. ICCAT, 75(6): 1301-1314.

6. ATLANTIC BLUEFIN TUNA (*Thunnus thynnus*) LARVAE IDENTIFICATION IN THE BAY OF BISCAY

Task Leader: María Santos (AZTI)

Participants:

AZTI: Beatriz Beldarrain, Miguel Angel Pardo, Haritz Arrizabalaga

6.1. Introduction

Atlantic bluefin tuna (*Thunnus thynnus*) is composed of two separate populations. Their two spawning areas are widely separated. The western stock spawns in the Gulf of Mexico (including the Straits of Florida), and the eastern stock spawns in several spawning areas of the Mediterranean Sea. Although the western stock was the first to be under regulation (since 1999), the number of reproductive studies is lower than those undertaken for the eastern stock (Susca et al., 2001; Corriero et al., 2003; Karakulak et al., 2004; Aranda et al., 2011; MacKenzie & Mariani, 2012). Recently, Richardson et al.(2016) used larval collections to demonstrate a spawning ground in the Slope Sea, between the Gulf Stream and the northeast United States continental shelf (Richardson et al.2016).

Eastern Atlantic bluefin tuna migrates from the Mediterranean to the Bay of Biscay for feeding (Arrizabalaga et al.2019; Arregui et al.2018). But recently, there were indications that ABFT was spawning also in the Bay of Biscay, since larvae of the species have been found in this area (Rodriguez et al.2019). For that reason, the search for additional ABFT larvae in samples collected in past surveys in the Bay of Biscay was proposed for this study.

6.2. Material and Methods

6.2.1. Field samples

Historical plankton samples from different surveys were selected in the ABFT laying period (June-July-August) in order to look for ABFT larvae in the Bay of Biscay. The selection of samples was restricted to samples collected outside the continental shelf (≥ 200m depth), since the probability to find ABFT is higher in these zones. In some years some samples from the platform were analyzed as well.

Table 6.1 shows the samples selected for the analysis. 663 samples in total, from years 2003, 2008, 2009 and 2015. All larvae were in good conditions of preservation (all preserved in ethanol).

The first samples analyzed were taken in the survey ECOANCHOA1 from 27th of June to 13th of July 2008 with Bongo40, double oblique tows to 200 m or to 5m near the bottom in shallower waters, with 0.4 m diameter bongo nets having 0.335 mm mesh size, preserved in ethanol (Table 6.1). The identification started with the samples outside the platform (>200m depth), were the probability to find a BFT is higher. Afterwards some from the platform, in the area of the Gironde, were checked as well (Figure 6.1). In total 105 samples were analyzed with 2,297 larvae of different species that were checked looking for ABFT larvae. From the same survey 64 samples taken with the MIK (mesh size 1000µm) with 801 larvae, were checked for ABFT.

Afterwards ECOANCHOA2 samples from the 4th to the 24th of August 2009 were analyzed. 91 samples taken with BONGO40 (mesh size 225µm) with 843 larvae preserved in ethanol were revised for ABFT (Table 6.1). And additional 2,419 larvae were checked from 97 samples taken with the MIK (mesh size of 1000µm) in the same survey.

From project BABES 2015, 4 samples, 2 from July and 2 from August, were checked for ABFT, with 39 and 58 larvae respectively.

From project SAVOR 2003, 17 stations were analyzed, with 524 larvae checked for ABFT.

Table 6.1: Samples available to be checked for BFT larvae. The header shows: the research project; year and month the samples were taken; sampler; preserver; total number of stations with different spp of larvae; stations selected for the analysis, larvae revised and mean sea surface temperature during the survey.

Project	year	month	sampler	preserv	st with larvae	St	Larva	SST	SSS
SAVOR	2003	7	Bongo40	ethanol	29	17	524		
ECOANCHOA1	2008	6-7	MIK	ethanol	88	64	801	20.2	34.99
ECOANCHOA1	2008	6-7	Bongo40	ethanol	141	85	2,297	20.2	34.99
ECOANCHOA2	2009	8	Bongo40	ethanol	183	91	879	21.6	34.88
ECOANCHOA2	2009	8	MIK	ethanol	186	97	2,419	21.6	34.88
BABES	2015	8	Bongo40	ethanol	2	2	39	22.5	34.13
BABES	2015	7	Bongo40	ethanol	2	2	58	22.3	33.47
TOTAL					**663**	**358**	**7,017**		

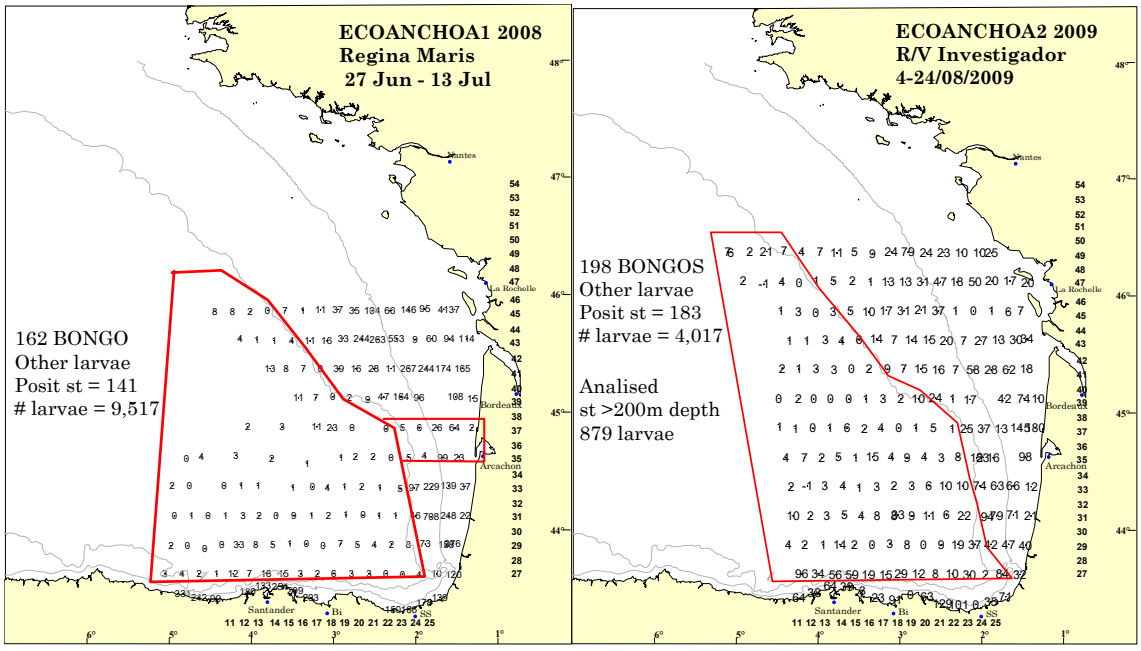

Figure 6.1: Left: Bongo40 samples taken during the survey Ecoanchoa1 2008. Right: Bongo40 samples taken during Ecoanchoa2 2009. The numbers are the larvae (different spp) taken in each station. The red line delimited the samples analyzed from each year.

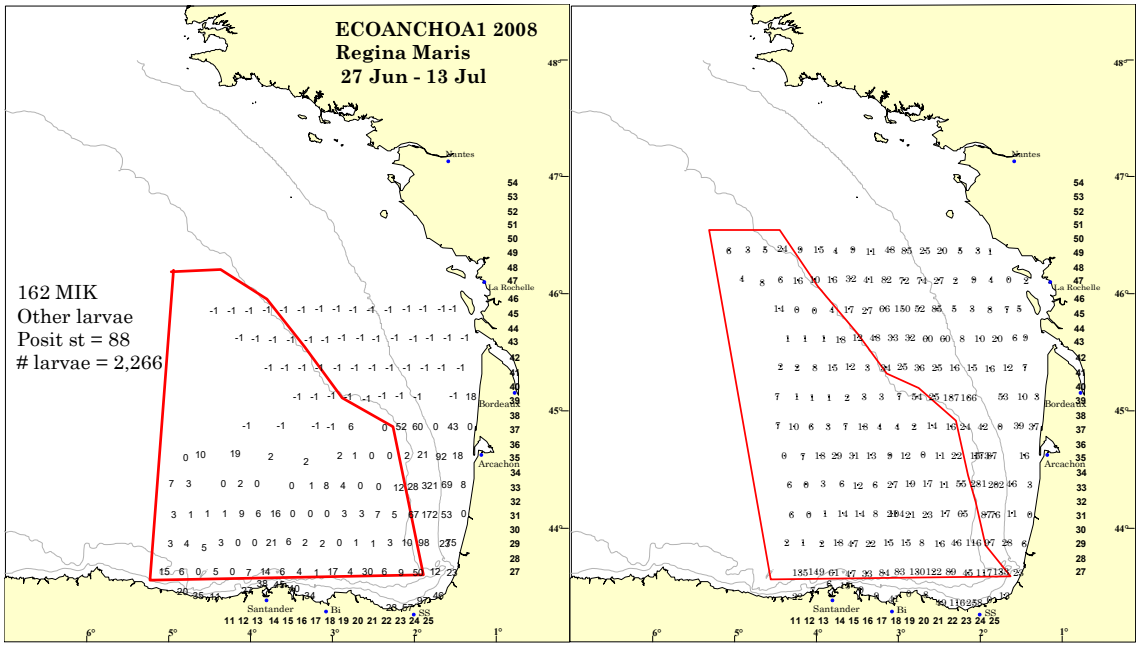

Figure 6.2: Left: MIK samples taken during the survey Ecoanchoa1 2008. Right: MIK samples taken during Ecoanchoa2 2009. The numbers are the larvae (different spp) taken in each station. The red line delimited the samples analyzed from each year for this study.

6.2.2. Microscopic identification

All larvae were extracted from the plankton samples and ABFT larvae were searched and identified under a stereoscopic microscope, using pigmentation patterns, number of myomers, morphologic and meristic characteristics, following the descriptions by Alemany (1997), Fahay (2007), Rodriguez et al. (2017), Puncher et al. (2015) and ABFT larvae photos from an incubation experiment carried out in 2012 by AZTI, in the laboratory of IEO Mazarrón-Murcia (Spain) and from a survey carried out in 2012 in the Balearic sea.

6.2.3. Genetic identification

To confirm the meristic and morphological identification, genetic identification of *T.thynnus* larvae, preserved in ethanol, was carried out following the AZTI's internal procedure MA-BM-02, accredited under ISO 17025. This procedure includes the isolation of DNA using the Genomic DNA Purification Kit (Qiagen) and amplification of

a pool of mitochondrial DNA fragments belonging to cytochrome b gene, including 7 polymorphisms, by Real Time PCR.

6.3. Results and discussion

Among the 7,017 larvae analyzed from 368 samples (Table 6.1), one larva collected in August 2009 (SST: 21.6ºC, SSS: 34.88) was identified as ABFT through microscopic identification and corroborated by genetic sequencing. This sample was taken west of Santander (43º37'61N 4º10'92 W) (Figure 6.6). This ABFT larva found was damaged but their myomere count was 39 and the morphologic and meristic characteristics were similar to that of ABFT and was afterwards corroborated by genetic sequencing. The standard length of the larva was 3.9mm. (Figure 6.3).

This larva could not have been transported into this area from any of the Mediterranean Sea spawning grounds. Instead it provided evidence for spawning in this region. This species relied heavily on environmental signals, and therefore their spawning habitats can vary depending on the environment (Reglero et al.2012). Atlantic bluefin tuna start to spawn once SST are over 20.5 °C, and preferentially in the range of 21.5–26.5 °C (Alemany et al.2010), the mean SST found during the survey where the larva was found is according to these parameters. This represents a single larva, adds to the larvae already found by Rodriguez et al (2019) in the Bay of Biscay. Anyway, further studies should be conducted to evaluate the existence of more ABFT larvae. The summer acoustic survey conducted in the Bay of Biscay during July (Goñi 2018) can be an opportunity to take plankton samples, although plankton sampling is limited in the open ocean.

Moreover, and again confirming the findings by Rodriguez et al. (2019) larvae from *Sarda sarda*, Atlantic bonito and *Auxis spp* were found among the samples checked for ABFT in the Bay of Biscay after the genetic sequencing. In August 2009 13 Auxis spp larvae were found spread in different stations (Figure 6.4 and Figure 6.6). The mean standard length was 5.4mm, the minimum was 3.3mm and the maximum 7.0mm. In August 2009 one *Sarda sarda* larva was found and in June-July 2008 13 were found (Figure 6.5 and Figure 6.6). The number of myomeres found in this specie was around 51.

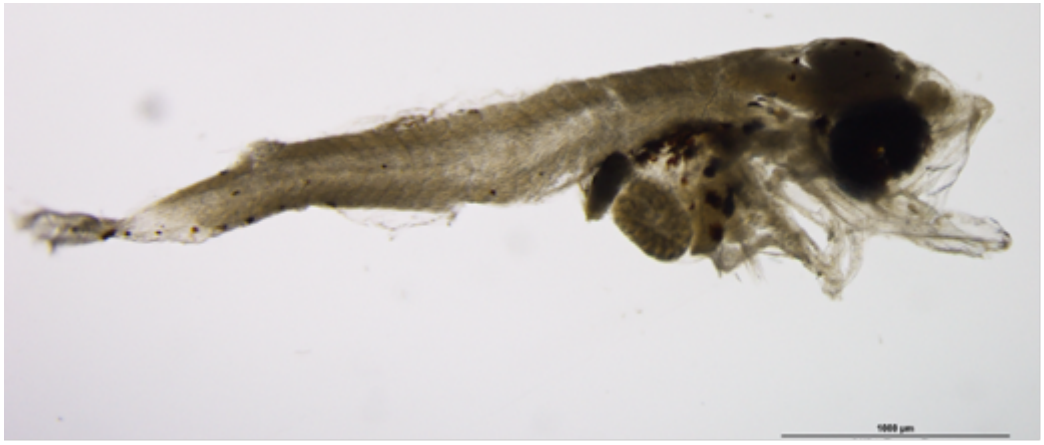

Figure 6.3: The ABFT larva encountered in August 2009 west of Santander. 3.9mm standard length.

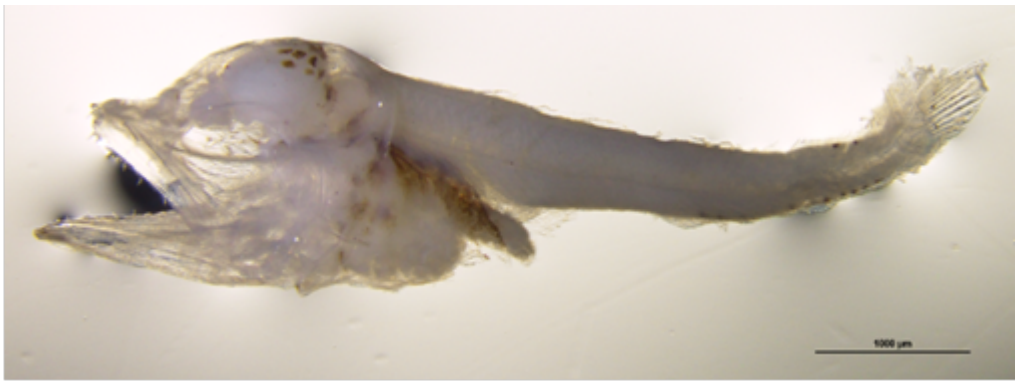

Figure 6.4: Photo of one of the 13 Auxis spp. larvae found in August 2009.

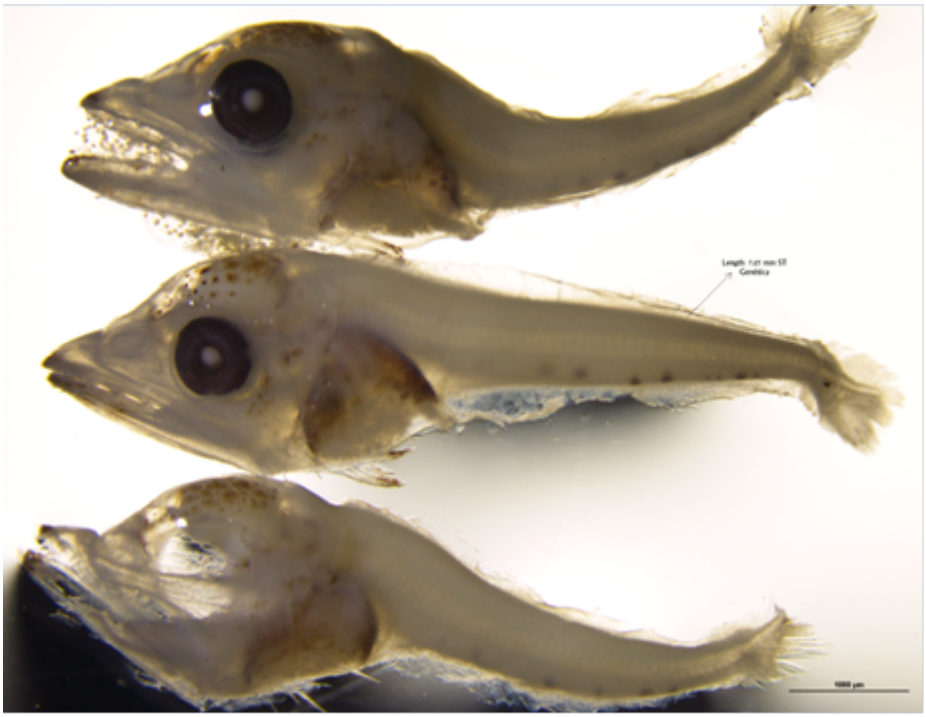

Figure 6.5: Photo of three of the 14 Sarda sarda larvae found in the samples.

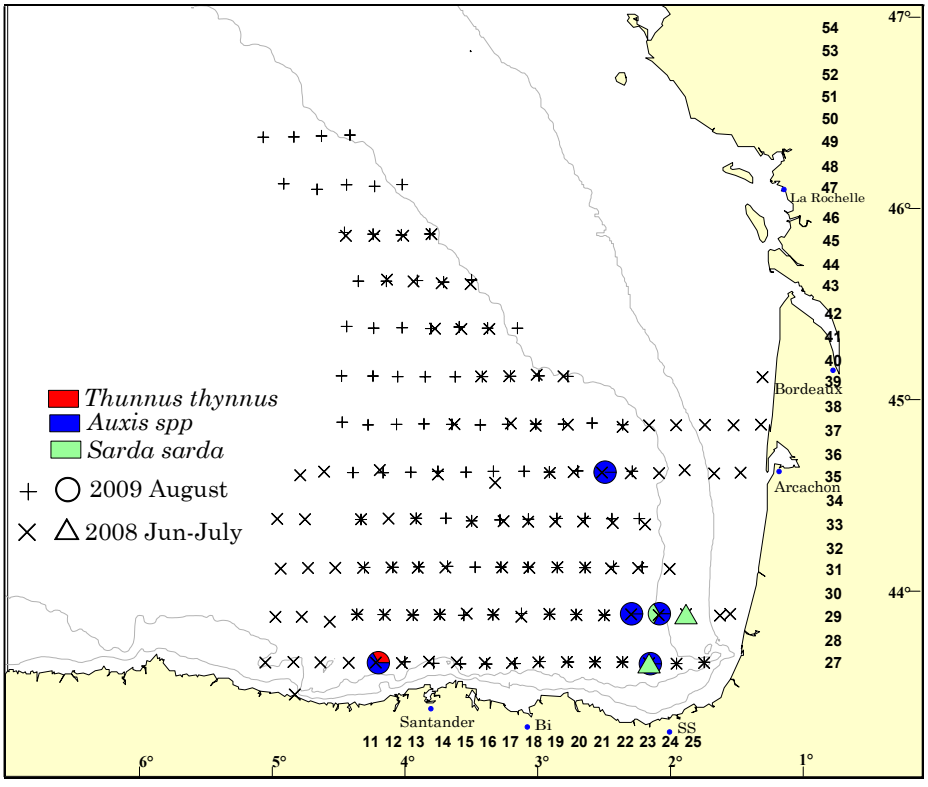

Figure 6.6: Distribution of the sampling stations analysed for ABFT in 2009 (addition sing) and 2008 (cross symbol) and larvae found in 2009 (circle) and 2008 (rectangle). The colours represent the different species: Thunnus thynnus (red), Auxis spp (blue) and Sarda sarda (green)

Acknowledgements

The samples used in this study were collected thanks to the projects ECOANCHOA funded by Department of Agriculture, Fisheries and Food of the Basque Country Government, BABES funded by the Department of Economic Development and Infrastructure of Basque Government and SAVOR (REN2002- 04205-C04-03) funded by the Spanish Ministry of Science and Technology.

References

Alemany F, Quintanilla L, Velez-Belchi P, Garcia A and others (2010) Characterization of the spawning habitat of Atlantic bluefin tuna and related species in the Balearic Sea (western Mediterranean). Prog Oceanogr 86: 21–38

Arregui, I., Galuardi, B., Goñi, N., Lam, C.H., Fraile, I., Santiago, J., Lutcavage, M. and Arrizabalaga, H. (2018) Movements and geographic distribution of juvenile bluefin tuna in the Northeast Atlantic, described through internal and satellite archival tags. ICES Journal of Marine Science doi:10.1093/icesjms/fsy056.

Arrizabalaga, H., Arregui, I., Medina, A., Rodríguez-Ezpeleta, N., Fromentin, J.-M. and Fraile, I. (2019) Life History and Migrations of Mediterranean Bluefin Tuna In: The Future of Bluefin Tunas: Ecology, Fisheries Management, and Conservation.B. Block (ed.) Johns Hopkins University Press, pp. 67-93.

Corriero A, Desantis S, Deflorio M, Acone F, Bridges CR, De la Serna JM, Megalofonou P, De Metrio G. Histological investigation on the ovarian cycle of the bluefin tuna in the western and central Mediterranean. Journal of Fish Biology. 2003;63(1):108–119. doi: 10.1046/j.1095-8649.2003.00132.x.

Goñi, N., Uranga, J., Arregui, I., Onandia, I., Martinez, U., Boyra, G., Melvin, G.D., Godard, I. and Arrizabalaga, H. (2018) ACOUSTIC-BASED FISHERY-INDEPENDENT ABUNDANCE INDEX OF JUVENILE BLUEFIN TUNAS IN THE BAY OF BISCAY: RESULTS FROM THE FIRST THREE SURVEYS AND CHALLENGES. Collect. Vol. Sci. Pap. ICCAT, 76(x): SCRS/2018/145

Karakulak S, Oray I, Corriero A, Deflorio M, Santamaria N, Desantis S, De Metrio G. Evidence of a spawning area for the bluefin tuna (Thunnus thynnus L.) in the eastern Mediterranean. Journal of Applied Ichthyology. 2004;20(4):318–320. doi: 10.1111/j.1439-0426.2004.00561.x

Mackenzie, Brian & Mariani, Patrizio. (2012). Spawning of Bluefin Tuna in the Black Sea: Historical Evidence, Environmental Constraints and Population Plasticity. PloS one. 7. e39998. 10.1371/journal.pone.0039998.

Puncher, G N, Alemany F, Arrizabalaga H, Cariani A and Tinti F. Misidentification of bluefin tuna larvae: a call for caution and taxonomic reform. Rev Fish Biol Fisheries (2015) 25:485–502 DOI 10.1007/s11160-015-9390-1

Reglero P., Ciannelli L., Alvarez-Berastegui D., Balbín R., Lopez-Jurado J.L., Alemany F., (2012) Geographically and environmentally driven spawning distributions of tuna species in the western Mediterranean Sea, Marine ecology progress series, 2012, 463:273-284 pp.

Richardson DE, Marancik KE, Guyon JR, Lutcavage ME, Galuardi B, Lam CH, Walsh HJ, Wildes S, Yates DA, Hare JA. Discovery of a spawning ground reveals diverse migration strategies in Atlantic bluefin tuna (Thunnus thynnus) Proceedings of the National Academy of Sciences of the United States of America. 2016;113(12):3299–3304. doi: 10.1073/pnas.1525636113.

Rodriguez J.M., Johnstone C.and Lozano-Peral D.2019. Is the southern Bay of Biscay a spawning ground for Thunnus thynnus and Sarda Sarda? SCRS/2019/201.

Rodriguez, J.M., Alemany, F. and Garcia A. 2017. A guide to the eggs and larvae of 100 common Western Mediterranean Sea bony fish species. FAO, Rome, Italy, 256 pp.

Susca V, Corriero A, Deflorio M, Bridges CR, De metrio G. New results on the reproductive biology of bluefin tuna (Thunnus thynnus) in the Mediterranean. ICCAT Collective Volume of Scientific Papers. 2001;52:745–751.

7. SORTING AND IDENTIFICATION OF ATLANTIC BLUEFIN TUNA LARVAE FOR POTENTIAL CLOSE-KIN ANALYSES

Task leader: Patricia Reglero (IEO)

7.1. Objective

The main objective of this task was to assess the capability of current BFT larval surveys for providing larvae to carry out different types of genetic analyses, and hence allowing to apply methods as the close kin approach. The initial goal was to get 10000 bluefin tuna larvae from a single survey useful for genetic analyses

7.2. Material & Methods

As a first step, the whole ichthyoplanktonic fraction from the formalin preserved replicate of the Bongo net 500 microns mesh size hauls carried out in a grid of stations sampled during the oceanographic survey conducted in 2017 in the Balearic Islands BFT spawning ground (Western Mediterranean), was sorted, and BFT larvae identified and counted. Formalin preserved samples are those routinely used to identify bluefin tuna larvae since formalin is the best preservation method for the maintenance of pigments used for taxonomic identification. In those stations where many BFT larvae were found then the Cytoscan preserved replicates were sorted out to separate larvae for DNA analyses.

In Autumn 2019, before finishing the envisaged sorting tasks on 2017 survey samples, the final results from a parallel study to compare the suitability of ethanol and Cytoscan preserved specimens for DNA extraction, carried out by CSIRO on larvae from the BFT larval survey carried out in 2016, were available. This study showed that whereas the larvae sorted directly from ethanol preserved samples worked perfectly for DNA extraction, individuals preserved in Cytoscan, and transferred temporary to water for sorting and identification, inhibited the DNA extraction.. Therefore, the analysis of 2017 larval survey BFT larvae was cancelled, after having sorted and identified bluefin tuna larvae from 45 formalin preserved samples and 15 Cytoscan preserved samples.

Therefore, in the view of results from the DNA genotyping some modifications to the original plan were made. Specifically, ethanol preserved ichthyoplankton samples from 2018 and 2019 surveys, taken following the same methodology than in 2017 and in which higher abundances of BFT larvae were expected according to observations carried out on boards, were analyzed. BFT larvae were sorted directly from the original sample, without transferring the zooplankters to water for sorting and identification tasks.

7.3. Results

The results from the analyses comparing Ethanol and Cytoscan preserved specimens from 2016 survey showed that whereas the ethanol preserved samples, not transferred to water for sorting, worked perfectly for DNA extraction, individuals preserved in Cytoscan inhibited the DNA extraction. Thus, DNA yields were very low for Cytoscan preserved larvae and did not produce any sequence whereas EtOH preserved larvae showed a tight high molecular weight band. The composition of Cytoscan was studied in depth to try to develop further protocols for DNA extraction. Such analyses showed that Cytoscan is mostly ethyl alcohol, normally 96% or 70%, depending on the concentration. In addition, it has some methanol, isopropyl alcohol and butanone to denature the ethyl alcohol. It was hypothesized that butanol or methanol was the culprit for destroying the DNA in the larvae. However, although when a mass spectrometry was done on the substance no butanol was detected. A second hypothesis was that given that Cytoscan preserved samples were sorted in water this process was affecting the quality of DNA. . Finally, 339 Atlantic bluefin tuna larvae preserved in ethanol from 22 stations in 2018 and 2019 were identified, which were sent to CSIRO for genetic analyses. This number is very much below the expected total of larvae since in the stations selected for 2018 and 2019, the number of larvae of bluefin tuna found was low. This low number is explained because in these surveys large patches of yolk sac larvae, which are the ones with the highest abundances, were not captured, and because the limited time left for analyzing 2018 and 2019 samples. However, the experience gained from the DNA extraction trials carried out within this study, which has allowed to develop a new larval preservation and handling workshop adequate for DNA extraction, as well the optimized BFT larval sampling methodologies developed along the time series of BFT larval surveys developed from 2001 in Balearic Sea, allows to confirm that current larval surveys developed in the Balearic sea could provide BFT larvae suitable for any type of

genetic studies, including those demanding a high number of larvae, as the Close Kin approach.

8. ACKNOWLEDGEMENTS

This work was carried out under the provision of the ICCAT Atlantic Wide Research Programme for Bluefin Tuna (GBYP), funded by the European Union, by several ICCAT CPCs, the ICCAT Secretariat and by other entities (see: https://www.iccat.int/GBYP/en/Overview.asp). The contents of this report do not necessarily reflect the point of view of ICCAT or of the other funders, which have not responsibility about them, neither do them necessarily reflect the views of the funders and in no ways anticipate the Commission's future policy in this area.

9. APPENDICES

Appendix 1: Database as of 10th April 2020 (see "Database_10_Apr_2020.xls). Note that this database is subject to change in the future as new samples are integrated.